

**ISÓTOPOS DE ENXOFRE DE COMPLEXOS ALCALINO-CARBONATÍTICOS NA
MARGEM DA BACIA DO PARANÁ - GOIÁS, MINAS GERAIS E SÃO PAULO**

**DISSERTAÇÃO DE MESTRADO
Nº 275**

CAROLINE SIQUEIRA GOMIDE

Orientador: JOSÉ AFFONSO BROD
Co-Orientador: BERNHARD MANFRED BÜHN

BRASÍLIA, 2011

ISÓTOPOS DE ENXOFRE DE COMPLEXOS ALCALINO-CARBONATÍTICOS NA MARGEM DA BACIA DO PARANÁ - GOIÁS, MINAS GERAIS E SÃO PAULO

DISSERTAÇÃO DE MESTRADO N° 275

CAROLINE SIQUEIRA GOMIDE

Área de Concentração: Mineralogia e Petrologia

Orientador: JOSÉ AFFONSO BROD

Co-Orientador: BERNHARD MANFRED BÜHN

Membros da Banca Examinadora:

José Affonso Brod- UFG/UnB

Lucieth Cruz Vieira - UnB

Sérgio de Castro Valente – UFRRJ

**15/03/2011
BRASÍLIA/DF**

AGRADECIMENTOS

Agradeço a meus filhos, Gael e Iuri, eles são minha força nos momentos mais difíceis, minha alegria de viver e razão pela qual enfrento todos os momentos com a garra e energia necessária. Ao amor da minha vida, responsável por dar dois solzinhos em minha vida, Luiz Zarref, meu companheiro, marido, amado, amante, namorado, paixão...que sempre me deu força e apoio em todos os sentidos.

Agradeço ao meu pai, Afonso, pelo esforço, dedicação e ensinamentos, e aos meus irmãos, Guilherme e Ramon, pela cumplicidade e amizade. À minha avó, pedagoga da família, que sempre me apoiou em minhas decisões acadêmicas e se orgulha da netinha que gosta dessa vida. À minha "Mãezinha", Natalícia, e ao seu José Carlos, que sempre me acolheram, apoiaram e compreenderam mesmo sem entender porque tanta correria. À tia Neusinha e Jaqueline que cuidaram com tanto carinho do meu pequeno Iuri enquanto estive escrevendo em Catalão.

Agradeço a família buscapé, Paulinho, Gustavo, Luci, Isabela e Dindinha, pelo apoio, ajuda e por tornar possível a morada em comunidade.

A todos os amigos e amigas, pelos momentos de alegria, estudos, farras e reflexões. Em especial, agradeço à Katita, Bela, Raquel, Bibi, Jean, Cupim, Juça e tantos que colaboraram e foram fundamentais nesta etapa de minha vida, e que mesmo sem entender "porque diabos essa menina estuda tanto", sempre me apoiaram e compreenderam meus sumiços.

Aos amigos da geologia, pelo apoio e partilha da choradeira do "nunca acaba", pelos lanchinhos na hora do desespero para uma energia a mais, pela ajuda com o trabalho, pelos papos nos intervalos para um cafezinho...Em especial Diana, Luiz Paulo, Mari Bege e Ana Catarina.

Aos multirões geocronógicos para ajudar a Carol, em especial à Bárbara (de babá a mãe do netuno) e Jaqueline (de babá a pessoa que resolve todas as coisas). Também agradeço ao Mancini que me aturou demais com as perguntas e amostras a serem analisadas, Érico com a ajuda e paciência, Lucieda pela companhia e atenção e à Jô (sempre disponível, incrível como ela consegue!).

Agradeço o professor Elton, pelo apoio e ajuda sempre que solicitado. Ao professor Bernhard pela orientação e ensinamentos para que esse trabalho fosse possível.

Agradeço especialmente aos meus orientadores Affonso e Tereza Brod, meus "pais geológicos" que foram fundamentais em minha formação e que com tanto carinho, dedicação, firmeza e sabedoria auxiliaram, participaram e compartilharam tantos momentos de superação e aprendizado.

À Capes, pela bolsa, quesito fundamental para a realização deste trabalho.

Por fim, agradeço a todos e todas que não foram lembrados neste agradecimento, mas que foram e são importantes no meu processo de formação.

ABSTRACT

This thesis presents petrographic, chemical, and sulphur isotope data, in order to contribute to elucidate the origin, evolution and differentiation mechanisms (e.g. fractional crystallization, liquid immiscibility, magma mixing and degassing) in alkaline-carbonatite complexes of the Alto Paranaiba Igneous Province (APIP) and in the Jacupiranga complex, from the Ponta Grossa Province.

The APIP is one of the largest ultrapotassic-ultramafic provinces worldwide, and one of the few known kamafugite-carbonatite associations. It includes six carbonatite complexes (Catalão I, II, Serra Negra, Salitre, Araxá, Tapira), which are multiphase intrusions formed by rocks belonging to the bebedourite, phoscorite and carbonatite series. The Ponta Grossa Province, unlike APIP, is dominated by sodic alkaline rocks. Jacupiranga was the sole complex studied from this province, and is composed of rocks of the carbonatite and ijolite series.

The rocks from carbonatite complexes, especially those of the carbonatite series, often contain sulphides (pyrite, pyrrhotite, chalcopyrite, galena, bornite, pentlandite) and sulphates (mainly barite). Therefore, sulphur is an important element for research in the petrogenesis of these rocks. This work presents the first sulphur isotope data from APIP and Ponta Grossa complexes. The main tools used in this study include petrography, mineral chemistry and isotopic analysis of sulphides and sulphates in carbonatites, phoscorites and bebedourites, in APIP, and carbonatites and jacupirangites, in Jacupiranga.

The studied samples show mesoscopic and microscopic quench textures, such as bladed carbonate and sulphide crystals, with interstitial microgranular aggregates of carbonate, barite and sulphides. These are interpreted as the result of rapid crystallization during degassing of a supercooled carbonatite magma.

The CO₂ degassing at APIP complexes was studied in previous works by the Research Group in Alkaline Rocks and Associated Mineralizations and this work adds degassing of sulphur gaseous phases (H₂S and/or SO₂) to that picture.

The sulphur isotope results in sulphides from samples showing evidence of degassing vary from core to rim, with the latter showing higher (less negative) $\delta^{34}\text{S}$, compared with the former, which indicates that degassing took place in an oxidizing environment.

Isotopic data indicates that as magma differentiation progresses it consumes particularly heavier isotopes into the solid phases, leaving a residual magma/fluid enriched in ^{32}S . On the other hand, sulphur loss by degassing under oxidizing conditions lead the residue to evolve toward higher $\delta^{34}\text{S}$.

The sulphur isotope composition of the studied complexes is consistent with the expected values for igneous rocks and carbonatite complexes. Data for worldwide carbonatites of various ages suggest that the sulphur isotope global composition in the mantle might have progressively changed towards more negative $\delta^{34}\text{S}$ values with time.

RESUMO

Esta dissertação apresenta dados petrográficos, de química mineral e de isótopos estáveis de enxofre, com o intuito de contribuir para elucidar a gênese, evolução e mecanismos de diferenciação (processos como cristalização fracionada, imiscibilidade de líquidos, mistura de magmas e desgaseificação) em complexos alcalino-carbonatíticos da Província Ígnea do Alto Paranaíba (APIP) e em Jacupiranga, um complexo Carbonatítico da Província Ponta Grossa.

A Província Ígnea do Alto Paranaíba (APIP) é uma das maiores províncias ultramaficas-ultrapotássicas mundiais e uma das poucas associações kamafugíticas-carbonatíticas conhecidas. Inclui 6 complexos carbonatíticos (Catalão I, II, Serra Negra, Salitre, Araxá, Tapira) que são intrusões multifásicas formadas por rochas das séries bebedourítica, carbonatítica e foscorítica. A Província de Ponta Grossa, diferente da APIP, é dominada por rochas alcalinas sódicas. Jacupiranga, o único complexo desta província estudado no presente trabalho, é composto de rochas das séries carbonatítica e ijolítica.

As rochas dos complexos carbonatíticos, principalmente as da série carbonatítica, frequentemente contêm sulfetos (pirita, pirrotita, calcopirita, galena, bornita, pentlandita) e sulfatos (principalmente barita). Portanto, o enxofre é um elemento importante no estudo de processos de formação dessas rochas. Este é o primeiro trabalho a apresentar dados isotópicos de S nos complexos da APIP e Ponta Grossa.

As principais ferramentas utilizadas para o estudo incluem petrografia, química mineral e análise isotópica de sulfetos e sulfatos em rochas das séries carbonatítica, foscorítica e bebedourítica, na APIP, e de carbonatitos e jacupiranguitos, em Jacupiranga.

A petrografia das amostras permitiu o reconhecimento de texturas interpretadas como de resfriamento rápido, como cristais alongados (laminares) principalmente de carbonato e sulfeto, cujos interstícios estão preenchidos por agregados microgranulares de carbonato, barita e sulfetos. Estas texturas são interpretadas como resultado de congelamento (*quench*) durante a desgaseificação de um magma super-resfriado.

A desgaseificação de CO₂ nos complexos da APIP foi estudada em trabalhos anteriores do Grupo de Pesquisa em Rochas Alcalinas e Mineralizações Associadas e este trabalho agrega a desgaseificação de gases sulfetados (H₂S e/ou SO₂).

As análises de isótopos de S em amostras com evidências petrográficas de desgaseificação apresentam uma diferença núcleo e borda do grão de sulfeto, onde a borda possui maiores valores (menos negativos) de $\delta^{34}\text{S}$ em relação ao núcleo, o que leva à conclusão de que o processo de desgaseificação ocorreu em ambiente oxidante.

Os dados isotópicos indicam que a medida que os processos de diferenciação progredem, os isótopos mais pesados são consumidos deixando o magma residual enriquecido em ^{32}S , ao passo que que durante a desgaseificação de voláteis com S, em condições oxidantes, o magma residual enriquece em ^{34}S nos complexos estudados.

A composição isotópica de enxofre dos complexos estudados coincide com os valores esperados para rochas ígneas e para complexos carbonatíticos. Os dados de carbonatitos mundiais, de várias idades, sugerem que a composição isotópica de enxofre no manto pode ter mudado progressivamente ao longo do tempo geológico, em direção a valores mais negativos de $\delta^{34}\text{S}$.

Índice

CAPÍTULO 1	1
Introdução.....	1
CAPÍTULO 2	5
Métodos.....	5
Análises em Microssonda Eletrônica	5
Preparação de amostras	5
Procedimentos analíticos.....	6
Isótopos de Enxofre	7
Revisão bibliográfica	7
Preparação de amostras	9
Laser ablation multiple-collector inductively coupled plasma mass spectrometry (LA-MC-ICP-MS)	9
Procedimentos analíticos.....	11
Tratamento dos dados.....	12
CAPÍTULO 3	13
Sulfur isotopes from alkaline carbonatite complexes along the borders of the Paraná Basin - Goiás, Minas Gerais and São Paulo States, Brazil.....	13
Abstract.....	13
1. Introduction.....	13
2. Geological setting	15
3. Sample description	19
4. Analytical methods	34
5. Results.....	35
5.1. Mineral Chemistry.....	38
5.2. Sulfur isotope variations in the APIP complexes and Jacupiranga	40
5.3. Sulfur isotope variations by rock type	42
5.4. Sulfur isotope variations from rim to core	44
5.5. Sulphide-sulphide isotopic variation	46
5.6. Sulphide-sulphate isotopic variation and fractionation	47
5.7. Comparison with other carbonatites.....	49
6. Conclusions.....	51
7. References	55
CAPÍTULO 4	62
Conclusões	62
REFERÊNCIAS BIBLIOGRÁFICAS	66
ANEXOS	i
Análises de Isótopos de Enxofre	i
Dados de Química Mineral de Barita	v
Dados de Química Mineral de Sulfeto	viii

Índice de Figuras

Figura 2.01 - Desenho esquemático do sistema MC-ICP-MS (Manual Thermo Finnigan 2003).....	10
Figure 3.01 – Carbonatite occurrences surrounding the Paraná Basin. The carbonatite complexes studied in this work are shown as stars. Modified from Oliveira et al. (2004) and Wooley & Kjarsgaard (2008).....	16
Figure 3.02 – Carbonatite from the Catalão II complex. A: phlogopite (phl), magnetite (mgt) and recrystallized pyrite (py). cbt=carbonate Field width: 5mm. Plane polarized light; B: Same as A in reflected light. C: Back-scattered image of a carbonate (cbt) + barite (brt) mass in carbonatite from the Catalão II complex. D: Higher magnification view of the back-scattered image in A.....	20
Figure 3.03 – Textural features of nelsonites from the Catalão II complex. A: Apatite (Ap) and pyrochlore (Pcl) in nelsonite, plane polarized light. Field width: 5mm. B: Same as A, in reflected light, showing chalcopyrite (Cpy) and subordinate pyrite (Py). Field width: 5mm. C: Phlogopite (Phl), apatite (Ap), pyrochlore (Pcl), carbonate (Cbt) and magnetite (Mgt) in nelsonite, plane polarized light. Field width: 5mm. D: Pyrite (Py) and rare chalcopyrite (Cpy) replacing magnetite; note that the earlier magnetite contained ilmenite (Ilm) exsolution lamellae that remained preserved upon dissolution and substitution of the magnetite grain, forming a trellis texture, reflected light. Field width: 1,5mm.....	21
Figure 3.04 – Textural features of sulphides and barites in carbonatites from the Catalão I complex. A: Apatite (Ap), carbonate (Cbt) and phlogopite (Phl) in cross polarized light. Field width: 5mm. B: Same as A in reflected light, showing a smooth surface for pyrite (Py). Field width: 5mm. C: Phlogopite (Phl), carbonate (Cbt), barite (Brt); note the intergrowth of pyrite and barite. Cross polarized light. Field width: 5mm. D: Same as C in reflected light, pyrite (Py) and magnetite (Mgt); note the intergrowth of pyrite and barite. Field width: 5mm. E: Pyrite (Py) with pitted surface, probably resulting from recrystallization as microgranular aggregates. Reflected light. Field width: 5mm. F: Pyrite (Py) with skeletal appearance and irregular surfaces, probably resulting from recrystallization as microgranular aggregates. Reflected light. Field width: 5mm.....	22
Figure 3.05 – Textural features of sulphide phoscorites from the Catalão I complex A: Apatite (Ap) and phlogopite (Phl) from phoscorites in cross polarized light. Field width: 5mm. B: Same as A in reflected light, showing a pitted surface in various pyrite (Py) individual grains and very fine grained chalcopyrite (Cpy) aggregates with a “dusty” appearance. Field width: 5mm. C: Apatite (Ap) and phlogopite (Phl). Plane polarized light. Field width: 5mm. D: Same as C, in reflected light showing pyrite (Py); note the amoeboid geometry of the interstitial pyrite aggregates, suggesting that they formed from an immiscible sulphide liquid. Field width: 5mm.....	23
Figure 3.06 – Textural features of nelsonites from the Catalão I complex. A: Apatite (Ap), carbonate (Cbt), pyrochlore (Pcl) and phlogopite (Phl) in nelsonite, plane polarized light showing flow orientation of phlogopite and apatite crystals. Field width: 5mm. B: Pyrite (Py) grains with pitted surface and fine-grained chalcopyrite (Cpy) aggregates. Field width: 5mm.....	24
Figure 3.07 – Serra Negra carbonatites. A: Coarse-grained carbonate (Cbt) in cross polarized light; Field width: 5mm. B: Same as A, in reflected light, showing a small pyrite grain (Py). Field width: 5mm.....	25

- Figure 3.08** – Textural features of carbonatites from the Salitre complex. **A:** Apatite (Ap), carbonate (Cbt), phlogopite (Phl) and pyrochlore (Pcl) in plane polarized light. Field width: 5mm. **B:** Elongated sulphide grain, pyrrhotite (Po) is the grain with a smooth surface, pyrite (Py) is the irregular surface grain, and chalcopyrite (Cpy) is present in small amounts, bordering pyrrhotite and pyrite. Reflected light. Field width: 5mm. **C:** Carbonate (Cbt), barite (Brt) and pyrite (Py) showing zonation in carbonate crystals. Plane polarized light. Field width: 5mm. **D:** Carbonate (Cbt) and complexly zoned barite (Brt). Cross polarized light. Field width: 5mm.....26
- Figure 3.09** – Textural features of sulphide phoscorites from the Salitre complex. **A:** Coarse grained phoscorite, composed of olivine (Ol), phlogopite (Phl) in plane polarized light. Field width: 5mm. **B:** Same as A in reflected light, showing pyrite (Py) replacing magnetite; ilmenite (Ilm), chalcopyrite (Cpy) and pyrrhotite (Po). Field width: 5mm.....27
- Figure 3.10** – Bebedourite from the Salitre complex. **A:** Coarse grained bebedourite, composed of clinopyroxene (Cpx), phlogopite (Phl), magnetite, ilmenite, pyrite. Field width: 5mm. **B:** Same as A in reflected light, showing magnetite (Mgt) replacement by pyrite (Py). Field width: 5mm.....27
- Figure 3.11** – Textural features of fine-grained aggregates of sulphide, barite and carbonate in carbonatite from the Araxá complex. **A:** Cryptocrystalline carbonate mass, with intergrown of barite aggregates and sulphide, cross polarized light. Field width: 5mm. **B:** Same as "A", in reflected light. Field width: 5mm.....28
- Figure 3.12** – Textural features of sulphide and carbonate in carbonatite from the Araxá complex **A:** Typical texture of carbonatite pyrite (Py), with very irregular grain surfaces, probably resulting from recrystallization of microgranular aggregates and very fine-grained aggregates of chalcopyrite (Cpy), and subordinate pyrite, with a dusty appearance. Reflected light. Field width: 5mm. **B:** Sulphides with a blob aspect, showing round contours that may indicate segregation of a sulphide immiscible liquid, with pyrrhotite (Po), pyrite (Py) and chalcopyrite (Cpy). Reflected light. Field width: 5mm. **C:** Carbonate aggregates marked by subparallel curved lines. Plane polarized light. Field width: 5mm. **D:** Same as "C" in cross polarized light. **E:** Cross section of carbonate aggregates showing concentric growth lines. Plane polarized light. Field width: 5mm. **F:** Same as "E", in cross polarized light, showing a circling maltese cross similar to the spherulitic extinction.....29
- Figure 3.13** – Phoscorite. **A:** Phoscorite with magnetite (Mgt), phlogopite (Phl), apatite (Ap) and carbonate (Cbt). Plane polarized light. Field width: 5mm. **B:** Pyrite (Py) with pitted surface and magnetite (Mgt). Reflected light. Field width: 5mm.....30
- Figure 3.14** – Textural features of carbonatites from Tapira complex. **A:** Carbonatite with carbonate (Cbt), olivine (Ol) and apatite (Ap). Cross polarized light. Field width: 5mm. **B:** Carbonatite with some microgranular carbonates of colloidal aspect (arrow). Plane polarized light. Field width: 5mm.....31
- Figure 3.15** – **A:** BSE image of a fine-grained mass containing dolomite (Cbt) and skeletal barite (Brt). **B:** BSE image of a fine-grained mass containing different carbonate types and barite, 001: Barite; 002: Barite; 003: Sr-carbonate; 004: Sr-carbonate; 005: Dolomite; 006: Calcite; 007: Calcite.....31
- Figure 3.16** – Textural features of phoscorites from Tapira complex. **A:** Phoscorite showing carbonate (Cbt), olivine (Ol), apatite (Ap), granular chalcopyrite and pyrite with pitted surface. Cross polarized light. Field width: 5mm. **B:** Same as A,

showing granular chalcopyrite (Cpy) and pyrite (Py) with pitted surface under reflected light. Field width: 5mm.....	32
Figure 3.17 – Textural features of carbonatites from Jacupiranga complex. A: Carbonatite with apatite (Ap) and disseminated pyrrhotite (Po) in plane polarized light. Field width: 5mm. B: Texture suggestive of carbonate-sulphide immiscibility showing pyrrhotite (Po) and chalcopyrite (Cpy), note the blob-like aspect of the pyrrhotite near the lower-right corner. Reflected light. Field width: 5mm. C: Carbonatite with microgranular aggregates of pyrite (Py), forming concentric circular or amoeboidal lines. Ilm=ilmenite. Reflected light. Field width: 3.5mm.....	33
Figure 3.18 – Textural features of jacupirangites from Jacupiranga complex. A: Jacupirangite showing clinopyroxene (Cpx) with magnetite (Mgt) and interstitial chalcopyrite (Cpy). Cross polarized light. Field width: 5mm. B: Same as "A", in reflected light. C: Jacupirangite showing nepheline (Ne) with symplectic texture, titanite (Ttn) and clinopyroxene (Cpx). Plane polarized light. Field width: 5mm. D: Same as "C", in cross polarized light. Field width: 5mm.....	34
Figure 3.19 –Classification of sulphides according to Cu-S-Fe in atomic proportions.....	39
Figure 3.20 – Compared major element variations in the studied sulphides for each complex.....	39
Figure 3.21. Sulphur isotope data for alkaline carbonatite complexes from APIP and Ponta Grossa Province. Red bars represent sulphide data and blue bars represent sulphate data.....	41
Figure 3.22. Sulphur isotope data for sulphides and sulphates from the APIP and Jacupiranga alkaline carbonatite complexes, by host rock type and complex.....	43
Figure 3.23. Sulphur isotope data for samples with evidence of degassing, showing different values from core to rim. Note that both the variation in single grains and the comparison between different rock types indicate increasing values of $\delta^{34}\text{S}$ with progressive degassing.....	45
Figure 3.24. Sulphur isotope data for sulphides from the studied alkaline carbonatitic complexes. Black solid horizontal bar: magmatic sulphide; Unfilled horizontal bar: sulphide from fenites.....	47
Figure 3.25. Sulphur isotope composition for sulphide and sulphate in the same sample.....	47
Figure 3.26. Modelling of sulphide-sulphate fractionation (Miyoshi et al., 1984) for the studied samples.....	48
Figure 3.27. Sulphur isotope data from alkaline carbonatite complexes in the World. APIP results (this work) are shown as vertical bars in the top section of the figure – blue and red bars represent barite and sulphides, respectively. The horizontal bars (solid colors = sulphides, unfilled bars = barite) in the bottom section represent other worldwide complexes, in order of increasing age from top to bottom: Bearpaw Mountain (Mitchell & Krouse 1975; ~48Ma - Duke, 2009), Magnet Cove (Mitchell & Krouse, 1975; 99Ma - Wooley & Kjarsgaard, 2008), Oka (Mitchell & Krouse 1975; 117Ma - Wooley & Kjarsgaard, 2008), Tuva (118Ma, Nikiforov et al. 2006), Jacupiranga (this work; 131Ma - Wooley & Kjarsgaard, 2008 #), Kola Province (Mitchell & Krouse 1975, Shin & Lee 2007; ~250-340Ma - Downes et al 2005), Swartbooisdrif (Druppel 2006; 750Ma - Wooley & Kjarsgaard, 2008), Mountain Pass (barite data only) (Mitchell & Krouse 1975; 1.4Ga - Wooley & Kjarsgaard, 2008), Superior Province (Farrel et al. 2010; 1,897 Ma to 1,093 Ma Farrel et al. 2010), Phalaborwa (Mitchell & Krouse 1975; 2.02Ga - Wooley & Kjarsgaard, 2008).....	50

Figure 3.28. Correlation of sulphur isotope composition of worldwide carbonatites with the respective ages. Note the log scale of the age axis. Data sources as in figure 3.27.....51

Índice de Tabelas

Tabela 2.01 – Limites de detecção para cada elemento, nas análises de sulfeto.....	6
Tabela 2.02 – Limites de detecção para cada elemento, nas análises de sulfato.....	6
Tabela 2.03 – Parâmetros de configuração do espectrômetro para análises <i>in situ</i>	12
Table 3.01 – Representative $\delta^{34}\text{S}$ ‰ results.....	36
Table 3.02 – Representative and average chemical compositions of the studied s sulphides.....	37
Table 3.03 – Representative compositions of the studied sulphates.....	38
Table 3.04 – Sulphur isotope data for the samples that present differences between rim and core.....	46

CAPÍTULO 1

Introdução

Processos como cristalização fracionada, imiscibilidade de líquidos, mistura de magmas e desgaseificação vem sendo estudados pelo Grupo de Pesquisa em Rochas Alcalinas e Mineralizações Associadas, da Universidade de Brasília e Universidade Federal de Goiás. Esta dissertação se insere nesse contexto trazendo dados de isótopos estáveis que colaboram na elucidação da gênese, evolução e mecanismos de diferenciação em Complexos Alcalinos da Província Ígnea do Alto Paranaíba (APIP) e do Complexo de Jacupiranga, na Província Ponta Grossa.

Diversos estudos geoquímicos, mineralógicos, de isótopos estáveis (principalmente C, O) e radiogênicos (Sr, Nd, Pb, além dos sistemas Re-Os e Lu-Hf) tem sido realizados na APIP e outras províncias alcalinas da borda da Bacia do Paraná (e.g. Gibson *et al.*, 1995b, Buzzi *et al.*, 1995, Comin-Chiaromonti e Gomes, 1996, 2005, Carlson *et al.*, 2007, Cordeiro *et al.*, 2011). Entretanto, embora as rochas dos complexos carbonatíticos da APIP, em particular as das séries foscorítica e carbonatítica, frequentemente contenham sulfetos (pirita, pirrotita, calcopirita, bornita) e sulfatos (principalmente barita), elas ainda não haviam sido estudadas do ponto de vista de isótopos estáveis de S.

Esta técnica tem sido aplicada a problemas petrológicos e metalogenéticos em complexos carbonatíticos como, por exemplo, Swartbooisdrif, Namibia (Drüppel *et al.* 2006), e Magnet Cove, Bearpaw e Mountain Pass, EUA (Mitchell e Krouse, 1975). Dentre as principais aplicações, destacam-se:

- Determinação da origem magmática ou hidrotermal do enxofre responsável pela formação de sulfetos e sulfatos em carbonatitos e rochas associadas (Nikiforov *et al.* 2006)
- Determinação da variação isotópica com temperatura, fugacidade de oxigênio e estado de diferenciação do magma (Drüppel *et al.* 2006).
- Monitoramento de processos tardios como fenitização e mineralizações (Drüppel *et al.* 2006).
- Desgaseificação de espécies voláteis como SO₂ e H₂S a partir de magmas (Zheng, 1990).

Na APIP, esta dissertação constitui o primeiro estudo de isótopos de S. O trabalho aborda a composição isotópica tanto de sulfetos quanto de sulfatos presentes em diversos litotipos dos complexos alcalino-carbonatíticos da província e incluiu, além das análises isotópicas, a obtenção de dados petrográficos, imagens de microscopia eletrônica, análise de química mineral e geoquímica de rocha total. Os resultados permitiram estabelecer diferenças entre complexos e dentro de um mesmo sistema, as quais podem estar relacionadas a processos de diferenciação, como cristalização fracionada e desgaseificação. Resultados analíticos representativos são apresentados no capítulo 3 e as tabelas com os resultados completos são apresentadas ao final do trabalho, como anexos.

A Província Ígnea do Alto Paranaíba, oeste de Minas Gerais e sul de Goiás, resulta de intenso magmatismo alcalino que gerou corpos intrusivos (diques, condutos, diatremas e complexos plutônicos) e extrusivos (lavas e piroclásticas) de afinidade kamafugítica (Leonardos *et al.*, 1991, Almeida e Svisero, 1991, Gibson *et al.*, 1995b, Carlson *et al.*, 1996, 2007, Brod *et al.*, 2000, 2004, Comin-Chiaromonti e Gomes, 2005). É uma das maiores províncias ultramaficas-ultrapotássicas mundiais (Gibson *et al.* 1995a,b), e uma das poucas associações kamafugíticas-carbonatíticas conhecidas (Brod *et al.*, 2000). Sonoki & Garda (1988) e Gibson *et al.* (1995b) fornecem idades radiométricas entre 80 e 90 Ma para a Província. Os complexos carbonatíticos da APIP (Catalão I, II, Serra Negra, Salitre I, II, III, Araxá, Tapira) são intrusões multifásicas formadas por rochas das séries bebedourítica, carbonatítica e foscorítica.

Catalão I, situado 20 km a NE da cidade de Catalão, é aproximadamente circular, com 6 km na direção N-S e 5,5 km E-W, encaixado em rochas metassedimentares do Grupo Araxá. Consiste de dunitos, bebedouritos, carbonatitos, foscoritos e nelsonitos, além de flogopititos metassomáticos, e abriga importantes depósitos de P, Nb, terras raras, Ti e vermiculita (Carvalho & Bressan, 1997, Brod *et al* 2004, Ribeiro, 2008).

Catalão II, cerca de 10 km a NNW de Catalão I, intrude rochas do Grupo Araxá, formando um pequeno alto topográfico irregular, alongado na direção NE-SW e com margens sinuosas, sugerindo a existência de intrusões múltiplas. Machado Junior (1992) descreve os tipos litológicos como piroxenitos, quartzo sienitos, feldspato alcalino sienitos, calcita carbonatitos, silico-carbonatitos, dolomita carbonatitos e lamprófiros, além de flogopititos metassomáticos. Além destes litotipos,

Palmieri *et al.* (2009) e Jácomo *et al* (2010) reportam a ocorrência de nelsonitos na porção sul do Complexo.

Serra Negra, a leste da cidade de Patrocínio, é o maior complexo carbonatítico da APIP, com 65 km². Intrude quartzitos do Grupo Canastra, formando uma estrutura dômica muito pronunciada. É composto por calcita carbonatito, dolomita carbonatito, foscorito, bebedourito, dunito e peridotito (Brod *et al.* 2004, Grasso *et al.*, 2009).

Salitre, imediatamente a sul do complexo Serra Negra, forma com este um sistema de intrusões coalescentes (Mariano & Marchetto, 1991), e consiste de 3 intrusões distintas. Salitre I, com 35 km², é composto por bebedourito, tinguaito, traquito, fenito, apatita carbonatito, calcita carbonatito, dolomita carbonatito e foscorito (Barbosa *et al.* 2004, 2008, 2009). Salitre II, com 2,5 km², situado entre Serra Negra e Salitre I, contém principalmente rochas ultramáficas (dunito, perovskitito, bebdourito, localmente cortados por diques e veios carbonatíticos). Salitre III é um pequeno corpo a sul de Salitre I, essencialmente formado por piroxenitos, com foscoritos subordinados (Brod *et al* 2004).

Araxá (Barreiro) é um complexo relativamente pequeno (15km²), circular, localizado a cerca de 6 km a sul da cidade de Araxá, composto por carbonatitos, foscoritos, bebedouritos, dunitos, lamprófiros (flogopita-picrítos) e um grande volume de flogopítitos derivados do metassomatismo sobre as rochas ultramáficas (Issa Filho *et al.*, 1984, Traversa *et al.*, 2001). A intrusão gerou uma estrutura dômica nos xistos e quartzitos do Grupo Ibiá (Seer, 1999).

Tapira, 30 km a SE da cidade de Araxá, é aproximadamente elíptico, com 35km², composto principalmente por bebedourito, com carbonatito e sienito subordinados e raros melilitolito e dunito, todos cortados por diques ultramáficos de afinidade kamafugítica (Brod *et al*, 2000, 2003).

A Província de Ponta Grossa, borda leste da bacia do Paraná, é dominada por rochas alcalinas sódicas – Ne-sienito, malignito, melteigito, ijolito, fonolito, carbonatito, lamprófiro, pulaskito, dunito, piroxenito, urtito, ankaratrito, gábro alcalino, sienogábro, sienodiorito, sienito, fonolito peralcalino, olivina gábro alcalino, sienodiorito, essexito, basanito, fonotefrito, shonkinito e traquito (Morbidelli *et al.* 1995). A província é composta por estruturas plutônicas denominadas Banhadão, Itapirapuã, Jacupiranga, Juquiá e Tunas, pipes and plugs – Barra do Ponta Grossa, Barra do Teixeira, Cerro Azul, Mato Preto, Morro do Chapéu e Sete Quedas (Ruberti *et al.* 2005).

Jacupiranga, o único complexo da Província de Ponta Grossa estudado neste trabalho, está localizado cerca de 10km a oeste da cidade de Jacupiranga e imediatamente a norte da cidade de Cajati no estado de São Paulo. O complexo intrudiu o grupo Açungui (Ruberti *et al.* 2005) e tem um formato oval (aproximadamente 65km²) com um pequeno núcleo alongado de carbonatito (Morro da Mina) que intrudiu jacupiranguitos. As rochas que compõem o complexo são piroxenitos-jacupiranguitos, peridotitos serpentinizados, ijolitos, nefelina-sienitos, carbonatitos, essexitos, monchiquitos e tinguaítos (Gomes *et al.* 1990).

CAPÍTULO 2

Métodos

As principais ferramentas aplicadas no projeto incluem petrografia, química mineral e análise isotópica de sulfetos e sulfatos em rochas das séries carbonatítica, foscorítica e bebedourítica, na APIP, e carbonatitos e jacupiranguitos, em Jacupiranga.

As amostras foram selecionadas a partir de critérios texturais e mineralógicos conhecidos de estudos anteriores do Grupo. Parte das amostras já vinha sendo estudada por outros métodos e outra parte foi coletada especificamente para este projeto. Sempre que possível procurou-se obter amostras que contivessem ao mesmo tempo sulfetos e sulfatos. Devido ao processo de intemperismo que facilmente atinge essas rochas, todas as amostras são testemunhos de sondagem ou amostras de afloramentos frescos no interior das minas de fosfato, cedidas pela empresas de mineração Fosfértil (Catalão I, Serra Negra, Salitre), Anglo American (Catalão II), e Bunge (Tapira e Araxá).

Foram confeccionadas lâminas delgadas polidas, parte no laboratório de laminação da Universidade de Brasília – UnB e parte em laboratório externo à universidade. As amostras para as outras técnicas analíticas foram selecionadas a partir da descrição petrográfica dessas lâminas.

A composição isotópica de enxofre foi determinada em LA-MC-ICP-MS (Laser Ablation-Multi Collector-Inductively Coupled Plasma Mass Spectrometer) no Laboratório de Geocronologia do IG/UnB, em grão individuais de sulfetos e sulfatos.

A composição química de fases minerais foi determinada por microssonda eletrônica JEOL JXA-8230, em modo WDS, no Laboratório de Microssonda Eletrônica do IG/UnB.

Análises em Microssonda Eletrônica

Preparação de amostras

Os sulfetos e sulfatos foram separados manualmente com o auxílio de alicate e/ou micro-retífica com disco diamantado (raio de aproximadamente 1cm) e montados em resina com apenas um grão em cada seção. Várias montagens foram acopladas em uma seção polida que foi posteriormente limpa em ultrassom e metalizada com carbono para análise em microssonda eletrônica JEOL JXA-8230.

Algumas análises foram realizadas em lâminas delgadas polidas também metalizadas com carbono. O bom polimento é extremamente importante na análise, para evitar variações dos efeitos de absorção.

Procedimentos analíticos

Os sulfatos foram primeiramente investigados em modo de dispersão por energia (EDS - energy-dispersive spectroscopy) e observados em imagens de elétrons retro-espalhados (BSE - back-scattered electrons). Posteriormente, a análise quantitativa dos sulfetos e sulfatos foi realizada em modo de dispersão por comprimento de onda (WDS - wavelength-dispersive spectrometry).

O componente-chave do EDS é um detector semicondutor que é um contador proporcional. Este sistema é normalmente utilizado para análises qualitativas, e também permite a execução de análises semi-quantitativas rápidas (fração de segundo) e opera de 0 eV a 10 keV (informações internas do laboratório).

No sistema de Dispersão por Comprimento de Onda (WDS)- a amostra, o cristal de difração e o detector tipo contador proporcional estão contidos em uma mesma circunferência. O princípio de funcionamento do sistema segue a lei de difração de Bragg ($n\lambda=2d \cdot \sin\theta$), onde o sistema WDS é mais lento, com resolução em torno de 5 eV e consegue diferenciar a sobreposição de picos com diferença de energia menor do que 150 eV, o que não é possível no sistema EDS.

As amostras de sulfeto foram analisadas a 20 kV, os limites de detecção são apresentados na tabela 2.01.

Tabela 2.01 – Limites de detecção para cada elemento, nas análises de sulfeto.

As	Pb	Fe	Co	Ag	S	Se	Cu	Ni	Pt	Pd	Zn
38	96	40	45	43	18	138	50	40	52	21	42

As amostras de sulfato também foram analisadas a 20kV e os limites de detecção são apresentados na tabela 2.02.

Tabela 2.02 – Limites de detecção para cada elemento, nas análises de sulfato.

Mg	Si	Al	Ba	P	Ca	Cr	S	Fe	Se	Sr	Pb	Mn
29	92	59	563	149	93	204	104	232	1933	137	168	94

Isótopos de Enxofre

Revisão bibliográfica

O estudo de isótopos de S pode auxiliar na identificação da gênese e evolução das rochas estudadas. O fracionamento de enxofre pode ser causado por diversos processos e varia de acordo com a temperatura, fO_2 , balanço de massa, condições de óxido-redução do ambiente, diferenciação magmática, além de processos superficiais e interações com bactérias redutoras. Alguns estudos anteriores (Nikiforov *et al.* 2006, Drüppel *et al.* 2006, Farrel *et al.* 2010) abordam os controles da variação isotópica de S em função da temperatura, comparando diferentes carbonatitos em um mesmo complexo alcalino, ou distintos complexos entre si, bem como os efeitos da desgasificação de SO_2 e H_2S e da fenitização sobre a composição isotópica original. Esses estudos demonstram a importância dos isótopos estáveis de S no estudo de complexos carbonáticos, mas a técnica não havia ainda sido aplicada aos complexos da Província Ígnea do Alto Paranaíba, o que motivou o presente trabalho.

As variações na composição isotópica de sulfetos, sulfatos ou espécies de S aquoso resultam do fracionamento entre as fases minerais envolvidas, o qual é controlado fundamentalmente pela temperatura ou por reações de oxidação e redução (Seal, 2006):

- em alta temperatura (sistemas ígneos) as distintas fases minerais tendem a estar em equilíbrio isotópico,
- em temperatura intermediária (sistemas hidrotermais),
- em baixa temperatura (diagênese sedimentar) o fracionamento isotópico tende a prevalecer.

Além disso, processos superficiais (intempéricos) também geram fracionamento isotópico, que aparece localmente em registros geológicos (Seal, 2006).

Seal (2006) detalha o ciclo geoquímico do Enxofre e indica duas épocas onde a variabilidade isotópica de S é de grande importância nos processos superficiais.

Antes de 2,4 Ga, o registro sedimentar revela variação limitada de $\delta^{34}S$ entre sulfetos e sulfatos e ampla variação de $\delta^{33}S$, indicando que antes de 2,4 Ga o principal fracionamento de S era independente da massa. A partir de 2,4 Ga, com o aparecimento de uma atmosfera rica em oxigênio e

o consequente diminuição das reações fotoquímicas que geram o fracionamento independente da massa, a variação se inverte e começa a haver variação ampla de $\delta^{34}\text{S}$ e limitada de $\delta^{33}\text{S}$.

Há cerca de 0,7 Ga, outra grande mudança na variabilidade de $\delta^{34}\text{S}$ de sulfetos e sulfatos sedimentares ocorre, indicada por uma maior gama de composições, que novamente foi interpretada em termos de aumento de concentrações atmosféricas de oxigênio.

O registro isotópico das bactérias redutoras de sulfato pode ser encontrado em muitos pontos do ciclo do enxofre, desde sulfetos e sulfatos sedimentares, até camadas de carvão, depósitos hidrotermais de assoalho oceânico, depósitos continentais do tipo Mississipi Valey formados a partir de bacias de salmoura, e dos magmas de todas as composições que tiveram interação com rochas crustais (Seal, 2006).

Os estudos de isótopos estáveis de S podem elucidar aspectos da gênese e evolução de magmas alcalinos e carbonatitos, conforme os exemplos abaixo:

Zheng definiu que $\delta^{34}\text{S}$ de uma rocha ígnea pode se afastar do magma original simplesmente devido à destilação Rayleigh durante a desgaseificação de SO_2 e/ou H_2S , ou devido ao fluxo seletivo de enxofre através do fracionamento de equilíbrio por troca isotópica entre o sulfato e sulfeto na temperatura de solidificação do magma. A intensidade da mudança na composição isotópica de S depende da $f\text{O}_2$, do balanço de massa e da medida em que o sistema se abre.

O processo de desgaseificação Rayleigh pode ser identificado pela correlação de $\delta^{34}\text{S}$ e a concentração total de enxofre. O fracionamento isotópico e solubilidade de enxofre no magma está relacionado com a $f\text{O}_2$ que controla as razões sulfato/sulfeto e $\text{Fe}^{3+}/\text{Fe}^{2+}$ (Zheng, 1990).

Nikiforov *et al.* (2006) determinaram $\delta^{34}\text{S}$ em: fenocristais de pirita, de siderita e ankerita-calcita carbonatito primários; barita primária do siderita carbonatito; pseudomorfos de sulfatos epigenéticos hidrotermais (baritocelestina e celestina) sobre barita primária; e metacristais de pirita em rochas encaixantes do complexo carbonatítico de Tuva Central e detectaram desvios de $\delta^{34}\text{S}$ em relação a composição primária que podem ser explicados pela remoção isotópica de enxofre leve sob a forma de SO_2 , como resultado de uma intensa desgaseificação sob alta fugacidade de oxigênio. Os sulfatos hidrotermais apresentaram valores elevados de $\delta^{34}\text{S}$.

Mitchell e Krouse (1975) estudaram distintos complexos carbonatíticos e obtiveram resultados diferentes para cada um deles, relacionando a variação com os parâmetros T, $f\text{O}_2$ e pH durante a

formação. Os resultados indicaram que com a diminuição da T e aumento de fO_2 , a média de $\delta^{34}S$ fica mais negativa em relação à média do magma original.

Drüppel et al. (2006) determinaram a variação isotópica com temperatura, fugacidade de oxigênio e estado de diferenciação do magma e monitoraram processos tardios como fenitização e mineralizações em ferrocarbonatitos de Swartbooisdrif, Namíbia.

Preparação de amostras

Neste trabalho, as determinações da composição isotópica foram realizadas sobre as mesmas amostras analisadas em microssonda eletrônica, isto é, grãos separados manualmente, resinados e polidos. O equipamento utilizado foi um MC-ICP-MS Neptune (Thermo Finnigan) com laser New Wave UP213 Nd:YAG acoplado. Os padrões de referência para análise *in situ* de sulfetos já estavam prontos no laboratório de geocronologia, enquanto que os padrões de sulfato foram colocados sob pressão de 10 ton por 5 minutos usando uma prensa hidráulica PerkinElmer para confeccionar comprimidos.

Laser ablation multiple-collector inductively coupled plasma mass spectrometry (LA-MC-ICP-MS)

O MC-ICP-MS é um espectrômetro de massa capaz de medir diversas massas ao mesmo tempo. É composto por 3 módulos: um módulo ICP (inductively coupled plasma), um módulo ESA (electrostatic analyser) e um módulo multicoletor (Figura 2.01). As especificações e descrição do funcionamento do equipamento, apresentadas abaixo, foram retiradas do Manual Thermo Finnigan Neptune.

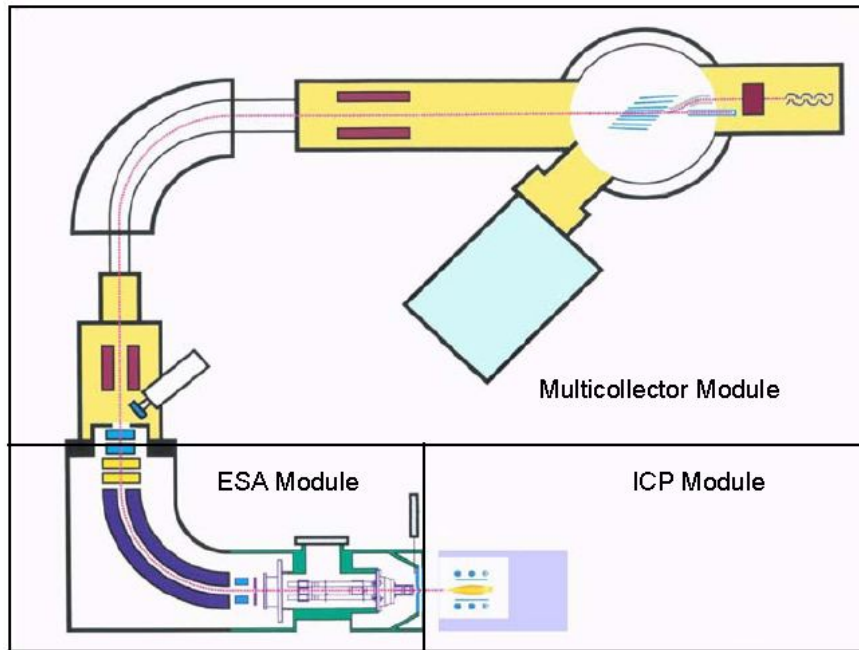


Figura 2.01 - Desenho esquemático do sistema MC-ICP-MS (Manual Thermo Finnigan 2003)

Módulo ICP

Este módulo está relacionado à geração de plasma. Ele inclui controladores de fluxo para o fornecimento de argônio (gás carreador da amostra), o gerador RF que liga o plasma, o estágio XYZ da posição da tocha, e, finalmente, a câmara de spray e a tocha em si.

A amostra (gás ou líquido) é alimentada continuamente na nebulização (sistema de admissão), onde um aerosol contendo argônio e a amostra é gerado. Este aerossol é guiado para a câmara de pulverização, que remove as gotas maiores. A mistura é então refinada em aerosol, direcionada para o injetor da tocha do plasma, injetada no centro do plasma e instantaneamente dissolvida e ionizada.

Módulo ESA

Este módulo é responsável por relançar e acelerar íons. Ele inclui a interface de plasma, sistema de lentes de transferência e o analisador eletrostático (ESA).

Os íons (assim como elétrons, prótons e todos os tipos de moléculas de gás) entram no espectrômetro de massa através dos orifícios na ponta do cone de amostragem. O fluxo de gás principal vai para a bomba de interface, enquanto os íons vão para o cone *skimmer*. Os íons são

extraídos do fluxo de gás através da lente de extração e seguem no sistema pela lente de transferência.

A partir do sistema de lentes de transferência, o feixe de íons entra no analisador eletrostático (ESA), que focaliza os íons. Íons com energias diferentes estão focalizados em pontos ligeiramente diferentes ao longo da imagem. Pouco antes da imagem intermediária, os íons são acelerados para o final de energia do feixe de íons a 10 keV.

Módulo Multicoletor

A seção final do instrumento abrange o ímã, o zoom óptico, o multicoletor e o sistema amplificador de corrente. A separação de massa e a detecção de íons ocorrem neste módulo.

O Netuno é equipado com um conjunto de lentes de zoom. Usando as duas lentes de quadrupolo posicionadas antes e depois do ímã, a dispersão de massa pode ser alterada em cerca de $\pm 5\%$. O zoom óptico dinâmico pode ser utilizado para compensar dispersões de massa ligeiramente diferentes para os diferentes elementos.

O Multicoletor é equipado com nove copos de medida Faraday (contagem em V) mais oito contadores de íons (contagem em cps). Os detectores são movidos a motor e podem ser posicionados precisamente ao longo do plano focal das lentes de íons.

A extração da amostra para análise foi realizada com laser acoplado. O laser utiliza He como gás carreador das partículas liberadas *in situ* pelo laser e se mistura com o Ar antes de entrar no módulo ICP, substituindo o nebulizador que somente é usado para análise de soluções.

Procedimentos analíticos

O equipamento foi calibrado, primeiramente, com soluções padrão medindo a massa ^{32}S no faraday L2, a massa ^{33}S no copo central e a massa ^{34}S no faraday H1 levando em consideração as interferências possíveis (^{16}O , ^{17}O , ^{18}O , ^{15}N , ^1H). Com a extração da amostra por laser essas interferências diminuem, mas ainda é feita mais uma calibração no laser para melhorar a intensidade do sinal e garantir a reprodução do padrão para análises *in situ*. As amostras são lidas em grupo de quatro leituras, para um branco e um padrão. Os padrões utilizados para calibração e correção dos

dados foram NBS-123, IAEA-S1, IAEA-S2, calcopirita (padrão interno) e pirita (padrão interno) para os sulfetos, e NBS-127 e IAEA-S3 para os sulfatos.

Os parâmetros utilizados para o laser foram 10 Hz de freqüência, 100 µm de tamanho do feixe e 53% da energia do laser. Já os parâmetros de operação do espectrômetro podem variar a cada dia de análise. Os parâmetros aproximados são apresentados na tabela 2.03.

As análises foram realizadas em modo raster (linha de análise), que é mais utilizado do que o modo ponto, para obter um material de análise mais homogêneo em relação ao tempo (Craddock *et al.* 2008).

Tabela 2.03 – Parâmetros de configuração do espectrômetro para análises *in situ*.

Cool Gas	15
Aux Gas	0,7
Sample Gas	0,998
Add Gas 1	0
Add Gas 2	0,44
Posição X	0,810
Posição Y	0,970
Posição Z	0,320

Tratamento dos dados

Os resultados são expressos na notação comum delta per mil ($\delta\text{\textperthousand}$), que representa uma comparação com o padrão de referência Vienna Canyon Diablo Troilite (V-CDT) que é calculado da seguinte maneira:

$$\delta = \left(\frac{R_{\text{amostra}} - R_{\text{padrão}}}{R_{\text{padrão}}} \right) \times 10^3$$

Onde R é a razão isotópica ($^{34}\text{S}/^{32}\text{S}$) medida para a amostra e para o padrão que é o valor de referência. A precisão analítica foi em torno de 0,1‰ a 0,5‰.

CAPÍTULO 3

Sulfur isotopes from alkaline carbonatite complexes along the borders of the Paraná Basin - Goiás, Minas Gerais and São Paulo States, Brazil

C.S. Gomide ^a, J.A. Brod ^b, T.C. Junqueira-Brod ^b, B. Buhn ^a, E.S.R. Barbosa ^b, P.F.O. Cordeiro ^a, M. Palmieri ^c, C.B. Grasso ^d, M.G. Torres ^e

^a Instituto de Geociências, Campus Universitário Darcy Ribeiro, Universidade de Brasília (UnB), CEP 70910-900, Brasília, DF – Brazil.

^b Instituto de Estudos Sócio-Ambientais, Universidade Federal de Goiás (UFG), Caixa Postal 131, CEP 74001-970, Goiânia, GO – Brazil.

^c Anglo American.

^d Fosfertil.

^e Universidade Católica de Brasília.

Abstract

This work presents petrographic, chemical, and sulphur isotope data in alkaline-carbonatite complexes of the Alto Paranaiba Igneous Province (APIP) and in the Jacupiranga complex, from the Ponta Grossa Province. The rocks from carbonatite complexes, especially those of the carbonatite series, often contain sulphides (pyrite, pyrrhotite, chalcopyrite, galena, bornite, pentlandite) and sulphates (mainly barite). Therefore, sulphur is an important element for research in the petrogenesis of these rocks. This work presents the first sulphur isotope data from APIP and Ponta Grossa complexes.

The studied samples show mesoscopic and microscopic quench textures, such as bladed carbonate and sulphide crystals, with interstitial microgranular aggregates of carbonate, barite and sulphides. These are interpreted as the result of rapid crystallization during degassing of a supercooled carbonatite magma. The CO₂ degassing at APIP complexes was studied in previous works from Research Group in Alkaline Rocks and Associated Mineralizations and this work adds degassing of sulphur gaseous phases (H₂S and/or SO₂) to that picture. The sulphur isotope results in sulphides from samples showing evidence of degassing vary from core to rim, with the latter showing higher (less negative) $\delta^{34}\text{S}$, compared with the former, indicating that degassing took place in an oxidizing environment.

Isotopic data indicates that as magma differentiation progresses it consumes particularly heavier isotopes into the solid phases, leaving a residual magma/fluid enriched in ³²S. On the other hand, sulphur loss by degassing under oxidizing conditions lead the residue to evolve toward higher $\delta^{34}\text{S}$.

Keywords: Carbonatite, sulphide, sulphate, APIP, Jacupiranga, sulphur isotope, degassing.

1. Introduction

The carbonatite complexes and alkaline rocks from the Alto Paranaíba Igneous Province (APIP) and from other alkaline provinces occurring at the borders of the Paraná Basin have been the subject of studies comprising geochemistry, mineralogy, and stable (mostly C, O) and radiogenic (Sr, Nd, Pb, Re-

Os, Lu-Hf) isotopes (e.g. Gibson *et al.*, 1995a, Comin-Chiaromonti & Gomes, 2005, Carlson *et al.*, 2007). Although many of the rocks in these complexes, particularly those belonging to the carbonatite and phoscorite petrogenetic series (e.g. Barbosa, 2009), contain sulphides and/or sulphates, they were not yet studied for sulphur isotopic composition.

This technique has been applied to assess petrological and metallogenetic problems in other carbonatite complexes, such as Swartbooisdrif, Namibia (Drüppel *et al.* 2006), and Magnet Cove, Bearpaw and Mountain Pass, in the USA (Mitchell & Krouse, 1975). Sulfur isotopes studies have been successful in determining the magmatic or hydrothermal origin of the sulphur (Nikiforov *et al.* 2006), assessing the variation of isotope composition with temperature, oxygen fugacity and differentiation stage of magma, as well as studying fenitization and mineralization processes (Drüppel *et al.* 2006) and degassing of SO₂ and H₂S from magmas (Zheng, 1990).

Mitchell & Krouse (1975) stated that each carbonatite appears to have its own mean sulphide or sulphate isotopic composition. Deines (1989) compiled the $\delta^{34}\text{S}$ composition of sulphides from carbonatites and found that it varied from -20‰ to +5‰ suggesting that some differences between carbonatite complexes may reflect S isotope heterogeneity in the mantle.

In this study we report the first S isotope data for carbonatites in Brazil. We discuss S stable isotope and petrographic data for various rock types and minerals in carbonatite complexes from the Alto Paranaíba Igneous Province (APIP) and for the Jacupiranga complex (Ponta Grossa Alkaline Province), with the aims of understanding the genesis and evolution of these complexes and comparing them with other complexes worldwide.

In various APIP complexes, C and O stable isotope data define a degassing trend for CO₂ (Junqueira-Brod *et al.* in preparation, Gomide *et al.*, 2008, Cordeiro *et al.*, 2011). However, these rocks may also degass sulphur, taking into account that they usually contain crystallized sulphides and/or sulphates, and that sulphur is an important volatile constituent in alkaline magmas associated with CO₂ and halogens (Bailey & Hampton, 1990). Furthermore, Zheng (1990) interpreted the significant differences in the sulphur isotope composition of some igneous rocks relatively to meteorites and primary mantle as the result of Rayleigh outgassing and selective flux process. In this work we propose that the degassing process in alkaline carbonatites magmas drives sulphur isotope ratios to positive values,

whereas fractionation from less evolved (bebedourites, in the APIP, and jacupiranguites, in the Jacupiranga complex) to more evolved rocks (carbonatites) drives these ratios to negative values.

2. Geological setting

A voluminous Cretaceous alkaline magmatism occurred in central and southern Brazil, and in eastern Paraguay (Comin-Chiaromonti and Gomes, 1996, 2005). Almeida (1983) argued that alkaline rocks spreading over a large area of the South American Platform south of the 15°S latitude are divided in 3 groups: those located at the borders of the Paraná basin, those in the east coastal region and those in eastern Bolivia. That author adopted the concept of Alkaline Province to divide and describe geographic groups showing petrographic relations with each other and belonging to a particular age range. The Provinces were named as Poços de Caldas, Alto Paranaíba, Rio Verde-Iporá, Paraguai Oriental, Mariscal, Piratini, Santa Catarina, Ponta Grossa, Ipanema, Serra do Mar, Velasco and Candelária. In this work we study carbonatite complexes of the Alto Paranaíba and Ponta Grossa Provinces.

Gibson *et al.* (1995a) interpreted the Early-Cretaceous alkaline magmatism (approximately 130Ma) and the contemporaneous Paraná magmatism as related with the Tristan da Cunha mantle plume, whereas Gibson *et al.* (1995b, 1997) and Brod *et al.* (2005) correlated the Late-Cretaceous magmatism (about 85Ma) at the north and northeast borders of the Paraná Basin with the impact of the Trindade mantle plume (Gibson *et al.* 1995b) at the sub-continental lithosphere of central Brazil. Thompson *et al.* (1998) state that the shifted trajectory of the Trindade plume generated the Serra do Mar province, in SE Brazil.

Ernesto (2005) argued against the mantle plume model based on paleomagnetic data, stating that these provinces (including the Paraná flood basalts) were never placed above plumes. This reinforced the alternative model proposed by Ernesto *et al.* (2002) according to which these provinces were generated by thermal sources unrelated with material transfer from the lower mantle to the lithosphere.

Some of the alkaline provinces surrounding the Paraná Basin contain carbonatite complexes, occurring as massive cores (plugs, stocks) usually displaying oval to circular outlines in map view

(Gomes *et al.* 1990). Among these, the APIP complexes, and the Jacupiranga complex in the Ponta Grossa Province were the subject of this research (figure 3.01).

The Alto Paranaíba Igneous Province, located in southern Goiás and western Minas Gerais States, results from an intense, Late-Cretaceous alkaline magmatism that generated intrusive (dykes, conduits, diatremes, and carbonatitic complexes) and extrusive (lavas and pyroclastic rocks) bodies (Leonardos *et al.*, 1991, Gibson *et al.*, 1995b, Brod *et al.*, 2000, Comin-Chiaromonti & Gomes, 2005, Carlson *et al.*, 2007). It is one of the largest ultramafic-ultrapotassic provinces of the world (Gibson *et al.* 1995b). Kamafugite is by far the dominant rock-type in the province, forming one of the few known kamafugite-carbonatite associations (Brod *et al.*, 2000).

The APIP alkaline carbonatite complexes (Catalão I, II, Serra Negra, Salitre I, II, III, Araxá and Tapira) are relatively shallow (e.g. Santos and Clayton, 1995; Brod *et al.*, 2001, Ribeiro *et al.*, 2005), multi-stage intrusions formed by rocks derived from various (bebedourite, carbonatite, and phoscorite) petrogenetic series related to each other by fractional crystallization, liquid immiscibility and degassing (Brod *et al.*, 2004, Ribeiro, 2008, Cordeiro *et al.*, 2010, Barbosa, 2009).

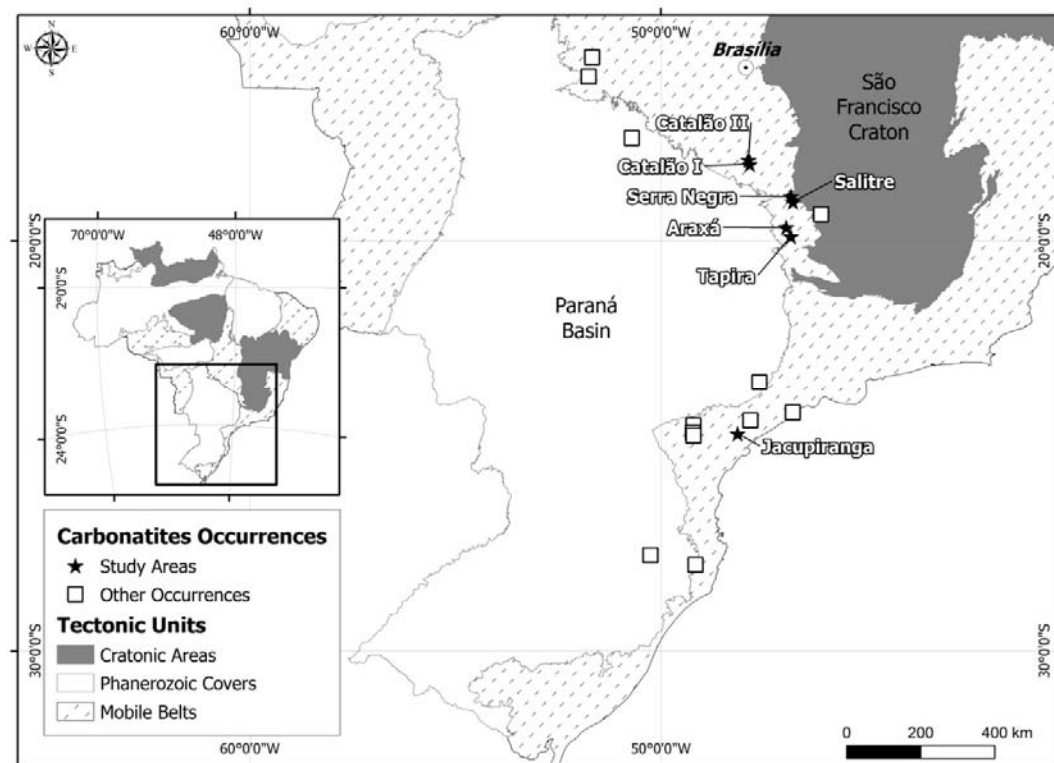


Figure 3.01 – Carbonatite occurrences surrounding the Paraná Basin. The carbonatite complexes studied in this work are shown as stars. Modified from Oliveira *et al.* (2004) and Wooley & Kjarsgaard (2008).

Catalão I, located 20km to the northeast of Catalão city, is a multi-phase intrusion composed of dunite, clinopyroxenite, bebedourite, carbonatite, phoscorite, nelsonite and metassomatic phlogopitites, and hosts important deposits of phosphate, niobium, rare earth elements, titanium and vermiculite (Carvalho & Bressan, 1997, Brod *et al.*, 2004, Ribeiro, 2008, Cordeiro *et al.*, 2011). The complex evolved from a phlogopite-picrite magma by several stages of fractional crystallization and liquid immiscibility (Ribeiro, 2008). Magnesiocarbonatite is by far the dominant carbonatite type in the complex. Sulphides occur towards the more evolved stages in the complex, and are typically present in some phoscorites and in many nelsonites and carbonatites. Sulphate (barite) occurs at an even later stage, both in magmatic carbonatite and in late-stage, post magmatic veins.

Catalão II, nearly 10 km NNW from Catalão I, is an elongated (NE-SW) body with sinuous margins, suggesting the existence of multiple intrusions. Machado Junior (1992) describes pyroxenites, quartz syenites, alkali-feldspar syenites, calcite carbonatites, silico-carbonatites, dolomite carbonatites e lamprophyres, and metasomatic phlogopitites. Calciocarbonatites dominate over magnesiocarbonatites. Palmieri (2011) recognized at least two separate magmatic systems in the complex, one in the north, dominated by phoscorite and the other in the south, dominated by nelsonite. Sulphides and sulphates occur mainly in the southern (nelsonite) domain of the complex. Sulphides are common accessory phases both in nelsonites and in carbonatites. Sulphates occur in late-stage Ba-rich magnesiocarbonatites.

Serra Negra is located to the east of Patrocínio city, in western Minas Gerais and is the largest APIP carbonatite complex, with 65 km². It is dominantly composed of dunite, bebedourite, and carbonatite, with rare trachytes. Both calciocarbonatite and magnesiocarbonatite occur (Grasso *et al.* 2010). The complex intruded quartzites from Canastra Group and generated a very pronounced dome structure (Brod *et al.* 2004). Sulphides occur as accessory phases in carbonatites (especially magnesiocarbonatites).

Salitre consists of three bodies located to the south of the Serra Negra Complex, and compose with the latter a system of coalescing intrusions (Mariano & Marchetto, 1991). Salitre I, with 35 km², is composed of bebedourite, tinguaite, trachyte, fenite, apatite-carbonatite, calcite carbonatite and phoscorite. Salitre II, with 2.5 km², is located between Serra Negra and Salitre I, and contains mainly

ultramafic rocks (dunite, perovskitite, bebedourite, locally cut by carbonatitic dikes and veins). Salitre III is a small body to the south of Salitre I, formed by pyroxenites, with subordinated phoscorites (Brod *et al.* 2004, Barbosa, 2009). Both calciocarbonatite and magnesiocarbonatite occur in the complex. Sulphides are present in bebedourite, phoscorite and carbonatite, and sulphate occurs only in late-stage magnesiocarbonatite.

Araxá (also known as Barreiro) is a small (15 km^2) complex located approximately 6 km to the south of Araxá city. In many aspects, this complex is similar to Catalão I. It is composed of carbonatites, phoscorites and a large volume of phlogopites derived from the metasomatism of ultramafic rocks such as bebedourites and dunites (Issa Filho *et al.*, 1984, Traversa *et al.*, 2001). Magnesiocarbonatite is the dominant carbonatite type. The intrusion generated a domic structure in schists and quartzites of the Neoproterozoic Ibiá Group (Seer, 1999). Sulphide occurs as pyrite, chalcopyrite, sphalerite, galena and cobaltite in carbonatites, especially ferrocarbonatites, which are clearly subordinate to the previous carbonatite types (Traversa *et al.* 2001). Sulphate (barite) occurs in carbonatites. Samples containing both sulphide and sulphate were obtained from carbonatites and one sample from phoscorite.

Tapira, 30 km to the SE of Araxá city, is an approximately elliptical complex with 35 km^2 , composed mainly by bebedourite, with subordinate carbonatite and syenite and rare melilitolite and dunite, all cut by ultramafic dikes of kamafugite affinity (Brod, 1999, Brod *et al.*, 2000, Brod *et al.*, 2003). Calciocarbonatite dominates over magnesiocarbonatite

The Ponta Grossa Province is located at the eastern margin of the Paraná Basin. Unlike the APIP, this province is Early-Cretaceous in age, and dominated by sodic alkaline rocks – Ne-syenite, malignite, melteigite, ijolite, phonolite, carbonatite, lamprophyre, pulaskite, dunite, pyroxenite, urtite, ankaratite, alkali gabbro, syenogabbro, syenodiorite, syenite, peralkaline phonolite, alkali ol-gabbro, syenodiorite, essexite, basanite, phonotephrite, shonkinite and trachyte (Morbidelli *et al.* 1995). It comprises plutonic structures - Banhadao, Itapirapuã, Jacupiranga, Juquiá and Tunas, pipes and plugs – Barra do Ponta Grossa, Barra do Teixeira, Cerro Azul, Mato Preto, Morro do Chapeu and Sete Quedas (Ruberti *et al.* 2005).

Jacupiranga (also known as Cajati), the only complex from the Ponta Grossa Province studied here, is located ca. 10 km to the west of Jacupiranga city and northwards from the Cajati town, in São Paulo

State. It is emplaced into the Açuñui group (Ruberti *et al.* 2005) and has an oval-shape (about 65 km²) with a small elongated carbonatite core (Morro da Mina) that intruded into jacupiranguites. The main rock-types in the complex are pyroxenite-jacupirangite, serpentinized peridotite, ijolite, nepheline syenite, carbonatite, essexite, monchiquite, and tinguaite (Gomes *et al.* 1990). Both calciocarbonatite and magnesiocarbonatite are present in the complex. Sulphides are accessory phases in some carbonatites, and also occur, rarely, in jacupirangites.

3. Sample description

Catalão II

Samples from Catalão II include different types of carbonatites and nelsonites. The carbonatites (figure 3.02) vary from coarse grained to microcrystalline, and may contain various amounts of apatite. Phlogopite, tetra-ferriphlogopite, magnetite with ilmenite exsolution lamellae, and barite are common, pyrochlore is an accessory phase, and amphibole was found rarely. Pyrite, pyrrhotite and chalcopyrite are the sulphide phases. Pyrite is usually granular and euhedral, but often shows very irregular grain surfaces, probably resulting from recrystallization of microgranular aggregates (figure 3.02b). It is also found as veins or scattered grains. Chalcopyrite occurs as small anhedral grains. Pyrrhotite occurs restrictedly in the studied samples, as tabular grains or forming net texture. Barite is the only sulphate present, as fine grain aggregates or as a criptocrystalline mass together with carbonate. Barite is more abundant than sulphides in the carbonatites.

Carbonates in the Catalão II carbonatite samples have a cloudy aspect, marked by brownish irregular patches with a "dusty" aspect. Presumably this results from the quench precipitation of carbonate during oscillatory temperature behavior in heterogeneous regions created by CO₂ degassing in the magma chamber (Junqueira-Brod in preparation). Although carbonate is the dominant phase, barite, sulphides, and phlogopite may also be present in these criptocrystalline aggregates (figure 3.02c,d).

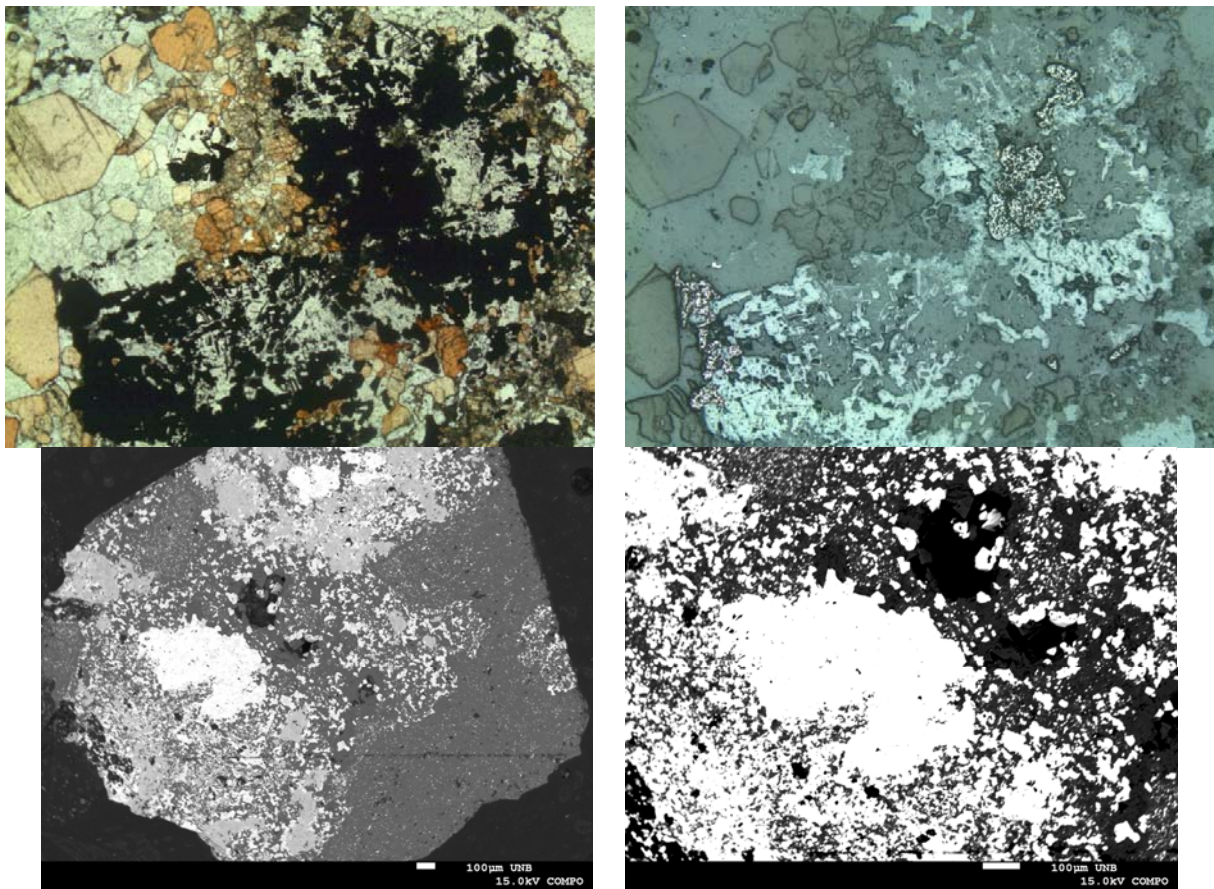
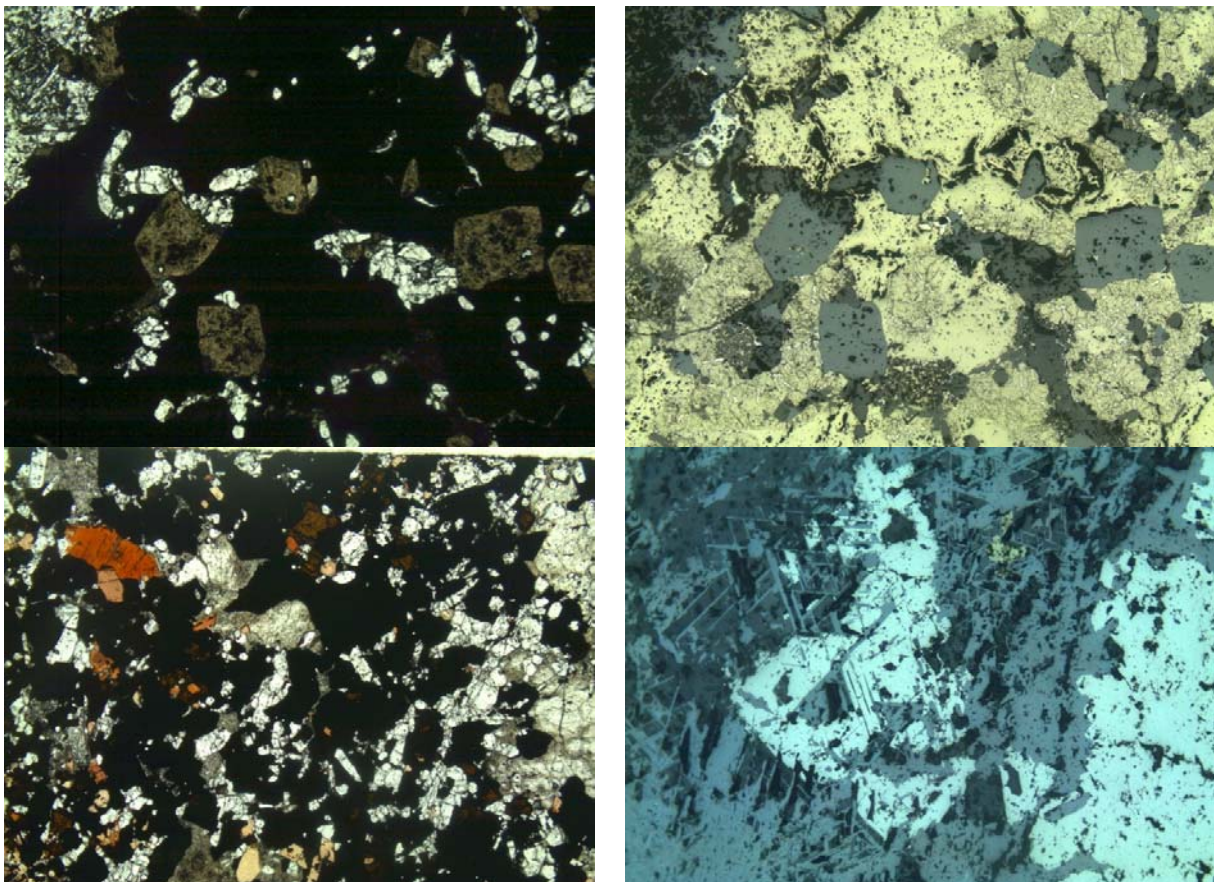


Figure 3.02 – Carbonatite from the Catalão II complex. A: phlogopite (phl), magnetite (mgt) and recrystallized pyrite (py). cbt=carbonate Field width: 5mm. Plane polarized light; B: Same as A in reflected light. C: Back-scattered image of a carbonate (cbt) + barite (brt) mass in carbonatite from the Catalão II complex. D: Higher magnification view of the back-scattered image in A

Nelsonites (figure 3.03) are fine to coarse-grained, composed of magnetite, apatite, phlogopite, carbonate, and variable amounts of pyrochlore. Sulphide is relatively abundant in these rocks. Pyrite occurs as euhedral grains, as veins, or as scattered crystals. It is often associated with magnetite and sometimes replaces this mineral (figure 3.03d), indicating a late-stage formation. Chalcopyrite may form concentrations about 1.5cm wide in some samples (figure 3.03b), and also occurs as very fine grain aggregates with a dusty appearance, associated with pyrite. Bornite is very rare, included in or intergrown with chalcopyrite Barite was not found in this rock-type.



*Figure 3.03 – Textural features of nelsonites from the Catalão II complex. **A:** Apatite (Ap) and pyrochlore (Pcl) in nelsonite, plane polarized light. Field width: 5mm. **B:** Same as A, in reflected light, showing chalcopyrite (Cpy) and subordinate pyrite (Py). Field width: 5mm. **C:** Phlogopite (Phl), apatite (Ap), pyrochlore (Pcl), carbonate (Cbt) and magnetite (Mgt) in nelsonite, plane polarized light. Field width: 5mm. **D:** Pyrite (Py) and rare chalcopyrite (Cpy) replacing magnetite; note that the earlier magnetite contained ilmenite (Ilm) exsolution lamellae that remained preserved upon dissolution and substitution of the magnetite grain, forming a trellis texture, reflected light. Field width: 1,5mm.*

Catalão I

The studied samples from Catalão I are carbonatites, phoscorites, nelsonites, magnetitites and fenites. The carbonatites (figure 3.04) are fine to coarse grained, and may contain various amounts of apatite, phlogopite, magnetite and barite, \pm tetra-ferriphlogopite, \pm perovskite, \pm pyrochlore. Common textural features are microgranular barite pockets, apatite with flow orientation, and aligned grains of magnetite. Sometimes magnetite contains ilmenite exsolution lamellae, and may develop a skeletal aspect if the host magnetite is dissolved or replaced. Some carbonatites display bladed carbonate and sulphide crystals (figure 3.04d,f) typical of rapid crystallization as described by Junqueira-Brod (in preparation). In these samples,

carbonates may also form granular (recrystallized) aggregates or diffuse masses like the ones described for Catalão II. Apatite prisms are often along the faces of bladed carbonate crystals.

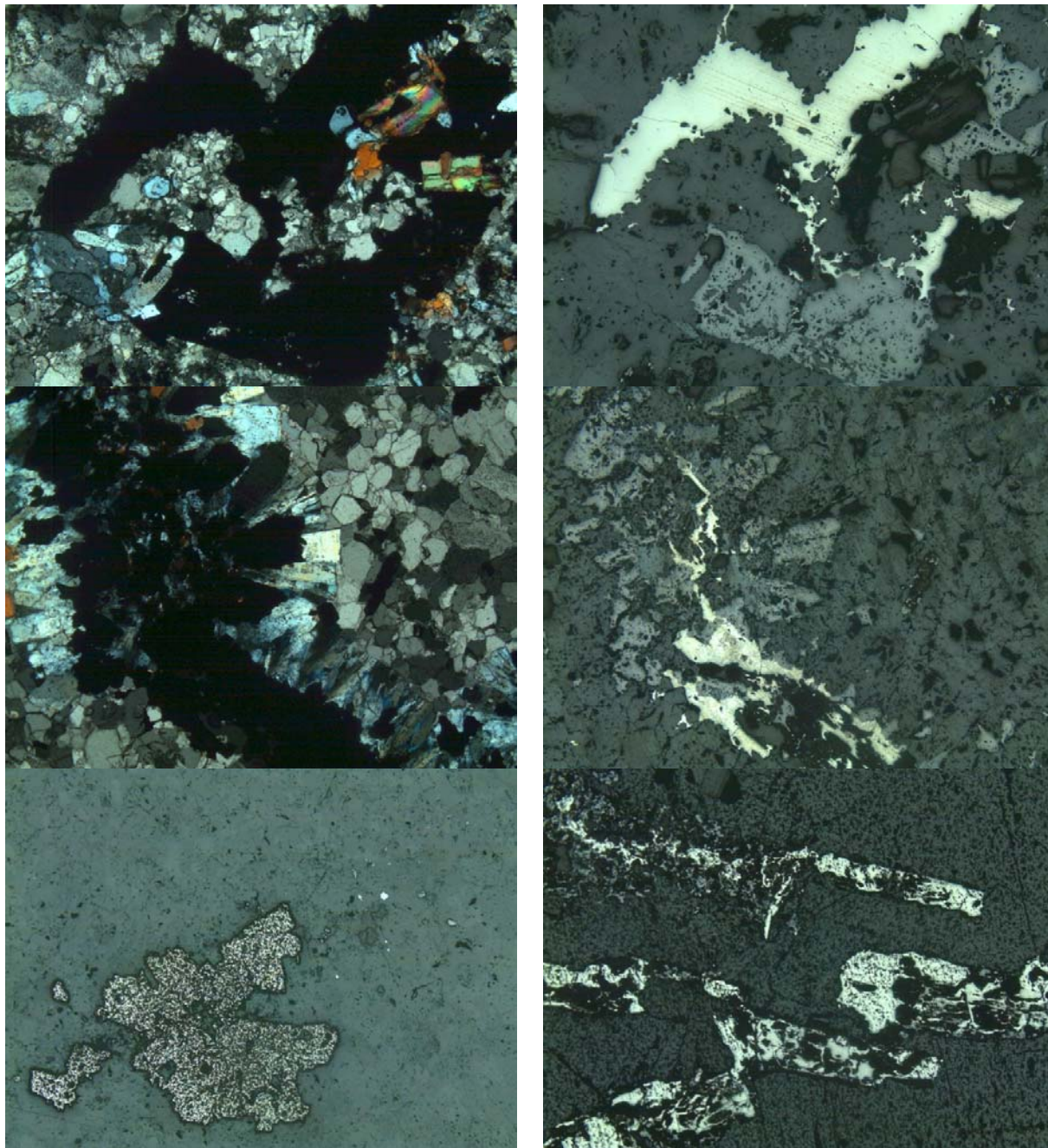
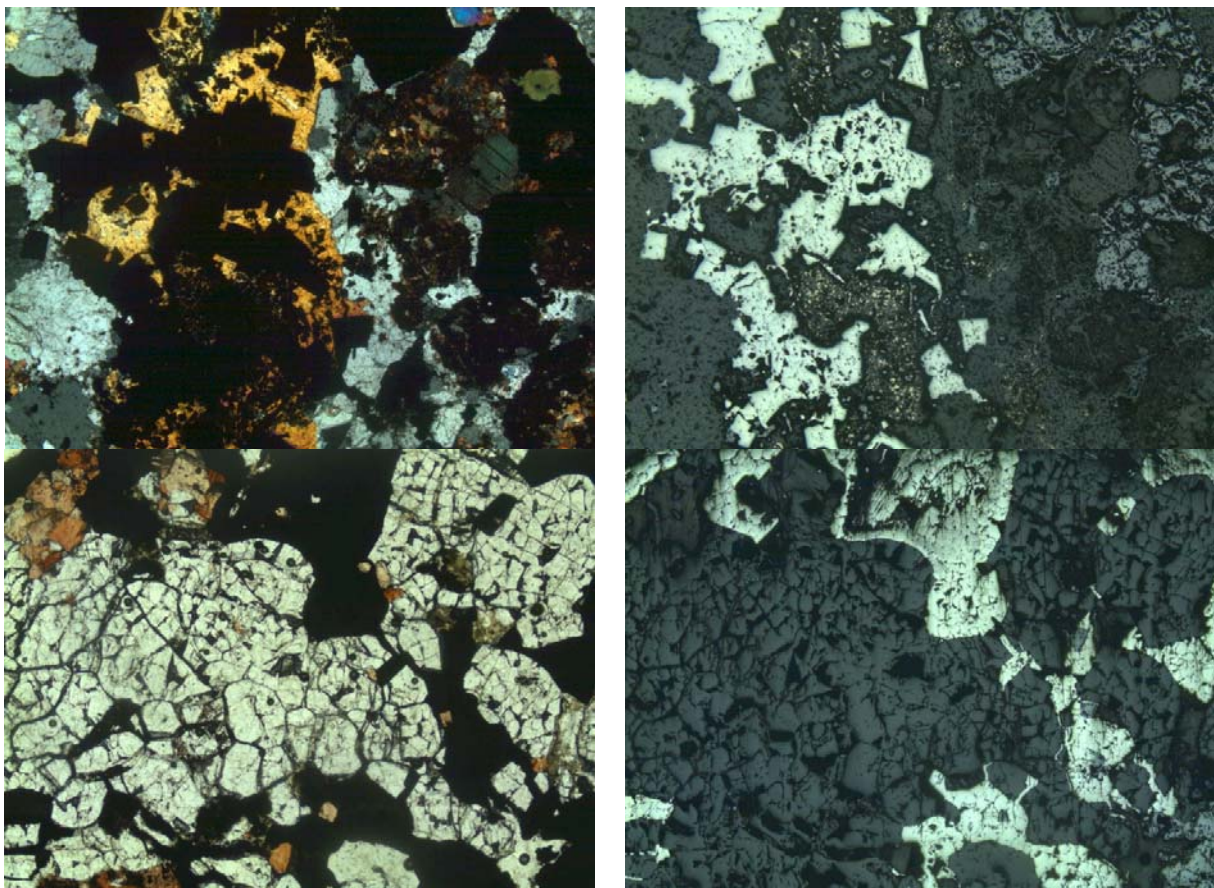


Figure 3.04 – Textural features of sulphides and barites in carbonatites from the Catalão I complex. A: Apatite (Ap), carbonate (Cbt) and phlogopite (Phl) in cross polarized light. Field width: 5mm. B: Same as A in reflected light, showing a smooth surface for pyrite (Py). Field width: 5mm. C: Carbonate (Cbt), barite (Brt); note the intergrowth of pyrite and barite. Cross polarized light. Field width: 5mm. D: Same as C in reflected light, barite, pyrite (Py) and magnetite (Mgt); note the intergrowth of pyrite and barite. Field width: 5mm. E: Pyrite (Py) with pitted surface, probably resulting from recrystallization as microgranular aggregates. Reflected light. Field width: 5mm. F: Pyrite (Py) with skeletal appearance and irregular surfaces, probably resulting from recrystallization as microgranular aggregates. Reflected light. Field width: 5mm.

Barite is a common phase in Catalão I carbonatites, occurring as radial aggregates, mixed in irregular carbonate masses and associated with sulphides or filling voids between bladed carbonate crystals, surrounded by small carbonate needles. The dominant sulphide species is granular, euhedral to anhedral pyrite mostly showing a smooth surface (figure 3.04b). More rarely pyrite may have a very pitted surface (figure 3.04e,f) analogous to those of Catalão II, or be interstitial. Chalcopyrite is rare and it was found only as small, very fine grained aggregates near pyrite.

Phoscorites (figure 3.05) are coarse grained to pegmatoid and essentially composed of apatite, magnetite, carbonate, and phlogopite, with or without olivine and rare sulphide. Phlogopite is often a pseudomorph over olivine. Pyrite and chalcopyrite show the same textural varieties as in the carbonatites (figure 3.05b). In phoscorites, the amoeboid contours of some pyrite aggregates suggest that it may have precipitated from an immiscible sulphide liquid (figure 3.05d).



*Figure 3.05 – Textural features of sulphide phoscorites from the Catalão I complex **A:** Apatite (Ap) and phlogopite (Phl) from phoscorites in cross polarized light. Field width: 5mm. **B:** Same as A in reflected light, showing a pitted surface in various pyrite (Py) individual grains and very fine grained chalcopyrite (Cpy) aggregates with a “dusty” appearance. Field width: 5mm. **C:** Apatite (Ap) and phlogopite (Phl). Plane polarized light. Field width: 5mm. **D:** Same as C, in reflected light showing pyrite (Py); note the amoeboid geometry of the interstitial pyrite aggregates, suggesting that they formed from an immiscible sulphide liquid. Field width: 5mm.*

Nelsonites (figure 3.06) are fine to medium-grained, composed of magnetite, apatite, phlogopite, carbonate, and pyrochlore, with sulphides as accessory phase. Sometimes the percentage of magnetite is high enough to allow the rock to be classified as a magnetitite. Sulphide (mostly pyrite and chalcopyrite) is relatively abundant in these rocks. Pyrite occurs as euhedral individual grains, as veins, as an interstitial phase, or as aggregates of bladed grains (figure 3.06b). The latter are interpreted as formed by rapid crystallization. Chalcopyrite is less abundant than pyrite and usually occurs as fine aggregates or small grains.

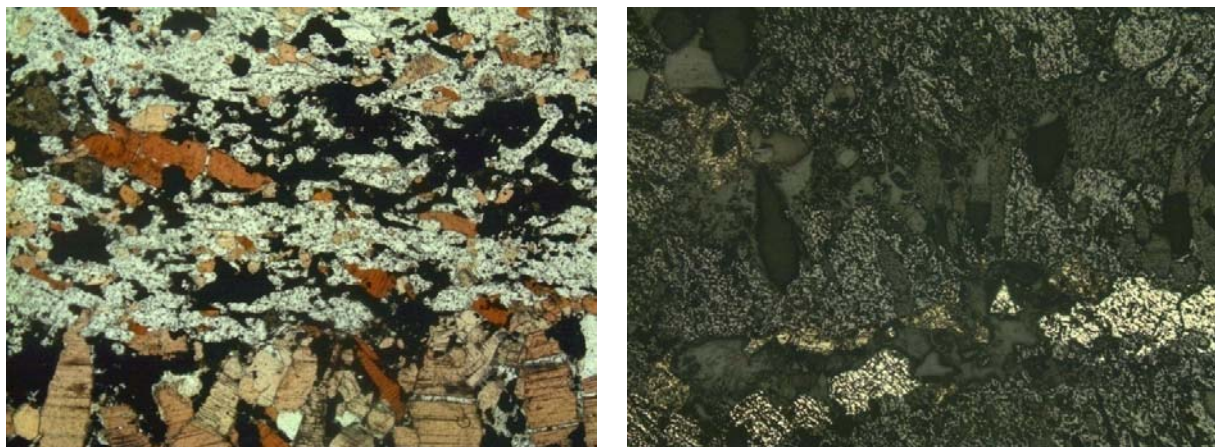


Figure 3.06 – Textural features of nelsonites from the Catalão I complex. A: Apatite (Ap), carbonate (Cbt), pyrochlore (Pcl) and phlogopite (Phl) in nelsonite, plane polarized light showing flow orientation of phlogopite and apatite crystals. Field width: 5mm. B: Pyrite (Py) grains with pitted surface and fine-grained chalcopyrite (Cpy) aggregates. Field width: 5mm.

Fenites occur both externally (fenitized Precambrian country rocks) and internally in the Catalão I complex. In this work we studied only the internal fenites, which result from a strong potassic metasomatism that converted the original ultramafic rocks (dunites, pyroxenites, and bebedourites) into magnetite-rich phlogopitites (e.g. Grasso *et al.*, 2006, Palmieri *et al.*, 2006, Ribeiro, 2008). These rocks are often cross cut by numerous carbonatite veins, and the phlogopite variety is typically fine-grained tetra-ferriphlogopite. The sulphide present is pyrite. Catalão I fenites were included in this study to assess the sulphur isotope composition of the metasomatic fluids involved in the late-stage evolution of the complex.

Serra Negra

The only rock-type analyzed from Serra Negra is carbonatite (figure 3.07). In the studied samples carbonate is subhedral, forming a roughly equigranular mosaic texture. Small amounts of apatite may be present. Both phlogopite and tetra-ferriphlogopite varieties are found in euehdral to subhedral lamellae, and the mica is usually associated with barite, when the second is present. Rare, disseminated, fine-grained pyrite is the sole sulphide found in these samples.

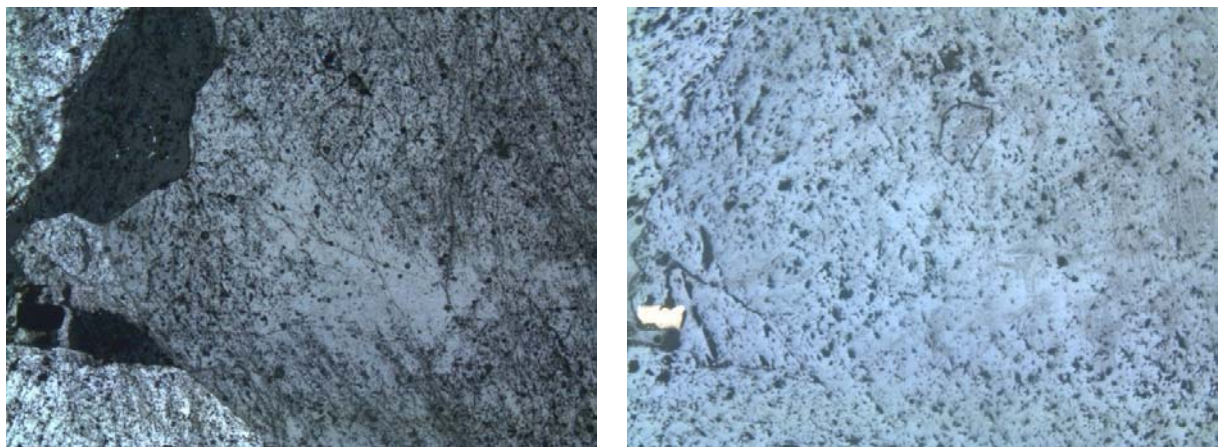
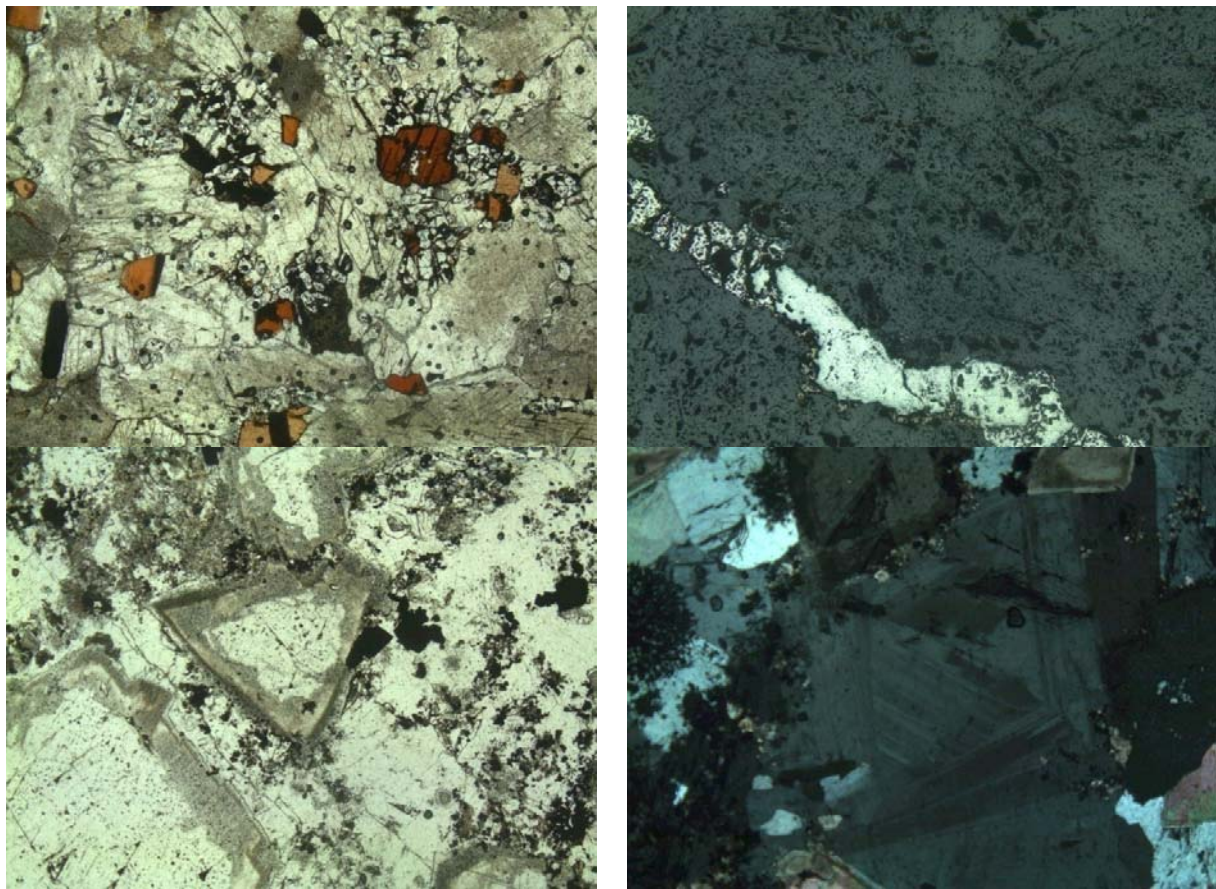


Figure 3.07 – Serra Negra carbonatites. **A:** Coarse-grained carbonate (Cbt) in cross polarized light; Field width: 5mm. **B:** Same as A, in reflected light, showing a small pyrite grain (Py). Field width: 5mm.

Salitre

Samples from the Salitre complex comprise carbonatites, phoscorites and bebedourites. The carbonatites (figure 3.08) are fine to coarse grained and contain variable amounts of apatite, phlogopite, magnetite, and barite. More rarely, was found pyrochlore. Apatite ranges from trace amounts to a major component, leading in extreme cases to a gradation to a carbonate-rich apatitite. Sulphides comprise pyrite, pyrrhotite, chalcopyrite (figure 3.08b) and galena but only the former two were large enough grains to be analysed for sulphur isotopes. Pyrite usually occurs as granular aggregates or as grains with irregular surface, disseminated in the rock. Pyrrhotite shows smooth surface and may form bladed cystals of scattered grains. Chalcopyrite forms discontinuous microgranular patches.



*Figure 3.08 – Textural features of carbonatites from the Salitre complex. **A:** Apatite (Ap), carbonate (Cbt), phlogopite (Phl) and pyrochlore (Pcl) in plane polarized light. Field width: 5mm. **B:** Elongated sulphide grain, pyrrhotite (Po) is the grain with a smooth surface, pyrite (Py) is the irregular surface grain, and chalcopyrite (Cpy) is present in small amounts, bordering pyrrhotite and pyrite. Reflected light. Field width: 5mm. **C:** Carbonate (Cbt) and pyrite (Py) showing zonation in carbonate crystals. Plane polarized light. Field width: 5mm. **D:** Carbonate (Cbt) and complexly zoned barite (Brt). Cross polarized light. Field width: 5mm.*

Phoscorites (figure 3.09) are coarse grained, composed of apatite, magnetite, carbonate, phlogopite, olivine, \pm perovskite. Sulphides comprise pyrite, pyrrhotite and chalcopyrite, usually occurring together. In some cases the textural relationships indicate late-stage substitution of other minerals (e.g. figure 3.09b) but, in others, they are disseminated grains. Pyrite has irregular surface, and is disseminated in the rock or replacing magnetite (figure 3.09b). Pyrrhotite is typically granular. Chalcopyrite is rare, occurring as “dusty” aggregates near pyrite grains.

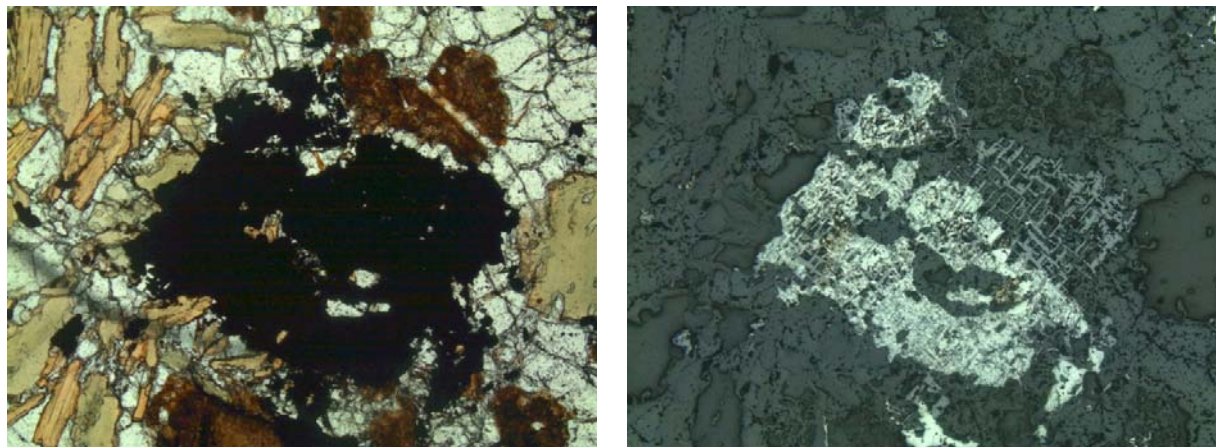


Figure 3.09 – Textural features of sulphide phoscorites from the Salitre complex. A: Coarse grained phoscorite, composed of olivine (Ol), phlogopite (Phl) in plane polarized light. Field width: 5mm. B: Same as A in reflected light, showing pyrite (Py) replacing magnetite; ilmenite (Ilm), chalcopyrite (Cpy) and pyrrhotite (Po). Field width: 5mm.

Bebedourites (figure 3.10) are coarse grained, composed of diopside, phlogopite, apatite, magnetite, \pm perovskite, \pm melanite, \pm titanite). Sulphide, usually pyrite, is rare, disseminated and interstitial.

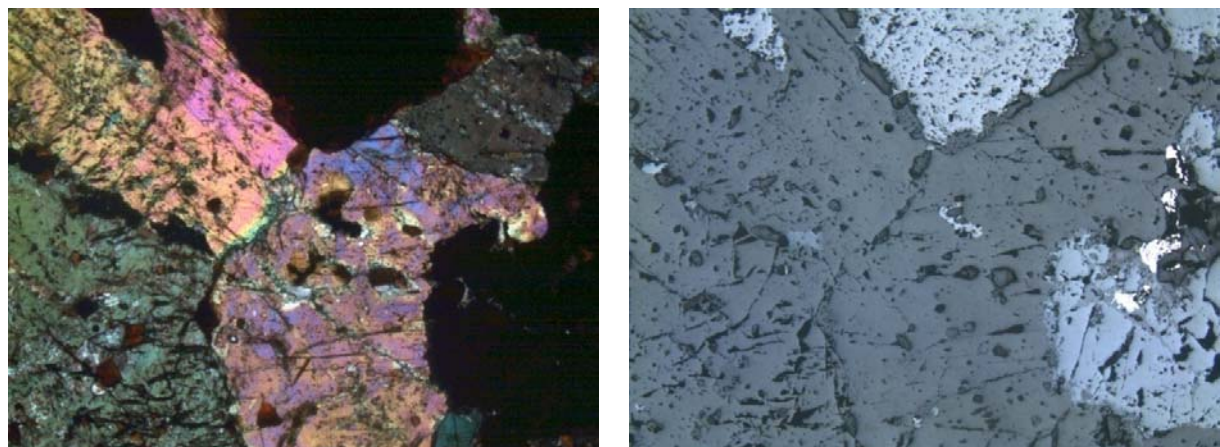


Figure 3.10 – Bebedourite from the Salitre complex. A: Coarse grained bebedourite, composed of clinopyroxene (Cpx), phlogopite (Phl), magnetite, ilmenite, pyrite. Field width: 5mm. B: Same as A in reflected light, showing magnetite (Mgt) replacement by pyrite (Py). Field width: 5mm.

Araxá

Most of the Araxá samples studied in this work are carbonatites, and one sample is a phosphorite. The carbonatite (figure 3.11 and 3.12) samples are fine to coarse grained, formed by carbonate, apatite, phlogopite, magnetite and barite. Sulphide is either disseminated or shows a bladed texture. Alternatively, it has a blob aspect, with round contours, which may represent segregation of a sulphide immiscible liquid (figure 3.12b). Pyrite, pyrrhotite and chalcopyrite are present. Pyrite and pyrrhotite show pitted surface, occurring as aggregates (figure 3.12a). Chalcopyrite is rare, forming a fine-grained cloudy mass (figure 3.12a) next to pyrite and pyrrhotite. Some of the carbonate, barite and sulphide textures are interpreted as the result of rapid crystallization resulting in cryptocrystalline aggregates like those described for Catalão II but, at Araxá, this aggregates seems to be the interface between the cryptocrystalline masses and the bladed crystals (figure 3.11).

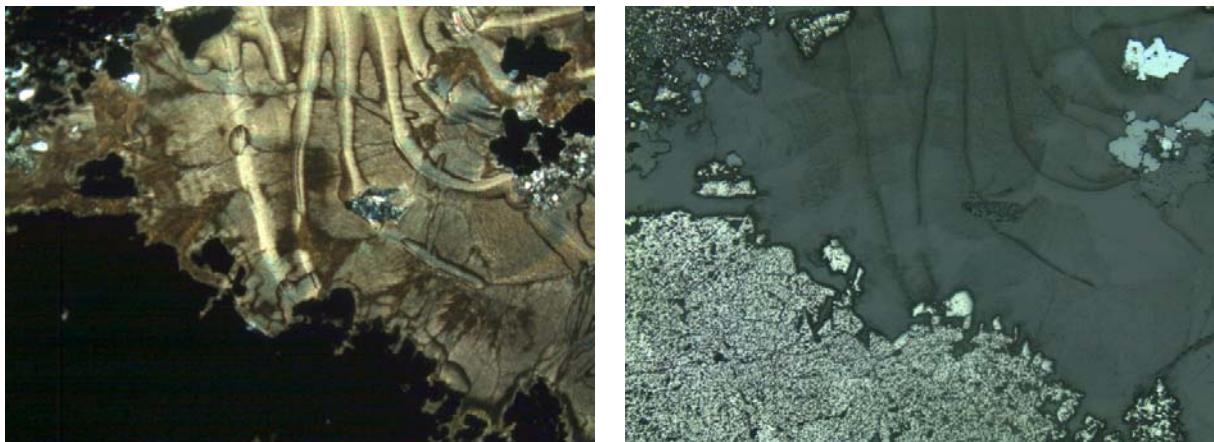


Figure 3.11 – Textural features of fine-grained aggregates of sulphide, barite and carbonate in carbonatite from the Araxá complex. A: Criptocrystaline carbonate mass, with intergrown of barite aggregates and sulphide, cross polarized light. Field width: 5mm. B: Same as "A", in reflected light. Field width: 5mm.

Carbonates are sometimes microcrystalline showing a colloidal aspect. These carbonate masses form elongate aggregates marked by subparallel curved lines (figure 3.12c,d). In cross section, they have an almost circular profile and may show alternating concentric circular lines (figure 3.12e,f) marked by different shades of brown in plane polarized light. Under crossed polars they show a circling maltese cross similar to the spherulitic extinction.

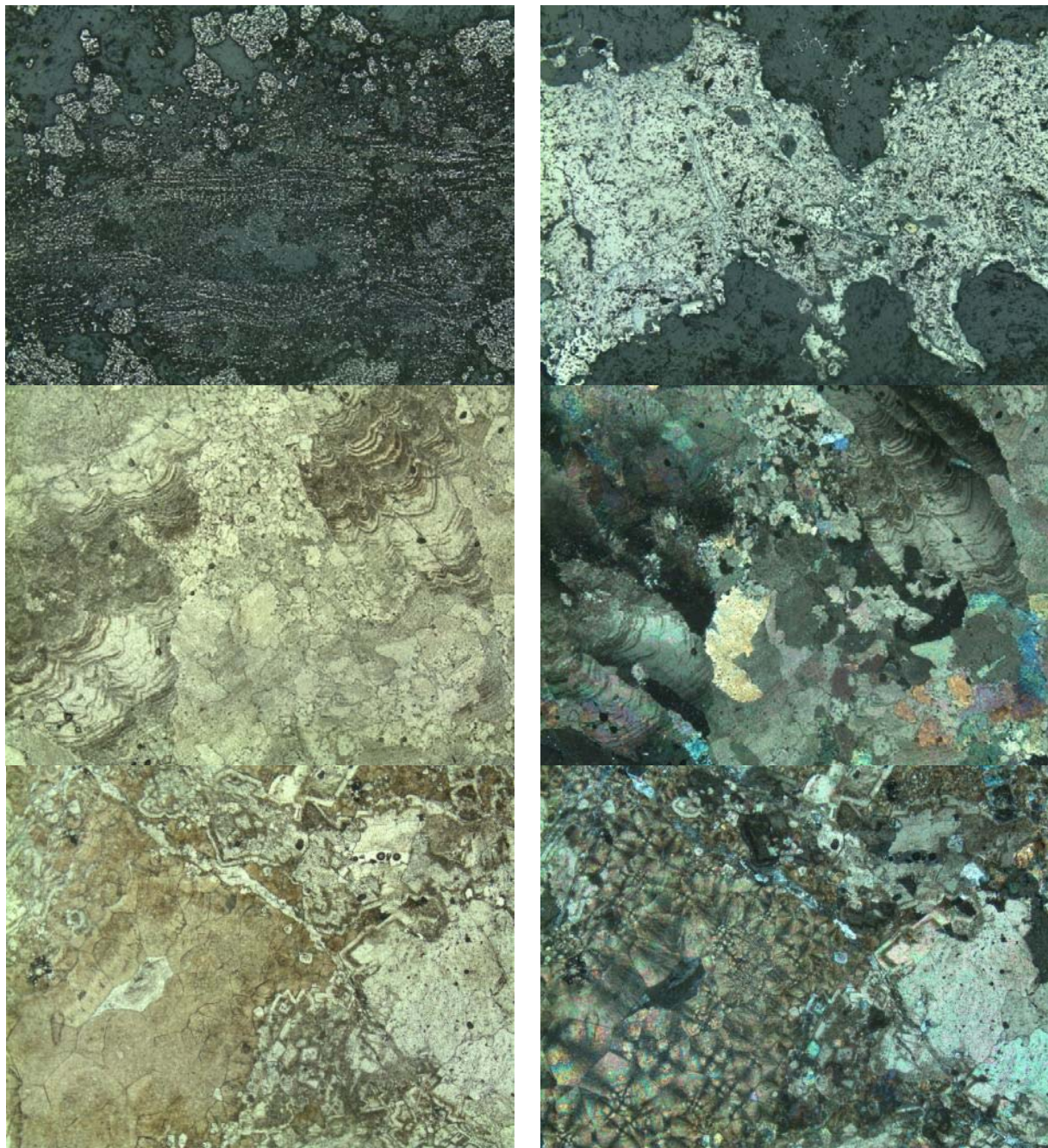


Figure 3.12 – Textural features of sulphide and carbonate in carbonatite from the Araxá complex **A:** Typical texture of carbonatite pyrite (Py), with very irregular grain surfaces, probably resulting from recrystallization of microgranular aggregates and very fine-grained aggregates of chalcopyrite (Cpy), and subordinate pyrite, with a dusty appearance. Reflected light. Field width: 5mm. **B:** Sulphides with a blob aspect, showing round contours that may indicate segregation of a sulphide immiscible liquid, with pyrrhotite (Po), pyrite (Py) and chalcopyrite (Cpy). Reflected light. Field width: 5mm. **C:** Carbonate aggregates marked by subparallel curved lines. Plane polarized light. Field width: 5mm. **D:** Same as "C" in cross polarized light. **E:** Cross section of carbonate aggregates showing concentric growth lines. Plane polarized light. Field width: 5mm. **F:** Same as "E", in cross polarized light, showing a circling maltese cross similar to the spherulitic extinction.

Barite often fills tabular voids in aggregates of bladed carbonate. This texture is indicative of degassing-controlled crystallization, and similar to those described by Junqueira-Brod *et al.* (in preparation) for an analogous stage of degassing in the Catalão I Complex. As the degassing progresses, causing the decrease of temperature in the liquid, it facilitates the precipitation of carbonate marked by growth lines shown by the elongated aggregates.

The phoscorite (figure 3.13) sample is coarse-grained, composed of apatite, magnetite, carbonate, phlogopite, and olivine (figure 3.13a). Pyrite is the sulphide present in this rock. It is typically associated with magnetite and has an irregular surface like the one described for the other complexes (figure 3.13b).

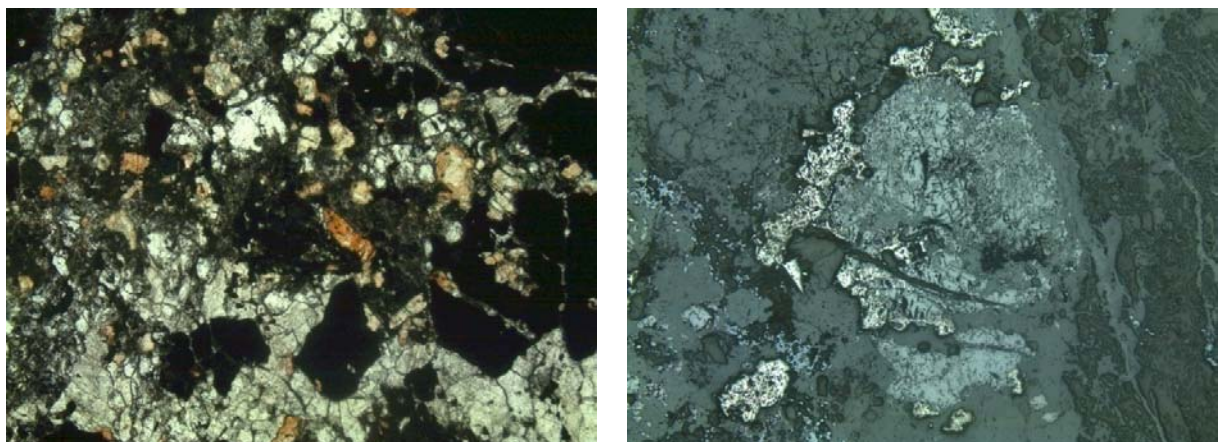


Figure 3.13 –Phoscorite. A: Phoscorite with magnetite (Mgt), phlogopite (Phl), apatite (Ap) and carbonate (Cbt). Plane polarized light. Field width: 5mm. B: Pyrite (Py) with pitted surface and magnetite (Mgt). Reflected light. Field width: 5mm.

Tapira

Most samples from Tapira are carbonatites, with a lesser number of bebedourites, phoscorites and fenites. The carbonatites (carbonate, apatite, phlogopite, magnetite, ilmenite and barite, ± olivine, ± tetra-ferriphlogopite, ± perovskite) (figure 3.14) are fine to coarse grained. The modal percentage of apatite varies from 2% to 20% approximately.

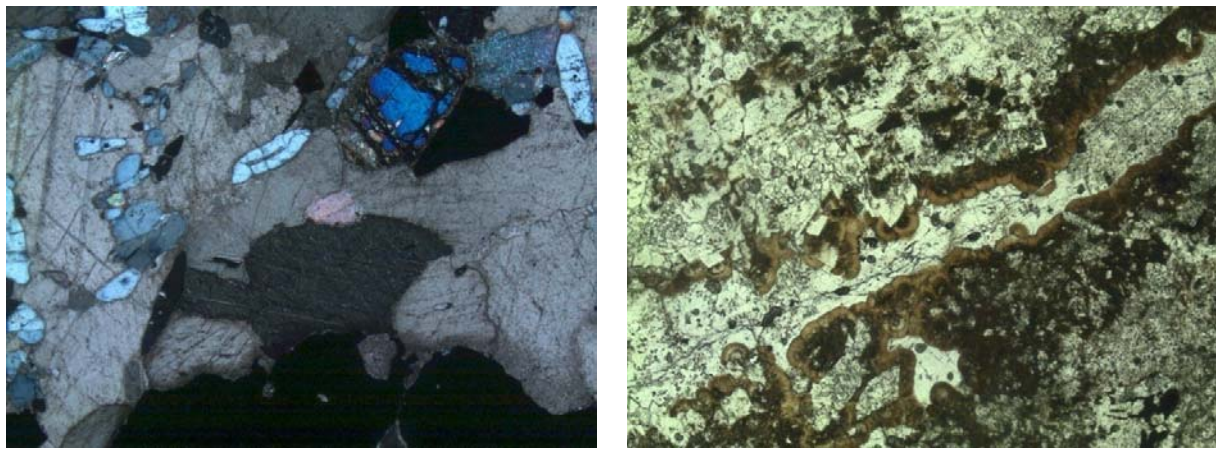


Figure 3.14 – Textural features of carbonatites from Tapira complex. A: Carbonatite with carbonate (Cbt), olivine (Ol) and apatite (Ap). Cross polarized light. Field width: 5mm. B: Carbonatite with some microgranular carbonates of colloidal aspect (arrow). Plane polarized light. Field width: 5mm.

Carbonates are sometimes microcrystalline showing a colloidal aspect (figure 3.14b) similar to that observed in samples from Araxá, and other cases form a criptocrystalline aggregate like that described for Catalão II (figure 3.15). The sulphides present are pyrite, pyrrhotite and chalcopyrite. Pyrite occurs as grains with pitted surface, as skeletal grains and as disseminated limpid grains. Pyrrhotite varies from well-formed grains to pit-surfaced. Chalcopyrite is rare and associated with the other two sulphides.

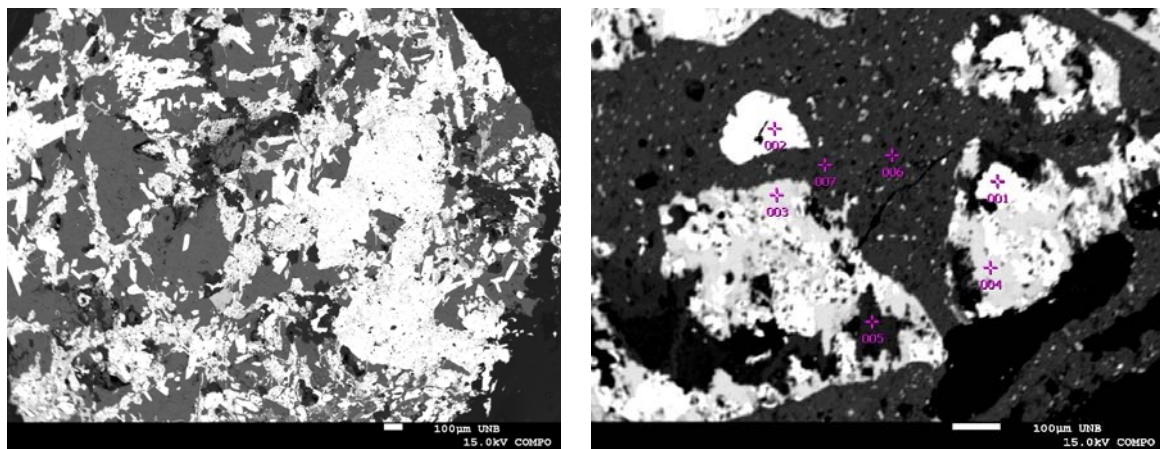


Figure 3.15 –A: BSE image of a fine-grained mass containing dolomite (Cbt) and skeletal barite (Brt). B: BSE image of a fine-grained mass containing different carbonate types and barite, 001: Barite; 002: Barite; 003: Sr-carbonate; 004: Sr-carbonate; 005: Dolomite; 006: Calcite; 007: Calcite.

Bebedourites are fine to medium grained, composed of diopside, phlogopite, apatite, magnetite, \pm perovskite, \pm titanite, with disseminated sulphides. The predominant sulphide species is pyrrhotite with subordinate chalcopyrite, both usually interstitial to the other phases.

Phoscorite is coarse-grained, composed of apatite, magnetite, carbonate, phlogopite, and olivine (figure 3.16a). Sulphide is disseminated and both chalcopyrite and pyrite are present. Pyrite shows an irregular surface like the one described to the other complexes, whereas chalcopyrite is found as well formed grains (figure 3.16b).

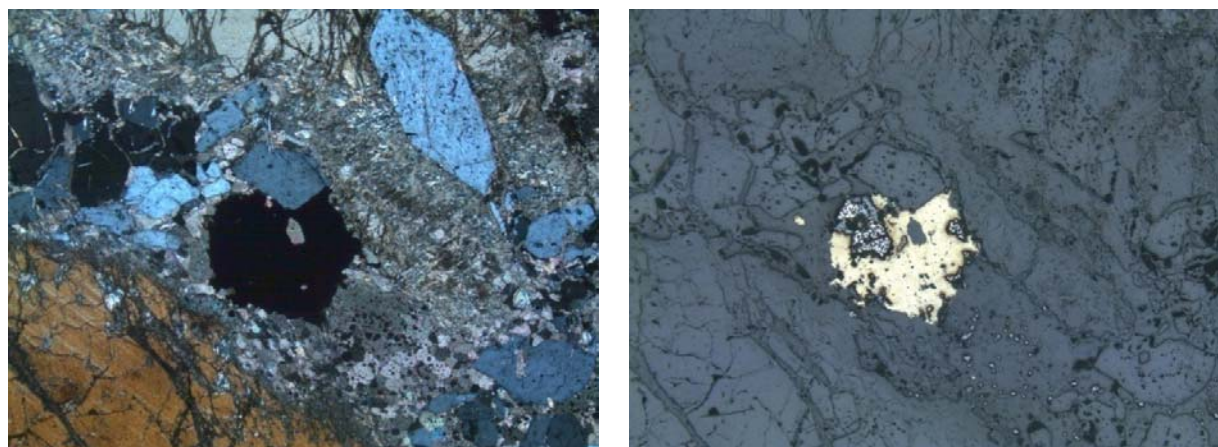


Figure 3.16 – Textural features of phoscorites from Tapira complex. A: Phoscorite showing carbonate (Cbt), olivine (Ol), apatite (Ap), granular chalcopyrite and pyrite with pitted surface. Cross polarized light. Field width: 5mm. B: Same as A, showing granular chalcopyrite (Cpy) and pyrite (Py) with pitted surface under reflected light. Field width: 5mm.

Tapira fenites have similar composition, texture and origin as those described in Catalão. The sulphide present is pyrite and is associated with carbonatite veins.

Jacupiranga

Jacupiranga samples are mostly carbonatites. Nevertheless, jacupirangite was also studied in order to compare its sulphur isotopes with bebedourites and other silicate rocks from the APIP. The carbonatites (figure 3.17) vary from fine to coarse grained and consist of carbonate, apatite, phlogopite, magnetite, ilmenite, \pm barite, \pm olivine, \pm tetra-ferriphlogopite, \pm perovskite. The most common sulphide is pyrrhotite followed by pyrite, chalcopyrite and pentlandite. Pyrrhotite varies from well formed to irregularly-surfaced grains whereas pyrite and chalcopyrite are rare and well formed.

Sulphides may appear as disseminated grains or a large aggregate that seems to be associated with carbonate-sulphide liquid immiscibility processes (figure 3.17b). Alternatively, pyrite occurs as concentric microgranular aggregates, forming circular lines (figure 3.17c). This may be the sulphide equivalent of the elongate carbonate aggregates and could be interpreted as the result of gradual precipitation of sulphide during sulphur gaseous loss.

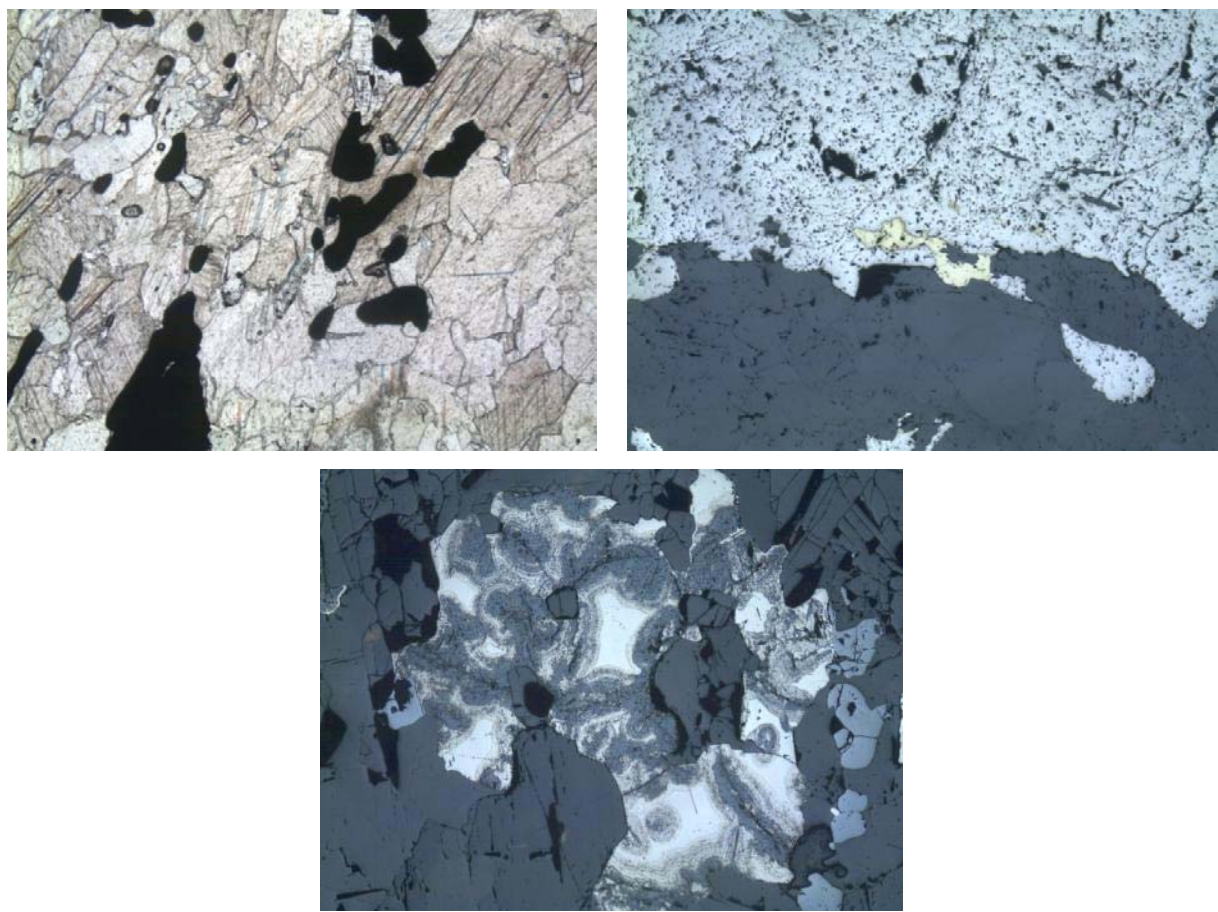


Figure 3.17 – Textural features of carbonatites from Jacupiranga complex. A: Carbonatite with apatite (Ap) and disseminated pyrrhotite (Po) in plane polarized light. Field width: 5mm. B: Texture suggestive of carbonate-sulphide immiscibility showing pyrrhotite (Po) and chalcopyrite (Cpy), note the blob-like aspect of the pyrrhotite near the lower-right corner. Reflected light. Field width: 5mm. C: Carbonatite with microgranular aggregates of pyrite (Py), forming concentric circular or amoeboidal lines. Ilm=ilmenite. Reflected light. Field width: 3.5mm.

Jacupirangites (figure 3.18) (clinopyroxene, nepheline, magnetite, apatite, phlogopite, carbonate, ± amphibole) are medium grained. The nepheline may show symplectitic texture (figure 3.18c,d). Sulphides (chalcopyrite and pyrite) are interstitial and well formed (smooth surface) (figure 3.18b).

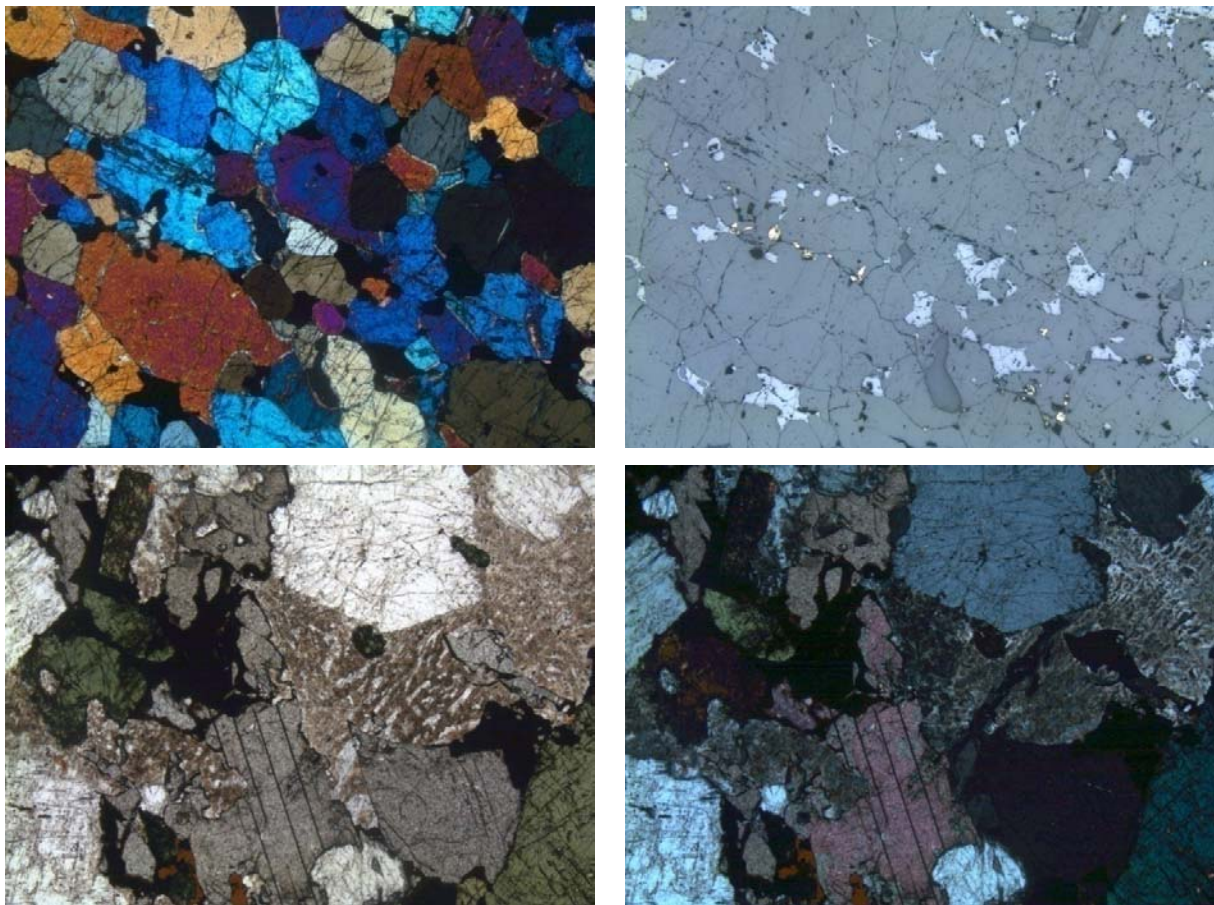


Figure 3.18 – Textural features of jacupirangites from Jacupiranga complex. A: Jacupirangite showing clinopyroxene (Cpx) with magnetite (Mgt) and interstitial chalcopyrite (Cpy). Cross polarized light. Field width: 5mm. B: Same as "A", in reflected light. C: Jacupirangite showing nepheline (Ne) with symplectic texture, titanite (Ttn) and clinopyroxene (Cpx). Plane polarized light. Field width: 5mm. D: Same as "C", in cross polarized light. Field width: 5mm.

4. Analytical methods

Sulfur isotopic compositions were determined at the Geochronology Laboratory of the Institute of Geosciences, University of Brasilia (UnB) by LA-MC-ICP-MS (Laser Ablation-Multi Collector-Inductively Coupled Plasma Mass Spectrometry) on handpicked minerals (sulphide and sulphate). The analyses were carried out using a Neptune MC-ICP-MS coupled with a NewWave UP213 Nd:YAG as ablation source for *in situ* analysis of solid samples.

Sulfur reference materials IAEA-S-1, S-2, S-3, NBS-127 and NBS-123 (Coplen and Krouse, 1998; Ding *et al.*, 2001; Qi and Coplen, 2003) were used to calibrate laboratory (in-house) standards (py-bsb and cpy-bsb) and to enable interlaboratory comparison against the V-CDT scale. The analytical precision

(1σ) was about $\pm 0.1\text{‰}$ to $\pm 0.5\text{‰}$. All sulfur isotope compositions are reported in the standard delta notation relative to V-CDT. Three percent HNO₃ blank solutions were used to quantify sulfur blanks throughout calibration sessions and during analysis. He flow were used to quantify sulfur blanks.

Powders of reference standards were prepared as pellets using a PerkinElmer hydraulic press. Pellets were pressed without addition of a binder under vacuum at 10 tons for 5 min, sulphide minerals were mounted independently on glass slides in epoxy resin and polished to give a flat surface suitable for laser ablation sampling. A line scan ('raster') protocol is used in preference to a single crater mode, in order to obtain a higher and more uniform rate of material removal with respect to time (Craddock *et al.* 2008).

Sulphides and sulphates chemical composition were obtained with a JEOL JXA-8230 microprobe at University of Brasilia. The sulphates were firstly explored by EDS (Energy-Dispersive Spectrometry) and observed by BSE (Back-Scatteres Electrons) and then analysed by WDS (Wavelength-Dispersive Spectrometry) at 20kV. Sulphides were directly analised by WDS at 20 kV.

5. Results

In sampling for this study we tried to systematically represent all available sulphide- and/or sulphate-bearing rock-types from which it was possible to mechanically extract these minerals for analysis. The set of analysed rock-types comprises: phoscorite and carbonatite from Araxá; carbonatite, phoscorite, nelsonite, magnetitite, and metassomatic phlogopitite from Catalão I; carbonatite and nelsonite from Catalão II; carbonatite from Serra Negra; bebedourite, phoscorite and carbonatite from Salitre; bebedourite, carbonatite, phoscorite, and metasomatic phlogopitite from Tapira; and carbonatite and jacupirangite from Jacupiranga.

Barite is the only sulphate found, usually occurring as masses in late-stage magnesiocarbonatites (e.g. Catalão I, Catalão II, Salitre and Tapira) or in post-magmatic veins (e.g. Catalão I).

The sulphides present in the sample set are pyrite, pyrrhotite, chalcopyrite, bornite and galena. Of these, bornite is rare and galena was found only in samples from Jacupiranga but it was too finely grained to allow a reliable analysis. Therefore, our discussion will focus on the three remainder sulphide species. Pyrite occurs in all petrographic types in a variety of textures: bladed phenocrysts or tabular aggregates associated with carbonate and/or magnetite in nelsonites and

magnesiocarbonatites (Junqueira-Brod *et al.* in preparation); interstitial grains sometimes replacing magnetite; millimetric pyrite veins and, very rarely, as centimetric massive pyrite intercepts in drill cores. Pyrrhotite occurs in carbonatites both as fenocrysts and interstitial grains, and also as a rare interstitial phase in bebedourites. Chalcopyrite occurs in all petrographic types and may be found as interstitial grains or as aggregates of anhedral grains, and sometimes replaces pyrite. Bornite is rare and occurs associated with chalcopyrite in nelsonite.

Table 3.01 shows representative sulphur isotope data, along with the analysed materials (S-bearing phase, host rock, and complex).

Table 3.01 – Representative $\delta^{34}\text{S}$ ‰ results .

Nº of	$\delta^{34}\text{S}$ ‰ V-CDT	Mineral	Rock	Complex
2	from 7.22 to 12.16	barite	Carbonatite	Catalao II
1	-6.25	chalcopyrite	Carbonatite	Catalao II
5	from -6.68 to -12.31	pyrite	Carbonatite	Catalao II
1	-6.68	pyrrhotite	Carbonatite	Catalao II
1	-5.28	bornite	Nelsonite	Catalao II
3	from -5.62 to -7.08	chalcopyrite	Nelsonite	Catalao II
2	from -4.86 to -5.98	pyrite	Nelsonite	Catalao II
4	3.26 to 12.88	barite	Carbonatite	Catalao I
2	from -17.36 to -24.55	pyrite	Fenite/Carbonatite	Catalao I
6	from -2.2 to -10.91	pyrite	Carbonatite	Catalao I
8	from -2.58 to -9.59	pyrite	Nelsonite	Catalao I
2	from -2.13 to 0.51	barite	Carbonatite	Salitre
2	from -4.66 to -5.03	pyrite	Bebedourite	Salitre
6	from -5.02 to -8.76	pyrite	Carbonatite	Salitre
5	from -2.84 to -12.36	pyrrhotite	Carbonatite	Salitre
1	-5.72	chalcopyrite	Phoscorite	Salitre
1	-5.98	pyrite	Phoscorite	Salitre
3	from -8.12 to -8.78	pyrite	Carbonatite	Serra Negra
1	-8.24	pyrrhotite	Carbonatite	Serra Negra
13	from -11.63 to -4.39	pyrite	Carbonatite	Araxa
3	from -7.93 to -11.69	pyrrhotite	Carbonatite	Araxa
1	-7.59	pyrite	Phoscorite	Araxa
4	from -1.31 to 16.75	barite	Carbonatite	Tapira
1	-6.49	chalcopyrite	Bebedourito	Tapira
3	from -2.59 to -9.55	pyrite	Bebedourito	Tapira
1	-2.19	pyrrhotite	Bebedourito	Tapira
6	from -6.79 to -13.15	pyrite	Carbonatite	Tapira
4	from -3.95 to -9.01	pyrrhotite	Carbonatite	Tapira
1	-8.61	pyrite	Fenito	Tapira
1	-1.70	chalcopyrite	Bebedourite	Jacupiranga
1	-0.84	pyrite	Bebedourite	Jacupiranga
5	from -3.15 to -6.08	pyrite	Carbonatite	Jacupiranga
10	from -3.15 to -5.37	pyrrhotite	Carbonatite	Jacupiranga

To discuss δ values it is initially necessary to note that the sulphur isotope composition of sulphur-rich minerals is strongly related with the redox conditions under which these minerals form. For example, in systems containing both sulphates and sulphides, the former are always heavier (higher $\delta^{34}\text{S}$) than the latter (e.g. Seal *et al.* 2006, Nikiforov *et al.* 2006, Miyoshi *et al.* 1984, Mitchell and Krouse, 1975). This is also true of the sulphide-sulphate pairs studied in this work. Similar relationships were obtained in degassing experiments in systems crystallizing sulphides only. In this case, sulphur degassing under oxidizing conditions drives $\delta^{34}\text{S}$ of the residual system towards higher values, whereas sulphur degassing under reducing conditions has the opposite effect (Zheng, 1990). In our work we adopt these concepts to compare the isotopic variations both in sulphate-sulphide and in sulphide- or sulphate-only systems.

Table 3.02 –Representative and average chemical compositions of the studied s sulphides.

mineral sample rock type	pyrite C8-7G* carbonatite	average #=252	pyrrhotite AT49* carbonatite	average #=76	chalcopyrite 165911C* nelsonite	average #=24	bornite 165911C1* nelsonite	average #=2
Fe	46.27	46.395	60.145	59.858	30.673	30.330	11.383	11.332
Cu	0.018	0.019	0	0.020	33.897	33.661	61.736	61.933
Pb	0.075	0.230	0.27	0.164	0.211	0.135	0	0
Co	0.185	0.155	0.079	0.195	0.036	0.037	0.008	0.022
Ag	0.021	0.004	0	0.003	0.018	0.024	0.281	0.259
Zn	0.005	0.005	0.024	0.002	0.016	0.023	0	0
Ni	0	0.020	0	0.028	0.009	0.006	0.063	0.039
Pt	0.01	0.004	0	0.006	0	0.003	0	0
Pd	0	0.002	0.001	0.002	0	0.002	0.008	0.004
S	53.368	53.008	39.414	39.104	34.833	34.596	25.293	25.410
As	0.074	0.025	0.004	0.002	0	0.001	0	0.0045
Se	0	0.029	0.087	0.036	0.06	0.034	0.095	0.0625
Total	100.03	99.90	100.02	99.42	99.75	98.85	98.87	99.07
	^a		^b		^c		^d	
Fe	0.995	1.001	0.875	0.879	1.012	1.009	1.035	1.028
Cu	0.000	0.000	0.000	0.000	0.982	0.984	4.934	4.937
Pb	0.000	0.001	0.001	0.001	0.002	0.001	0.000	0.000
Co	0.004	0.003	0.001	0.003	0.001	0.001	0.001	0.002
Ag	0.000	0.000	0.000	0.000	0.000	0.000	0.013	0.012
Zn	0.000	0.000	0.000	0.000	0.000	0.001	0.000	0.000
Ni	0.000	0.000	0.000	0.000	0.000	0.000	0.005	0.003
Pt	0.000	0.000	0.000	0.000	0.000	0.000	0.000	0.000
Pd	0.000	0.000	0.000	0.000	0.000	0.000	0.000	0.000
S	1.999	1.992	0.999	1.000	2.001	2.003	4.006	4.014
As	0.001	0.000	0.000	0.000	0.000	0.000	0.000	0.000
Se	0.000	0.000	0.001	0.000	0.001	0.001	0.006	0.004
total	3	3	1.88	1.88	4	4	10	10
Σ cations	1.00	1.01	0.88	0.88	2.00	2.00	5.99	5.98
Σ anions	2.00	1.99	1.00	1.00	2.00	2.00	4.01	4.02

* representative sample

^a atomic proportions for 3 ions

^b atomic proportions for 1 S

^c atomic proportions for 4 ions

^d atomic proportions for 10 ions

5.1. Mineral Chemistry

Data from 388 microprobe analyses are considered for this section. Table 3.02 shows representative results and averages for each sulphide species found and Table 3.03 shows representative barite analyses. Overall, pyrite is the most common S bearing phase. Barite is the only studied sulphate and was found in four of the seven Complexes (Catalão I, II, Salitre and Tapira).

Table 3.03 – Representative compositions of the studied sulphates.

sample rock complex	14405 4 carbonatite Catalão II	SH1BH 2 carbonatite Catalão I	ASL12B 2 carbonatite Salitre	AT132 1 carbonatite Tapira	average #=34
BaO	65.17	66.27	64.61	65.58	66.62
SO ₃	34.29	33.62	34.27	33.53	33.40
SeO ₂	0.50	0.00	0.00	0.00	0.18
MgO	0.00	0.02	0.01	0.00	0.00
SiO ₂	0.00	0.00	0.00	0.09	0.05
Al ₂ O ₃	0.11	0.04	0.08	0.05	0.06
P ₂ O ₅	0.07	0.00	0.02	0.00	0.05
CaO	0.00	0.00	0.00	0.12	0.06
Cr ₂ O ₃	0.00	0.00	0.00	0.00	0.00
FeO	0.11	0.02	0.01	0.04	0.03
SrO	0.00	0.09	1.11	0.12	0.08
PbO	0.00	0.00	0.00	0.00	0.00
MnO	0.02	0.00	0.02	0.00	0.00
Total	100.26	100.05	100.14	99.52	100.52
atoms per formula unit based on 4 oxygen					
Ba	0.9849	1.0201	0.9799	1.0109	1.0245
Pb	0.0000	0.0000	0.0000	0.0000	0
Sr	0.0000	0.0019	0.0250	0.0027	0.0019
Ca	0.0000	0.0000	0.0000	0.0048	0.0026
Si	0.0000	0.0000	0.0000	0.0037	0.0018
Al	0.0048	0.0019	0.0037	0.0023	0.0026
P	0.0022	0.0000	0.0008	0.0000	0.0016
Cr	0.0000	0.0000	0.0000	0.0000	0
Fe	0.0034	0.0006	0.0002	0.0012	0.0009
Mg	0.0000	0.0013	0.0005	0.0000	0
Mn	0.0007	0.0000	0.0007	0.0000	0
S	0.9925	0.9910	0.9954	0.9899	0.9836
Se	0.0105	0.0000	0.0000	0.0000	0.0038
sum	2.00	2.02	2.01	2.02	2.02

The compositional range of the analysed sulphides is very narrow, as can be observed from figure 3.19, where data from all 354 available analyses are included and plot very close to each other, close to each sulphide species ideal composition.

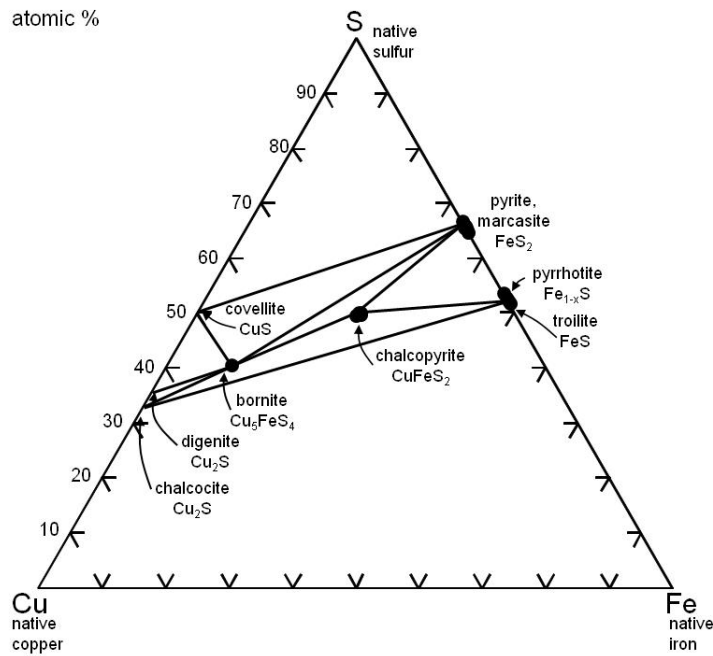


Figure 3.19 –Classification of sulphides according to Cu-S-Fe in atomic proportions (Klein, 2002).

The variation between complexes is also small, as shown in figure 3.20 where sulphur and iron ranges for each sulphide type were plotted according to their respective alkaline complex.

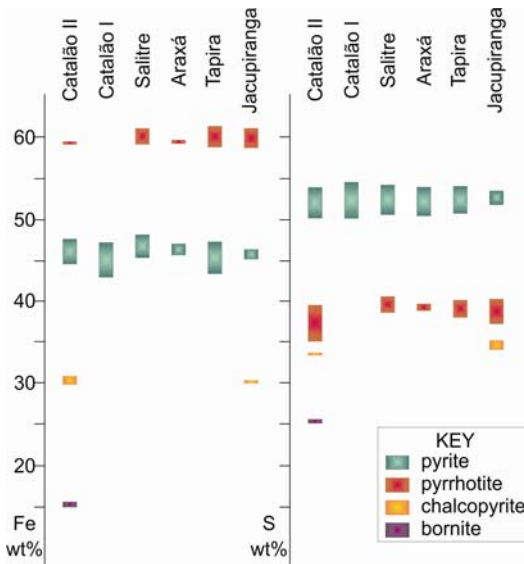


Figure 3.20 – Compared major element variations in the studied sulphides for each complex.

Trace elements detected in pyrite, pyrrhotite and chalcopyrite include Cu (major for chalcopyrite), Pb, Co, Ag, Zn, Ni, Pt, Pd, As and Se. Cobalt is always present in pyrite and can reach up to 2.7wt%. It is also important to note the presence of Ni and Pb at percentage levels (up to 0.7 wt. %

and 0.8 wt. %, respectively) in the pyrite analyses. In pyrrhotite (Fe_{1-x}S) the x parameter, representing Fe omission solid solution varies from 0.07 to 0.15. The trace elements found in pyrrhotite are the same as in pyrite, although generally in smaller amounts. Chalcopyrite usually shows the smallest trace elements contents. Many core/rim analyses were conducted, but none has detected significant changes in composition that could suggest zonning.

Barite also has a very steady composition. Strontium and selenium were the only significant trace elements in a total of 34 analyses (up to 1.87 wt% of SrO and 1.08 wt% of SeO_2). Other detected elements include Ca, Si, Al, P, Fe, Mg, Mn and Se.

5.2. Sulfur isotope variations in the APIP complexes and Jacupiranga

Sulphur isotope data are detailed for each studied complex in figure 3.21 and compared with the assumed primary mantle value of 0‰. The figure also emphasizes the difference between the isotopic composition of sulphides and sulphates. The occurrence of sulphide and sulphate in the complexes, sometimes in the same rock, indicate variable oxidizing/reducing conditions during magma evolution.

Samples from Catalão II yielded $\delta^{34}\text{S}$ ranges of -12.31‰ to -4.24‰, peaking at -4‰ for sulphides, and high positive values (7.22‰ to 12.16‰) for barite. The analyses of pyrite and barite from the same sample have yielded, respectively $\delta^{34}\text{S} = -9.17\text{\textperthousand}$ and 12.16‰, a ca. 21‰ difference.

Two types of sulphides may be distinguished in Catalão I on the basis of petrographic features and $\delta^{34}\text{S}$ results. Sulphides from samples lacking evidence of hydrothermal alteration range from -10.92‰ to -2.2‰, peaking at -6‰. These are dominantly pyrite, with one pyrrhotite analysis. In metasomatised rocks the analysed sulphide is also pyrite, and yielded substantially depleted $\delta^{34}\text{S}$ results (-17.36‰ to -24.55). Barite from Catalão I has a high positive $\delta^{34}\text{S}$, ranging from 3.27‰ to 12.88‰, as expected for sulphates. Coexisting pyrite and barite were analysed in two samples, one fresh and one showing evidence of metasomatism. In the first case, we obtained $\delta^{34}\text{S}_{\text{pyrite}} = -7.04\text{\textperthousand}$ and $\delta^{34}\text{S}_{\text{barite}} = 5.70\text{\textperthousand}$, a difference of ca. 13‰. The altered sample yielded $\delta^{34}\text{S}_{\text{pyrite}} = -24.55\text{\textperthousand}$ and $\delta^{34}\text{S}_{\text{barite}} = 11.00\text{\textperthousand}$, a striking 35‰ difference. The large difference between the reduced and oxidized form of sulphur in the altered sample probably indicates crystallization at different times, as observed by

Gomide *et al.* (2010) or, alternatively, coeval crystallization but at very low temperature (Miyoshi *et al* 1984).

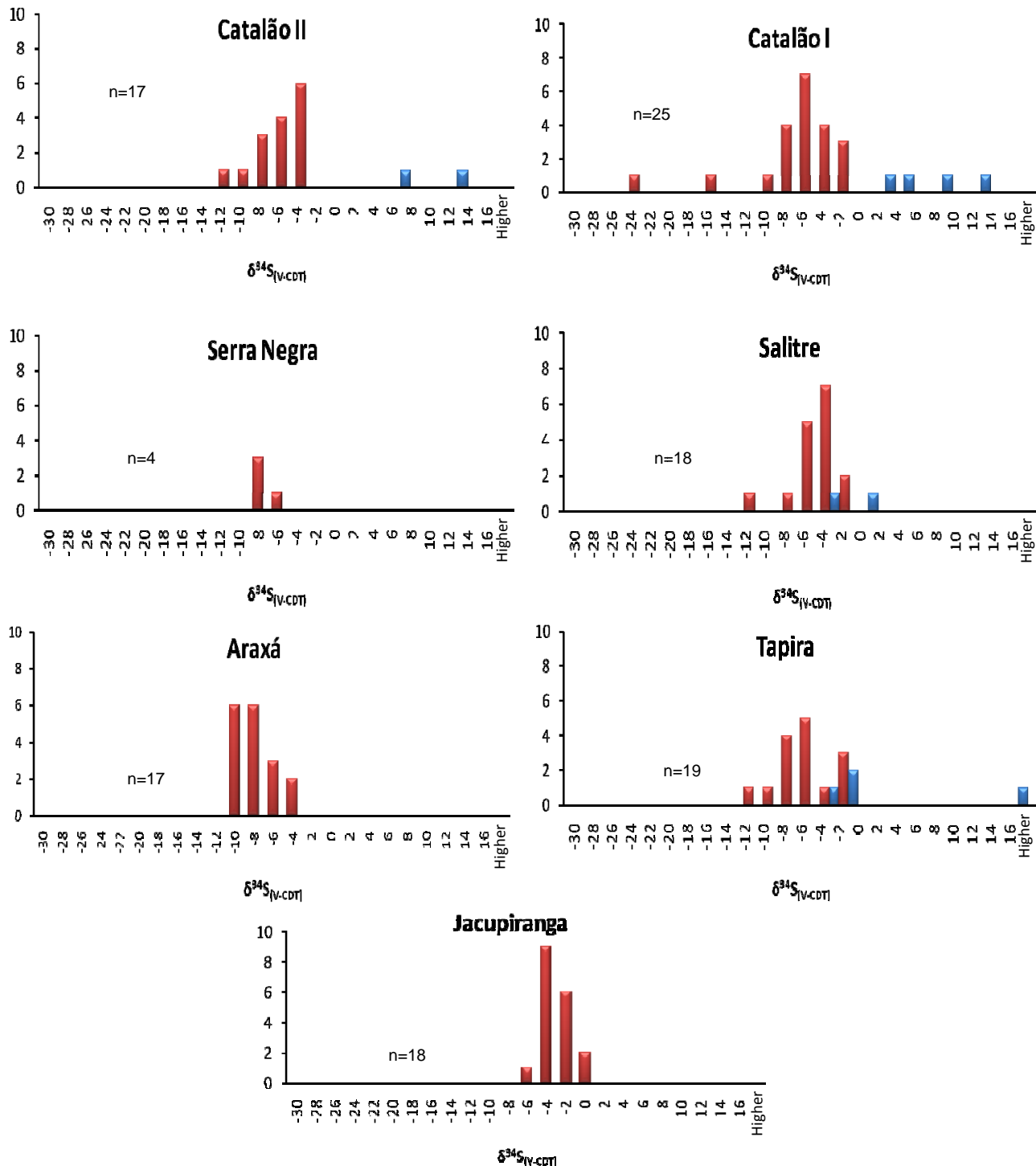


Figure 3.21. Sulphur isotope data for alkaline carbonatite complexes from the APIP and Ponta Grossa Province. Red bars represent sulphide data and blue bars represent sulphate data.

Serra Negra is the complex with the fewer analyses in our dataset: only 4 samples, which vary between -8.78‰ and -7.61‰. This is also the narrowest observed range, but this probably reflects the lack of a larger number of analytical determinations.

Sulphides from the Araxá complex (pyrite, chalcopyrite and pyrrhotite) plot between -11.69‰ and -4.4‰, with the most abundant values between -10‰ and -8‰. The Araxá complex is characterized by intense carbonatite metasomatism, similarly to Catalão I, but this was not represented in the sample set available for this work. Therefore, more $\delta^{34}\text{S}$ -depleted results would be expected should these metasomatic rocks be analysed in the future.

Salitre has a range from -8.77‰ to -2.84‰ with an isolated result at -12.36‰, representing a fresh carbonatite, which suggests that the primary sulphur composition range extends to this value. Salitre barite shows a narrow $\delta^{34}\text{S}$ range (-2.14‰ to +0.51‰). Among the studied complexes Salitre showed the smallest sulphide-sulphate fractionation. We obtained $\delta^{34}\text{S}$ values for pyrite and barite coexisting in the same sample of -5.7‰ and -2.14‰, respectively.

Sulphides from Tapira samples show a $\delta^{34}\text{S}$ range from -13.15‰ to -2.19‰, whereas barite varies from -3.94‰ to -1.31‰, with a single value of +16.75‰ in a sample where barite shows textural evidence of secondary origin. Two coexisting sulphide-sulphate pairs were analysed in carbonatites. One sample yielded $\delta^{34}\text{S}_{\text{Pyrrhotite}} = -11.59\text{\textperthousand}$ and $\delta^{34}\text{S}_{\text{Barite}} = -3.94\text{\textperthousand}$ and the other $\delta^{34}\text{S}_{\text{Pyrrhotite}} = -8.15\text{\textperthousand}$ and $\delta^{34}\text{S}_{\text{Barite}} = -1.31\text{\textperthousand}$. The sulphate-sulphide fractionation in these two cases is of similar magnitude (7.65 and 6.84‰ respectively).

Jacupiranga has a $\delta^{34}\text{S}$ range from -6.09‰ to -0.84‰, peaking at -4‰. It has a $\delta^{34}\text{S}$ distribution similar to Araxá, but suggesting less reducing conditions. Compared to the other analyzed complexes, Jacupiranga shows a much narrower range of $\delta^{34}\text{S}$ values.

5.3. Sulfur isotope variations by rock type

Figure 3.22 illustrates the difference between carbonatite, phoscorite, nelsonite and bebedourite for each complex. Overall, carbonatites show the wider S-isotope range of all rock-types. Sulphides from phoscorites tend to vary in a restricted range in each complex, with the exception of Catalão I nelsonites and Tapira bebedourites.

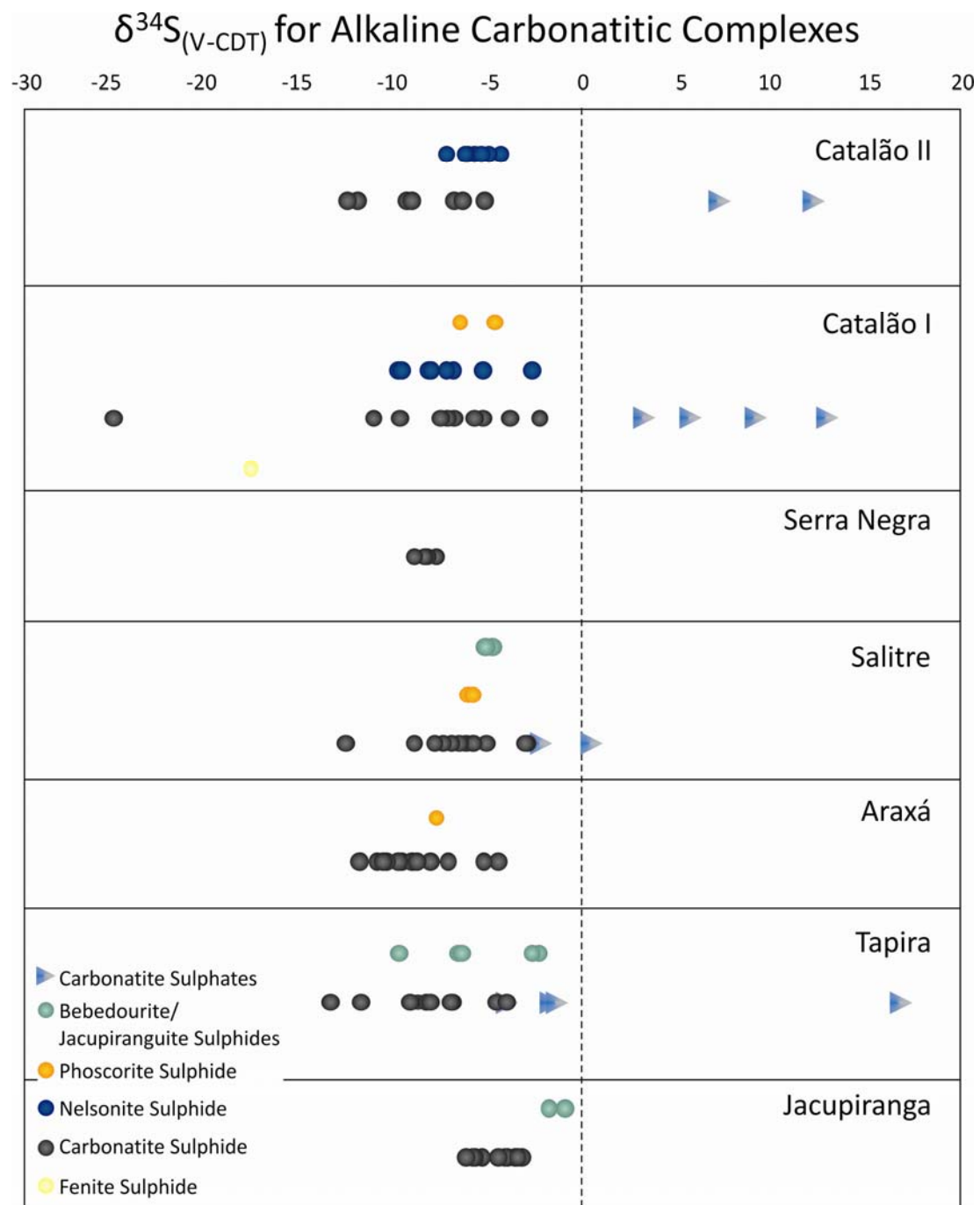


Figure 3.22. Sulphur isotope data for sulphides and sulphates from the APIP and Jacupiranga alkaline carbonatite complexes, by host rock type and complex.

Sulphides in nelsonites from Catalão II show a more restricted $\delta^{34}\text{S}$ range (-7.08‰ to -4.24‰) than carbonatites (-12.31‰ to -5.09‰). Nelsonites from Catalão I seem to span a similar range (-9.6‰

to -2.58‰) to the majority of the associated carbonatites, while phoscorites are very restricted (-6.37‰ to -4.56‰). Salitre carbonatites vary in a wide range (-12.36‰ to -2.84‰) while bebedourite (-5.03‰ to -4.66‰) and phoscorite (-5.98‰ to -5.72‰) have very restricted isotope compositions. Carbonatites from Araxá also span a relatively wide range (-11.69‰ to -4.40‰). In this complex there is only one analysed phoscorite sample, which does not allow to estimate stable isotope variations in this rock-type. Tapira shows wide ranges for both carbonatite (-13.15‰ to -3.95‰) and bebedourite (-9.55‰ to -2.19‰). Jacupiranga, the only complex that does not belong from APIP, is the one with the least S isotope variation in each rock-type, with values concentrated closer to zero than in the other studied examples. Jacupiranga carbonatites range in $\delta^{34}\text{S}$ from -6.09‰ to -3.15‰, and ultramafic rocks from -1.70‰ to -0.84‰, which is consistent with the highly-preserved character of the primary rocks in this complex and its deeper level of intrusion (e.g. Santos and Clayton, 1995).

Bebedourites/jacupirangites and phoscorites have values of $\delta^{34}\text{S}$ systematically closer to 0‰ (the primary mantle composition) compared to carbonatites for all complexes where data could be obtained for these rock types. This suggests that $\delta^{34}\text{S}$ becomes progressively more negative with the evolution of the complex. The fact that carbonatites (and possibly nelsonites) show a much wider range than other rocks may result of their genesis involving other petrogenetic processes besides crystal fractionation (e.g. liquid immiscibility and degassing) allow us to deduce that with evolution of the complex, $\delta^{34}\text{S}$ show more negative values until carbonatites that shows a large range because evolves other magmatic process beyond fractionation (nelsonites probably have a similar behavior).

5.4. Sulfur isotope variations from rim to core

The core and rim of some samples show different isotopic compositions, especially for Catalão I pyrite grains. The core is consistently more depleted in ^{34}S than the rim. This indicates that at the time of crystallization of the rim, the magma was more oxidized (or less reduced) than at an earlier stage when the core crystallized (figure 3.23). In addition to the *in situ* variation, Catalão I samples show a systematic change in isotopic composition, increasing in $\delta^{34}\text{S}$ from around -8‰ to values close to 0. Figure 3.23 illustrates the compositional variation and table 3.04 shows $\delta^{34}\text{S}$ results from core and rim.

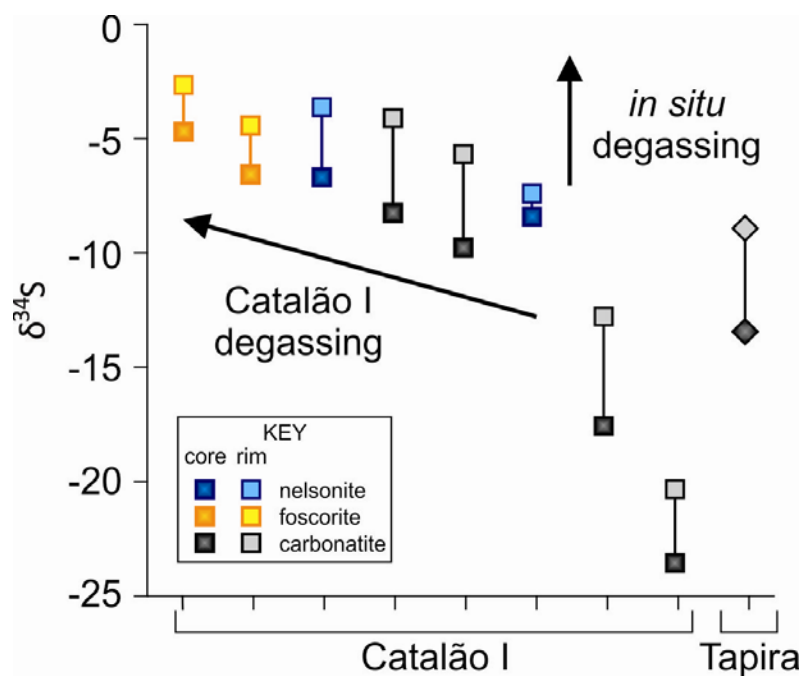


Figure 3.23. Sulphur isotope data for samples with evidence of degassing, showing different values from core to rim. Note that both the variation in single grains and the comparison between different rock types indicate increasing values of $\delta^{34}\text{S}$ with progressive degassing.

This variation can be correlated with the degassing of volatile species containing sulfur, altering not only the oxygen fugacity of the residue but its S isotopic composition as well. When the magma undergoes degassing, crystallization conditions change abruptly, immediately generating a quench-like fabric (Junqueira-Brod *et al.* in preparation). The crystallized phases register the difference in isotopic composition, since the core/border have not achieved equilibrium. Therefore it is reasonable to assume that magma evolves from an originally higher concentration of ^{32}S towards a heavier composition, richer in ^{34}S , as degassing takes place. This is evident by the $\delta^{34}\text{S}$ evolution depicted in figure 3.23. Comparatively the Tapira sample shown in the diagram recorded initial to early stages of S degassing in magma evolution.

Another important feature observed in figure 3.23 is that samples related with late stages of the complex evolution or with metassomatic alteration have very negative $\delta^{34}\text{S}$, between -25 and -10‰, but still show differences from rim to core.

Table 3.04 – Sulphur isotope data for the samples that present differences between rim and core.

Sample	rock	complex	core	rim
CB04	nelsonite	Catalão I	-4.48	-2.83
CB14	foscrite	Catalão I	-6.37	-4.56
AC328,30I	nelsonite	Catalão I	-6.41	-3.69
07C1CO3	Mg carbonatite	Catalão I	-8.05	-4.31
07C1CO3	Mg carbonatite	Catalão I	-9.54	-5.80
AC32830	nelsonite	Catalão I	-8.21	-7.57
C1 SH1	carbonatite	Catalão I	-17.46	-12.98
C1 SH3	carbonatite	Catalão I	-23.45	-20.55
AT 135	Mg carbonatite	Tapira	-13.58	-8.87

5.5. Sulphide-sulphide isotopic variation

Figure 3.24 shows histograms for $\delta^{34}\text{S}$ in the different sulphide types. The distribution is slightly asymmetric towards lower $\delta^{34}\text{S}$ for pyrite data, symmetric for chalcopyrite, and slightly asymmetric towards higher $\delta^{34}\text{S}$ for pyrrhotite. Sulphur isotope data for chalcopyrite, pyrite and pyrrhotite plot at different values (figure 3.24). Chalcopyrite is more depleted in ^{32}S than pyrite (small range) and this, in turn, is more depleted than pyrrhotite in the APIP results. For Jacupiranga, there is a smaller number of analyses and the ranges of pyrite and chalcopyrite overlap largely, although the latter extends to slightly more ^{34}S -depleted values. The overall sense of the progressive shift in $\delta^{34}\text{S}$ is in good agreement with pyrite-chalcopyrite and pyrite-pyrrhotite fractionation of S stable isotopes (e.g. Kajiwra and Krouse, 1971).

Metasomatic sulphide samples show a very depleted ^{34}S signature ($\delta^{34}\text{S}_{(\text{V}-\text{CDT})} = -25\text{\textperthousand}$ to $-14\text{\textperthousand}$), whereas sulphide from rocks without evidence of metasomatic alteration yield isotope data of $\delta^{34}\text{S}_{(\text{V}-\text{CDT})} = -11\text{\textperthousand}$ to 0\textperthousand , although a more restricted range is observed within individual complexes.

Pairs of coexisting sulphide species occur in some of the analysed samples, but this sulphides were not found to be in textural equilibrium. On the other hand, in many of the samples that did include more than one sulphide phase in equilibrium, one or more of the phases were too fine-grained to be reliably analysed by LA-MC-ICP-MS. These features prevent us from establishing a more detailed discussion on the sulphide-sulphide fractionation and crystallization temperatures at this stage.

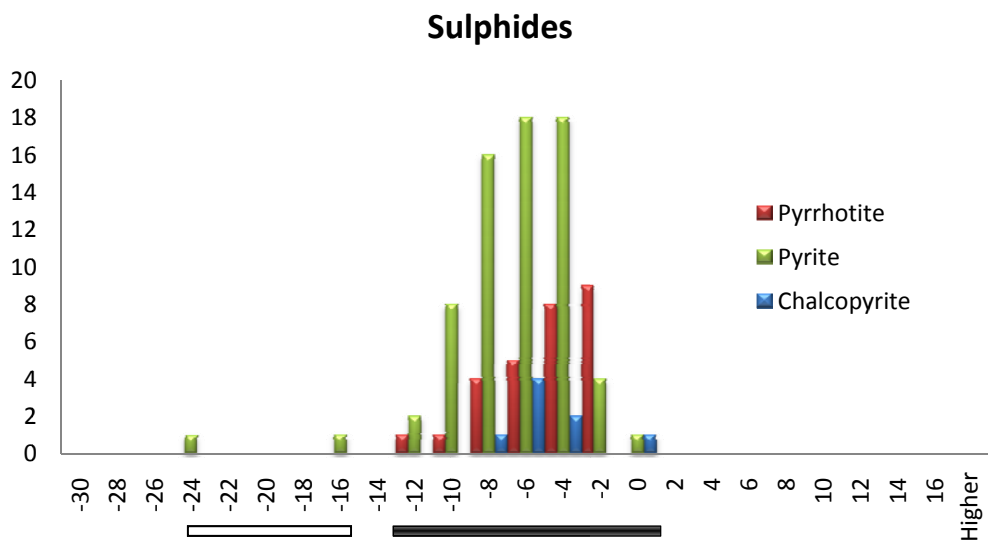


Figure 3.24. Sulphur isotope data for sulphides from the studied alkaline carbonatitic complexes. Black solid horizontal bar: magmatic sulphide; Unfilled horizontal bar: sulphide from fenites.

5.6. Sulphide-sulphate isotopic variation and fractionation

Figure 3.25 shows the isotopic difference between sulphide and sulphate in the same sample. Only samples from Catalão I, Salitre e Tapira were analysed for both minerals. Catalão I shows a large difference between sulphur isotope composition of pyrite and barite, whereas Salitre samples yielded the smallest fractionation values. Tapira shows an intermediate behaviour, except for one sample with a large fractionation between pyrrhotite and barite.

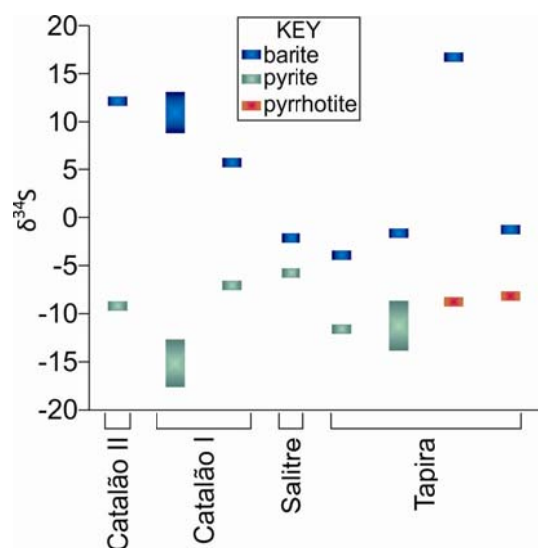


Figure 3.25. Sulphur isotope composition for sulphide and sulphate in the same sample.

We analysed sulphide-sulphate assemblages from eight carbonatite samples: one from Catalão II, two from Catalão I, one from Salitre and four from Tapira. However, in three of these samples the textural characteristics of barite suggest that it is secondary, particularly in some of the Tapira samples. The remaining five samples were used to model the crystallization temperatures as a function of sulphide-sulphate isotope fractionation, using the parameters of Miyoshi *et al.*(1984). The results are shown in figure 3.26.

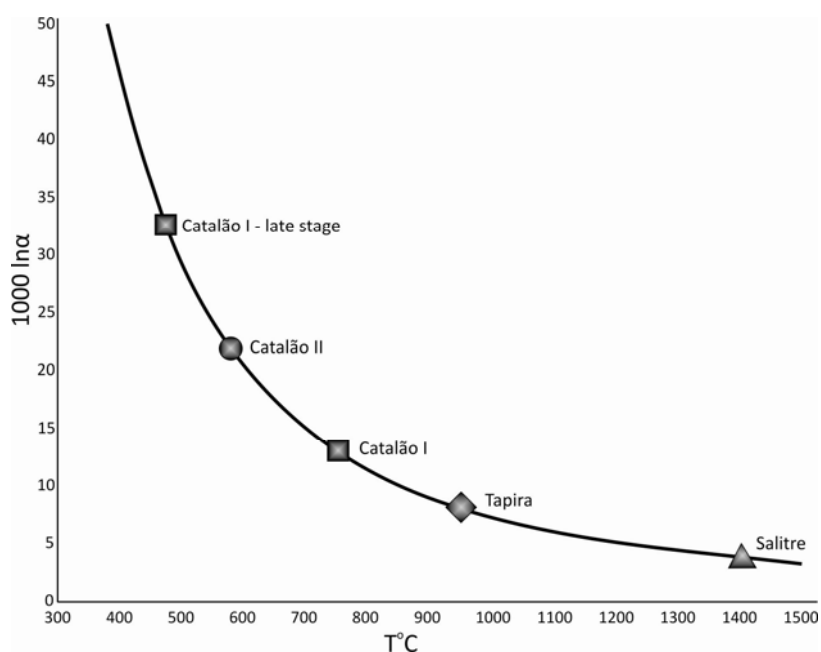


Figure 3.26. Modelling of sulphide-sulphate fractionation (Miyoshi *et al.*, 1984) for the studied samples.

Catalão II fractionation temperature plots about 550°C , compatible with the temperature of carbonatite formation (e.g. Wyllie, 1966).

Catalão I yielded temperatures close to 750°C for one sample of preserved carbonatite and 475°C for one sample of late carbonatite. In late-stage Ba- and REE-rich carbonatite magmas the liquid phase can persist to lower temperatures (543°C , Jones and Wyllie, 1983) then the normal carbonatite solidus, and temperatures measured in the erupting Oldoinyo Lengai lavas were as low as 490°C (Kraft and Keller, 1989). Thompson *et al.* (2002) reported temperatures as low as 420°C from the Swartbooisdrif ankerite carbonatite, Namibia.

Tapira shows a calculated temperature of 950°C. The Salitre sample plots at 1400°C, which is an exceedingly high temperature for this system. We could find no textural reason for this since the mineral assemblages appear to be in textural equilibrium, and the cause of this result is not yet clear.

5.7. Comparison with other carbonatites

Sulphur isotope ranges observed in the APIP and Jacupiranga are broadly comparable with other carbonatite provinces and localities.

Farrel et al (2010) found a more restricted sulphur isotope range in the Superior Province, Canada, where $\delta^{34}\text{S}$ from carbonatitic sulphides plot between -4.5‰ and +3.4‰ and sulphides from carbonatites have lighter S than the associated silicate rocks. In a compilation by Mitchell & Krouse (1975) of sulphur isotope data of some world carbonatites (Mountain Pass, Bearpaw, Magnet cove, Oka and Phalabora), sulphides (except for galena) plot in a range of -11‰ to +5‰ and sulphates from +2‰ to +12‰. Druppel et al (2006) studied the Swartbooisdrif carbonatite and $\delta^{34}\text{S}$ for the carbonatites are -3.3‰ to +5.1‰. Figure 5 compares the APIP complexes with other carbonatites in the world.

Seal et al. (2006) reported a sulphur isotope range for igneous rocks that varies from approximately -5‰ to +15‰. The sulphur isotope results from APIP and Jacupiranga compared with these databases, evidence a similarity with other world carbonatites, although the APIP rocks span a considerably wider range of sulphur isotope compositions.

Sulphur isotope data from APIP is illustrated in the histogram and the range of other carbonatites values are plotted below, as bars. The Oka alkaline-carbonatite complex, Quebec, shows the closest similarities with the APIP range. Russian Carbonatites also possess a similarly wide range, but this is shifted towards more positive values.

Other provinces have more restricted and/or near to 0‰ compositions. Despite the variations within each complex/province in figure 3.27, there is a clear trend of decreasing $\delta^{34}\text{S}$ of sulphides with decreasing age, which may suggest a long-term evolution of the sulphur isotope composition of the mantle. Available barite data are too few (Mountain Pass and Tuva) for their behavior to be assessed,

figure 3.28 presents the subset of $\delta^{34}\text{S}$ for sulphides only, versus carbonatites age (log scale) to depict S variation through age.

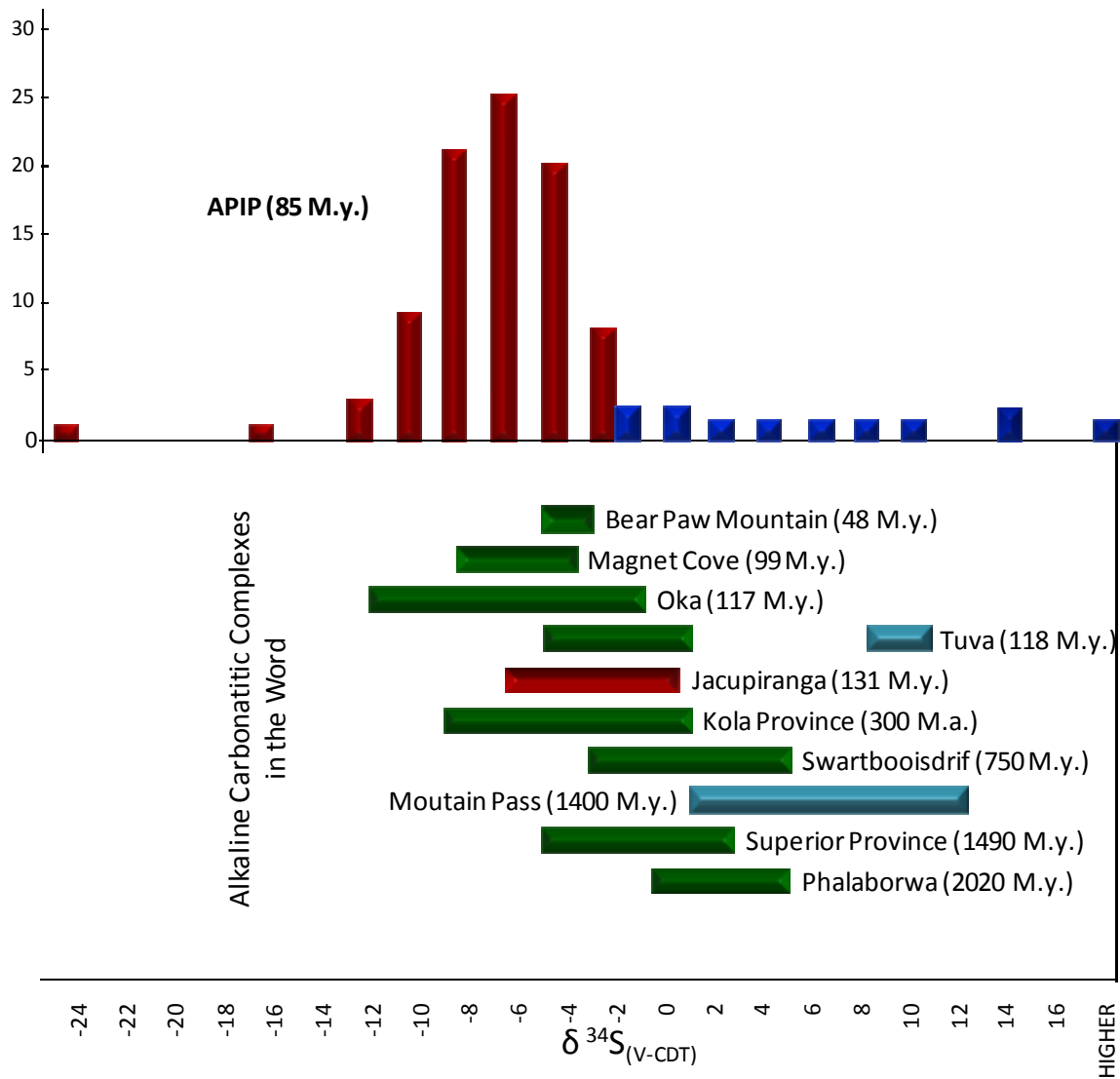


Figure 3.27. Sulphur isotope data from alkaline carbonatite complexes in the World. APIP results (this work) are shown as vertical bars in the top section of the figure – blue and red bars represent barite and sulphides, respectively. The horizontal bars (green = sulphides, light blue = barite) in the bottom section represent other worldwide complexes, in order of increasing age from top to bottom: Bearpaw Mountain (Mitchell & Krouse 1975; ~48Ma - Duke, 2009), Magnet Cove (Mitchell & Krouse, 1975; 99Ma - Wooley & Kjarsgaard, 2008), Oka (Mitchell & Krouse 1975; 117Ma - Wooley & Kjarsgaard, 2008), Tuva (118Ma, Nikiforov et al. 2006), Jacupiranga (this work; 131Ma - Wooley & Kjarsgaard, 2008 #), Kola Province (Mitchell & Krouse 1975, Shin & Lee 2007; ~250-340Ma - Downes et al 2005), Swartbooisdrif (Druppel 2006; 750Ma - Wooley & Kjarsgaard, 2008), Mountain Pass (barite data only) (Mitchell & Krouse 1975; 1.4Ga - Wooley & Kjarsgaard, 2008), Superior Province (Farrel et al. 2010; 1,897 Ma to 1,093 Ma - Farrel et al. 2010), Phalaborwa (Mitchell & Krouse 1975; 2.02Ga - Wooley & Kjarsgaard, 2008)

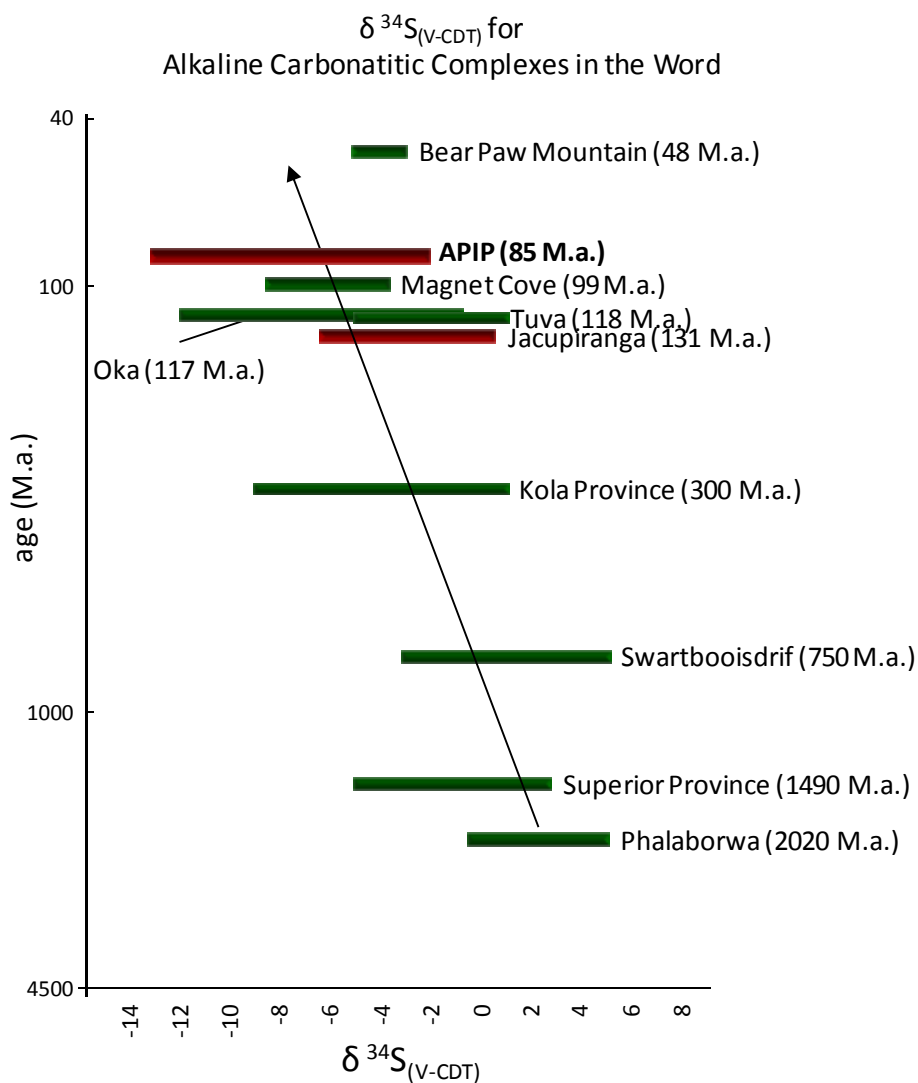


Figure 3.28. Correlation of sulphur isotope composition of worldwide carbonatites with the respective ages. Note the log scale of the age axis. Data sources as in figure 3.27.

6. Conclusions

In this work we presented petrographic, chemical and the first sulphur isotopic data for alkaline-carbonatite complexes of the Alto Paranaíba Igneous Province and for the Jacupiranga complex, in the Ponta Grossa Province.

Some key textural features allowed us to monitor the relationships between magma differentiation processes and sulphur isotope variations. The presence of bladed carbonate and sulphide crystals in some carbonatites indicates quenching, with rapid crystallization of these minerals (e.g. Gomide *et al.*, 2008, Junqueira-Brod *et al.*, in preparation). This is consistent with the presence of "dusty", microgranular to cryptocrystalline masses of carbonate, sulphide and barite interstitial to bladed carbonate crystals. Furthermore, the coexistence of sulphides and barite indicates important variations in the oxygen fugacity during crystallization. We interpret these textures as quench fabric, formed by rapid crystallization of a supercooled carbonatite magma during degassing. This process has consequences for the sulphur (see below) and carbon and oxygen (Junqueira-Brod *et al.*, in preparation) stable isotope variations.

Microprobe analyses of the studied sulphides did not show wide deviations from the respective ideal compositions. Some trace elements may be present in significant amounts in pyrite and, to a lesser extent, in pyrrhotite, whereas chalcopyrite analyses were always very close to stoichiometry. No significant chemical changes were noted between core and rim in the analysed sulfide grains.

Barite also shows little chemical variation: only strontium and selenium are significant trace substitutions. Sr is a common solid solution in sulphates (barite/celestine) and Se usually replaces sulphur in sulphides and sulphates structures (Deer *et al.* 1992). Our results show that Se replacement is more expressive in sulphate than in sulphide structure.

Serra Negra (on the basis of only a few analyses), Salitre, Araxá and Jacupiranga show narrow $\delta^{34}\text{S}$ ranges, and Salitre and Jacupiranga are characterized by values closest to primary mantle. Catalão I, Catalão II and Tapira show a wide range which may represent the effect of more variable differentiation process involved in the formation of these rocks.

This interpretation is also consistent with the sulphur isotope composition of barite, which shows wider ranges in Catalão I and Catalão II, but a narrow (near to 0‰) range for Salitre and Tapira.

Bebedourites/Jacupirangites and phoscorites have values of $\delta^{34}\text{S}$ systematically closer to 0‰ than those of carbonatites in all complexes where these rock types were analysed. Where data is available for both ultramafic silicate rocks and phoscorites, the former are even closer to 0‰ than the latter. This suggests that, in each complex, $\delta^{34}\text{S}$ shifts toward more negative values with magma evolution. Also, late-stage rocks, such as carbonatites and, probably, nelsonites, tend to undergo other

differentiation processes (e.g. liquid immiscibility and degassing) in addition to fractional crystallisation, which may partially explain the wider observed $\delta^{34}\text{S}$ ranges in these rocks.

Metasomatic sulphides show distinctly negative $\delta^{34}\text{S}$ values as shown by Drüppel *et al.* (2006) in fenites from Swartbboisdrif.

In a few of our nelsonite and carbonatite samples, the studied phases register differences in isotopic composition between core and rim of crystals, indicating that equilibrium was not achieved. In all cases the rim isotopes are heavier than in the corresponding core. Many of these samples show petrographic evidence of quenching, leading us to conclude that this difference is caused by degassing, and that magma evolves from a high ^{32}S content towards a heavier ^{34}S -rich composition, as degassing takes place. Comparatively, the sample from Tapira recorded sulphur degassing at an earlier stage in magma evolution than those of Catalão I.

The experimental work by Zheng (1990) showed that the Rayleigh distillation during outgassing of either SO_2 or H_2S can considerably change the isotopic composition of sulfur remaining in the melt, depending on the sulphate/sulphide ratio, which is controlled by $f\text{O}_2$, the fraction of sulfur remaining and the temperature at the time of outgassing. In the same study, Zheng (1990) argued that, at high $f\text{O}_2$, the $\delta^{34}\text{S}$ of the solidified rocks will be driven in the positive direction, due to equilibrium loss of the light gaseous sulfur species, whereas at low $f\text{O}_2$, the $\delta^{34}\text{S}$ of the crystallized rocks will shift in the negative direction. In carbonatite systems, the redox stage is also strongly dependent on CO_2 degassing, which greatly affects the $f\text{O}_2$ of the system (Gomide *et al.* 2009, Junqueira-Brod *et al.*, in preparation). Therefore, the redox state of such a system will depend on a complex interplay of distinct degassing events and conditions, in addition to fractional crystallization and, possibly, liquid immiscibility. The full comprehension of these controls requires complementary studies.

The results presented in this work indicate that as magma differentiation progresses from ultramafic rocks (jacupirangite, bebedourite) through phoscorites to nelsonites and carbonatites, it consumes particularly the heavier sulphur isotopes into the solid phases leaving a residual magma/fluid enriched in ^{32}S represented by lower $\delta^{34}\text{S}$. On the other hand, the observed core-to-rim variations in sulphides from samples with petrographic evidence of degassing showed that the residue of degassing evolved toward higher $\delta^{34}\text{S}$, and that sulphur loss happened at high $f\text{O}_2$.

Temperatures calculated using sulphide-sulphate isotope fractionation for Catalão II (ca. 550°C), Catalão I (ca. 750°C for an early-stage carbonatite and 475°C for a late-stage carbonatite) are within the expected ranges for this type of magma.

Sulphur isotope ranges observed in the APIP and in the Jacupiranga complex are broadly comparable with other carbonatite provinces and localities (Mitchell & Krouse 1975; Nikiforov *et al.* 2006; Shin & Lee 2007; Druppel 2006; Farrel *et al.* 2010) and with the expected variation of sulphur isotopes in igneous rocks (ca. -5‰ to ca. +15‰, Seal *et al.*, 2006), kimberlites (ca. -13‰ to ca. +5‰, Seal *et al.*, 2006) and carbonatites (ca. -13‰ to ca. +2‰, Deines, 1989). The comparison of sulphur isotopes results from carbonatites of different ages shows a general trend of decreasing $\delta^{34}\text{S}$ of sulphides with decreasing age. This may suggest a long-term evolution of the sulphur isotope composition of the mantle/source.

7. References

- Almeida, F.F.M. 1983. Relações Tectônicas das rochas alcalinas mesozóicas da região meridional da Plataforma Sul-Americana. Revista Brasileira de Geociências 13, 139-158.
- Bailey, D.K. and Hampton, C.M. 1990. Volatiles in alkaline magmatism. Lithos 26, 157-165.
- Barbosa, E.S.R., Brod, J.A., Junqueira-Brod, T.C., Gaspar, J.C., Ribeiro, C.C., Boaventura, G.R., 2004. Petrografia e geoquímica de carbonatitos do Complexo de Salitre, Congresso Brasileiro de Geologia, XLII.
- Barbosa, E.S.R., Junqueira-Brod, T.C., Brod, J.A., Dantas, E.L., 2008. Petrology of bebedourites from the Salitre phoscorite-carbonatite complex, Brazil, 9th International Kimberlite Conference, Frankfurt.
- Barbosa, E.S.R. 2009. Mineralogia e Petrologia do Complexo Carbonatítico-Foscorítico de Salitre, MG. Tese (Doutorado em Geologia) – Universidade de Brasília.
- Barbosa, E.S.R., Brod, J.A., Junqueira-Brod, T.C., Cordeiro, P.F.O., Santos, R.V., Dantas, E.L., 2009. Mineralogia e geoquímica dos foscoritos do Complexo de Salitre, MG, Simpósio de Geologia do Centro-Oeste, XI, Cuiabá, MT.
- Brod, J.A., 1999. Petrology and geochemistry of the Tapira alkaline complex, Minas Gerais State, Brazil. Ph. D. Thesis, University of Durham, Durham, UK, 486 pp.
- Brod, J. A., Gaspar, J. C., de Araújo, D. P., Gibson, S. A., Thompson, R. N. & Junqueira-Brod, T. C. (2001). Phlogopite and tetra-ferriphlogopite from Brazilian carbonatite complexes: petrogenetic constraints and implications for mineral-chemistry systematics. Journal of Asian Earth Sciences 19, 265-296.
- Brod, J.A., Gibson, S.A., Thompson, R.N., Junqueira-Brod, T.C., Seer, H.J., Moraes, L.C., Boaventura, G.R.. 2000. The kamafugite-carbonatite association in the Alto Paranaíba Igneous Province, southeastern Brazil. Revista Brasileira de Geociências 30 (3),. 404-408.
- Brod, A. J., Junqueira-Brod, T. C., Gaspar, J. C., Gibson, S. A., Thompson, R. N. 2003. Mineral-Chemistry fingerprints of liquid immiscibility and fractionation in the Tapira alkaline-carbonatite complex (Minas Gerais, Brazil).8th International Kimberlite Conference Long Abstract.
- Brod, J.A., Ribeiro, C.C., Gaspar, J.C., Junqueira-Brod, T.C., Barbosa, E.S.R., Riffel, B.F., Silva, J.F., Chaban, N., Ferrari, A.J.D. 2004. Excursão 1: Geologia e Mineralizações dos Complexos Alcalino-Carbonatíticos da Província Ígnea do Alto Paranaíba. São Paulo: Sociedade Brasileira de Geologia, (Guia de excursão).

- Brod, J. A. ; Barbosa, E.S.R. ; Junqueira-Brod, T. C. ; Gaspar, J.C. ; Diniz-Pinto, H.S. ; Sgarbi, P. B. A. ; Petrinovic, I.A. 2005 . The Late-Cretaceous Goiás Alkaline Province (GAP), Central Brazil. In: Piero Comin-Chiaromonti; Celso de Barros Gomes. (Org.). Mesozoic and Cenozoic alkaline magmatism in the Brazilian Platform. São Paulo: Edusp, p. 261-316.
- Carlson, R.W., Araújo, A.L.N., Junqueira-Brod, T.C., Gaspar, J.C., Brod, J.A., Petrinovic, I.A., Hollanda, M.H.B.M., Pimentel, M.M., Sichel, S.E. 2007. Chemical and Isotopic Relationships between Peridotite Xenoliths and Mafic-Ultrapotassic Rocks from Southern Brazil. *Chemical Geology*, v. 242, p. 418-437.
- Carvalho, W.T., Bressan, S.R. 1997. Depósitos de Fosfato, Nióbio, Titânio, Terras Raras e Vermiculita de Catalão I - Goiás. In: Schobbenhaus Filho, C., Queiroz, E.T., Coelho, C.E.S. (Eds.), *Principais Depósitos Minerais do Brasil*. DNPM, Brasília, pp. 69-93.
- Comin-Chiaromonti, P., Gomes, C.B., 1996. Alkaline magmatism in Central-Eastern Paraguay. Relationships with coeval magmatism in Brazil. Edusp/Fapesp, São Paulo, 458 pp.
- Comin-Chiaromonti, P. & Gomes, C. B. (eds). 2005. Mesozoic to Cenozoic Alkaline Magmatism in the Brazilian Platform. 750 pp.
- Coplen, T.B., and Krouse, H.R. 1998. Sulphur isotope data consistency improved: *Nature*, v. 392, p. 32.
- Cordeiro, P.F.O., Brod, J.A., Dantas, E.L., Barbosa, E.S.R. 2010. Mineral chemistry, isotope geochemistry and petrogenesis of niobium-rich rocks from the Catalão I carbonatite-phoscorite complex, Central Brazil. *Lithos* 118, 223-237.
- Cordeiro, P.F.O., Brod, J.A., Santos, R.V., Dantas, E.L., Oliveira, C.G., Barbosa, E.S.R., 2011. Stable (C, O) and radiogenic (Sr, Nd) isotopes of carbonates as indicators of magmatic and post-magmatic processes of phoscorite-series rocks and carbonatites from Catalão I, central Brazil. *Contributions to Mineralogy and Petrology*, 161(3): 451-464.
- Craddock, P.R., Rouxel, O.J., Ball, L.A., Bach, W. 2008. Sulfur isotope measurement of sulfate and sulfide by high-resolution MC-ICP-MS. *Chemical Geology*, v.253, p.102-113.
- Deer, W.A., Howie, R.A., Zussman, J. 1992. An Introduction to the Rock-Forming Minerals. Longman Pub Group.
- Deines, P. 1989. Stable isotope variations in carbonatites. In: Bell K. (ed) *Carbonatites: genesis and evolution*, Unwin Hyman, p 301-359.

- Ding, T., Valkiers, S., Kipphardt, H., De Bièvre, P., Taylor, P.D.P., Gonfiantini, R., Krouse, R. 2001. Calibrated sulfur isotope abundance ratios of three IAEA sulfur isotope reference materials and V-CDT with reassessment of the atomic weight of sulfur. *Geochimica et Cosmochimica Acta* 65, 2433-2437.
- Downes, H., Balaganskaya, E., Beard, A., Liferovich, R., Demaiffe, D. 2005. Petrogenetic process in the ultramafic, alkaline and carbonatitic magmatism in the Kola Alkaline Province: A review. *Lithos* 85, 48-75.
- Drüppel, K., Wagner, T., Boyce, A. J. 2006. Evolution of Sulfide Mineralization in Ferrocarbonatite, Swartbooisdrif, Northwestern Namibia: Constraints from Mineral Compositions and Sulfur Isotopes. *The Canadian Mineralogist* 44, 877-894.
- Duke, G.I. 2009. Black Hills-Alberta carbonatite-kimberlite linear trend: Slab edge at depth? *Tectonophysics* 454, 185-194.
- Ernesto, M., Marques, L.S., Piccirillo, E.M., Molina, E.C., Ussami, N., Comin-Chiaromonti, P., Bellieni, G. 2002. Paraná Magmatic Province-Tristan da Cunha plume system: fixed versus mobile plume, petrogenetic considerations and alternative heat sources. *Journal of Volcanology and Geothermal Research* 2484, 1-22.
- Ernesto, M. 2005. Paleomagnetism of the post-paleozoic alkaline magmatism in the Brazilian platform: questioning the mantle plume model. In: Comin-Chiaromonti, P. & Gomes, C. B. (eds). *Mesozoic to Cenozoic Alkaline Magmatism in the Brazilian Platform*. 750 pp.
- Farrel, S., Bell, K., Clark, I. 2010. Sulphur isotopes in carbonatites and associated silicate rocks from the Superior Province, Canada. *Miner. Petrol.* 98, 209-226.
- Gibson, S.A., Thompson, R.N., Dickin, A.P., Leonardos, O.H. 1995a. High-Ti and low-Ti mafic potassic magmas: Key to plume-lithosphere interactions and continental flood-basalt genesis. *Earth Planetary Science Letters* 136, 149-165.
- Gibson, S. A., Thompson, R. N., Leonardos, O. H., Dickin, A. P. & Mitchell, J. G. 1995b. The Late Cretaceous impact of the Trindade mantle plume - evidence from large-volume, mafic, potassic magmatism in SE Brazil. *Journal of Petrology* 36, 189-229.

- Gibson, S.A., Thompson, R.N., Weska, R., Dickin, A.P. and Leonardos, O.H. 1997. Late Cretaceous rift-related upwelling and melting of the Trindade starting mantle plume head beneath western Brazil. Contributions to Mineralogy and Petrology 126, 303-314.
- Gomes, C.B., Ruberti, E., Morbidelli, L. 1990. Carbonatite complexes from Brazil: A review. Journal of South American Earth Sciences 3, 51-63.
- Gomide, C.S., Brod, J.A., Palmieri, M., Santos, R.V., Junqueira-Brod, T.C., Marchão, M.O., Silva, P.G.N., Braga, L.M.V., Paulino, F., Silveira, D.A. 2008. Estudo preliminar de isótopos estáveis de carbono e oxigênio na associação kamafugito-carbonatito-foscorito da Província Ígnea do Alto Paranaíba. IV Simpósio de Vulcanismo, Foz do Iguaçu-PR.
- Gomide, C.S., Junqueira-Brod, T.C., Brod, J.A., Dardenne, M.A., Palmieri, M., Santos, R.V. Relações entre Geoquímica e processos de desgasificação em carbonatitos do complexo de Catalão I, Goiás. 2009. XI Simpósio de Geologia do Centro-Oeste, Cuiabá, MT, 1 pp.
- Gomide, C.S., Brod, J.A., Buhn, B.M. 2010. Sulfur isotopes from de Catalão I alkaline carbonatite complex, Alto Paranaiba Igneous Province, GO, Brazil. VII South American Symposium on Isotope Geology, Brasilia, Brazil.
- Grasso, C.B., Ribeiro, C.C., Brod, J.A., Gaspar, J.C., 2006. Mapeamento de detalhe (1:2000) das frentes de lavra da mina da Fosfértil Fertilizantes Fosfatados S.A. In: Silva, M.G., Franca-Rocha, W.J.S. (Editors), Congresso Brasileiro de Geologia, XLIII. SBG, Aracaju, pp. 796-801.
- Grasso, C.B., Brod, J.A., 2009. As séries bebedourítica, carbonatítica e foscorítica no complexo de Serra Negra, MG, Simpósio de Geologia do Centro-Oeste, Cuiabá, MT, pp. 1 pp.
- Grasso, C.B., Brod, J.A., Santos, R.V., 2010. Oxygen and carbon isotope study of the Serra Negra Complex, Alto Paranaíba Igneous Province, SE Brazil, South American Symposium on Isotope Geology, VII, Brasília, pp. 273-276.
- Issa Filho, A., Lima, P.R.A.S., Souza, O.M., 1984. Aspectos da geologia do complexo carbonatítico do Barreiro, Araxá, MG, Brasil. In: CBMM (Ed.), Complexos Carbonatíticos do Brasil: Geologia. CBMM, São Paulo, pp. 20-44.
- Jácomo, M.H., Junqueira-Brod, T.C., Pires, A.C.B., Brod, J.A., Palmieri, M., Ferrari, A.J.D., 2010. Associação de magnetometria, gamaespectrometria, geoquímica e petrografia para modelamento

- tridimensional da mineralização de nióbio do depósito Morro do Padre, Goiás, Brasil, IV Simpósio Brasileiro de Geofísica, Brasília, pp. 4.
- Jones, A. P. & Wyllie, P. J. (1983). Low-temperature glass quenched from a synthetic, rare earth carbonatite: implications for the origin of the Mountain Pass deposit, California. *Economic Geology* 78, 1721-1723.
- Junqueira-Brod, T.C., Gomide C.S., Brod, J.A., Dardenne, M.A., Palmieri, M., Grasso, C., Santos, R.V. Fluidisation processes and breccia formation int the Catalão I and Catalão II Complexes, Alto Paranaíba Igneous Province - APIP, Central Brazil – Evidence for magma fragmentation inside carbonatite magma chambers. In Preparation.
- Kajiwra, Y. and Krouse, H.R. 1971. Sulfur isotope partitioning in metallic sulfide systems. *Canadian Journal of Earth Sciences* 8, 1397-1408.
- Klein, C. 2002. *Mineral Science*, 405 pp.
- Krafft, M. & Keller, J. (1989). Temperature-Measurements in Carbonatite Lava Lakes and Flows from Oldoinyo-Lengai, Tanzania. *Science* 245, 168-170.
- Leonardos, O. H., Ulbrich, M. N., Gaspar, J. C. 1991. The Mata da Corda volcanic rocks. 5th Int. Kimberlite Conf. Field Guide 65-73.
- Machado Junior D.L. 1992. Geologia do complexo alcalino-carbonatítico de Catalão II (GO). 37 Congresso Brasileiro Geologia (Bol. Res. Exp.). São Paulo, 94-95.
- Mariano A.N., Marchetto M. 1991. Serra Negra and Salitre carbonatite alkaline igneous complex. In O.H. Leonardos, H.O.A. Meyer, J.C. Gaspar (Eds.), 5th Internat. Kimb. Conf. (Field Guide Book). Araxá, CPRM, Sp. Publ. 3/91. 75-79.
- Mitchell, R. H., Krouse, H. R. 1975. Sulphur isotope geochemistry of carbonatites. *Geochimica et Cosmochimica Acta*, 39 (11), 1505-1513.
- Miyoshi, T., Sakai, H., Chiba, H. 1984. Experimental study of sulfur isotope fractionation factors between sulfate and sulfide in high temperature melts. *Geochemical Journal*, 18: 75-84.
- Morbidelli, L., Gomes, C.B., Beccaluva, L., Brotzu, P., Conte, A.M., Ruberti, E., Traversa, G. 1995. Mineralogical, petrological and geochemical aspects of alkaline and alkaline-carbonatite associations from Brazil. *Earth Science Reviews*, v.39. p.135-168.

- Nikiforov, A. V., Bolonim, A. V., Pokrovsky, B. G., Sugorakova, A. M., Chugaev, A. V., Lykhin, D. A. 2006. Isotope Geochemistry (O, C, S, Sr) and Rb–Sr Age of Carbonatites in Central Tuva. *Geology of Ore Deposits* 48 (4), 256–276.
- Oliveira, I.W.B., Sachs, L.L.B., Silva, V.A., Batista, I.H., 2004. In: Schobbenhaus,C., Gonçalves,J.H., Santos, J.O.S., Abram, M.B., Leão Neto, R., Matos, G.M.M., Vidotti, R.M., Ramos, M.A.B., Jesus, J.D.A. de (eds.). *Carta Geológica do Brasil ao Milionésimo: Sistema de Informações Geográficas - SIG e 46 folhas na escala 1 : 1.000.000*. Brasília: CPRM, 2004. 41 CD-ROM's.
- Palmieri, M., Ferrari, A.J.D., Brod, J.A., Barbosa, P.A.R., 2006. Geologia da mina de fosfato da Copebrás no Complexo Foscórtico-Carbonatítico de Catalão I, 43 Congresso Brasileiro de Geologia. Aracajú. Sociedade Brasileira de Geologia, Aracajú, SE, pp. 791-795.
- Palmieri, M., Silva, S.E., Brod, J.A., Ferrari, A.J.D., Barbosa, P.A.R., Jácomo, M.H., Junqueira-Brod, T.C., Cordeiro, P.F.O., 2009. A mineralização de nióbio do Alvo Morro do Padre, Catalão II, GO, Simpósio de Geologia do Centro-Oeste, XI, Cuiabá, MT, pp. 32.
- Palmieri, M., 2011. Modelo Geológico e Avaliação de Recursos Minerais do Depósito de Nióbio Morro do Padre, Complexo alcalino-carbonatítico Catalão II, GO, dissertação de mestrado. Universidade de Brasília, Brasília.
- Qi, H.P., and Coplen, T.B. 2003. Evaluation of the $^{34}\text{S}/^{32}\text{S}$ ratio of Soufre de Lacq elemental sulfur isotopic reference material by continuous flow isotope-ratio mass spectrometry: Chemical Geology 199, 183-187.
- Ribeiro, C.C., Brod, J.A., Junqueira-Brod, T.C., Gaspar, J.C., Petrinovic, I.A., 2005. Mineralogical and field aspects of magma fragmentation deposits in a carbonate-phosphate magma chamber: evidence from the Catalao I complex, Brazil. *Journal of South American Earth Sciences*, 18(3-4): 355-369.
- Ribeiro, C.C. 2008. Geologia, geometalurgia, controles e gênese dos depósitos de fósforo, terras raras e titânio do Complexo Carbonatítico de Catalão I, GO. Tese (Doutorado em Geologia) - Universidade de Brasília.
- Ruberti, E., Gomes, C.B., Comin-Chiaromonti, P. 2005. The alkaline magmatism from the Ponta Grossa Arch. In: Comin-Chiaromonti, P. & Gomes, C. B. (eds). *Mesozoic to Cenozoic Alkaline Magmatism in the Brazilian Platform*. 750 pp.

- Santos, R. V. & Clayton, R. N. (1995). Variations of oxygen and carbon isotopes in carbonatites: a study of Brazilian alkaline complexes. *Geochimica et Cosmochimica Acta* 59, 1339-1352.
- Seal, R.R. 2006. Sulfur Isotope Geochemistry of Sulfide Minerals. *Reviews in Mineralogy & Geochemistry*, v.61, p.633-677.
- Seer H.J. 1999. Evolução Tectônica dos Grupos Araxá e Ibiá na Sinforma de Araxá-MG. Universidade de Brasília (Tese de Doutorado) 267p.
- Shin, D.B. and Lee, M.J. 2007. Oxygen and sulfur isotope characteristics of Salmagora Complex, Kola Peninsula. *Goldschmidt Conference Abstracts* A932.
- Thompson, R.N., Gibson, S.A., Mitchell, J.G., Dickin, A.P., Leonardos, O.H., Brod, J.A., Greenwood, J.C. 1998. Migrating Cretaceous-Eocene Magmatism in the Serra do Mar Alkaline Province, SE Brazil: Melts from the Deflected Trindade Mantle Plume? *Journal of Petrology* 39, 1493-1526.
- Thompson, R.N., Smith, P.M., Gibson, S.A., Matthey, D.P., Dickin, A.P. 2002. Ankerite carbonatite from Swartbooisdrif, Namibia: the first evidence for magmatic ferrocarbonatite. *Contributions to Mineralogy and Petrology* 143, 377-395.
- Traversa, G., Gomes, C.B., Brotzu, P., Buraglini, N., Morbidelli, L., Principato, M.S., Ronca, S., Ruberti, E., 2001. Petrography and mineral chemistry of carbonatites and mica-rich rocks from the Araxá complex (Alto Paranaiba Province, Brazil). *Anais Da Academia Brasileira De Ciencias*, 73(1): 71-98.
- Wyllie, P.J. (1966): Experimental studies of carbonatite problems: the origin and differentiation of carbonatite magmas, in "Carbonatites", O.F. Tuttle and J. Gittins, eds. New York: Wiley, 311-352.
- Woolley, A.R., Kjarsgaard, B.A., 2008. Carbonatite Occurrences of the World: Map and Database, Geological Survey of Canada. 1 CD-ROM + 1 map.
- Zheng, YF. 1990. Sulfur Isotope Fractionation in Magmatic Systems: Models of Rayleigh Distillation and Selective Flux. *Chinese Journal of Geochemistry* 9 (1).

CAPÍTULO 4

Conclusões

A partir dos dados e argumentos expostos nos capítulos anteriores, é possível obter algumas características das rochas das séries bebedourítica, foscorítica e carbonatítica da APIP, e dos carbonatitos e jacupiranguitos de Jacupiranga (Província Ponta Grossa) e caracterizar seus respectivos sulfetos e sulfatos do ponto de vista petrográfico e da composição de isótopos de S.

Os métodos de análises de isótopos de enxofre, já em rotina no Laboratório de Geocronologia da Universidade de Brasília, desenvolvidos pelo professor Berhard Manfred Buhn, obtiveram bons resultados com precisão analítica em torno de 0,1‰ a 0,5‰. A preparação de amostras com o auxílio da micro-retífica com disco diamantado facilitou a separação das fases minerais de interesse e melhorou o controle (posição do grão na amostra macro e/ou lâmina delgada) dos grãos a serem analisados.

Algumas das características texturais permitiram monitorar as relações entre processos de diferenciação do magma e as variações de isótopos de enxofre. A presença de cristais alongados de carbonato e sulfeto em alguns carbonatitos indica cristalização destes minerais por resfriamento rápido (Gomide *et al.*, 2008, Junqueira-Brod *et al.*, em preparação). A presença de massas microgranulares a criptocristalinas de sulfeto, carbonato e barita, intersticiais aos cristais alongados de carbonato reforça a interpretação de cristalização rápida. Além disso, a presença de sulfeto e barita nessas massas indica importantes variações na fugacidade de oxigênio durante a cristalização. Estas texturas são interpretadas como de congelamento (“quench”), formadas pela cristalização rápida de um magma carbonatítico super-resfriado durante a desgasificação. Este processo tem consequências na variação de isótopos de enxofre (este trabalho) e de carbono e oxigênio (Junqueira-Brod *et al.* em preparação).

As análises de química mineral dos sulfetos estudados não mostraram um afastamento significativo da respectiva composição ideal. Entretanto, alguns elementos-traço (Cu, Pb, Co, Ag, Zn, Ni, Pt, Pd, As, Se) podem estar presentes na pirita, e em menores quantidades na pirrotita e calcopirita. Variações compostionais sistemáticas ou significativas entre núcleo e borda não foram observadas nos sulfetos analisados.

A barita também mostra pouca variação em sua composição química: apenas Sr e Se são elementos-traço relevantes, encontrados em pequenas quantidades. A solução sólida entre bário e estrôncio é comum em sulfatos (barita/celestita) e Se é substituto do S em sulfetos e sulfatos (Deer *et al.* 1992). Os resultados de química mineral obtidos neste trabalho mostram que a substituição de S por Se é mais expressiva nos sulfatos do que nos sulfetos.

Serra Negra (com base em poucas amostras), Salitre, Araxá e Jacupiranga apresentam menores intervalos de $\delta^{34}\text{S}$, e Salitre e Jacupiranga têm os valores mais próximos de 0‰. Catalão I, Catalão II e Tapira mostram um intervalo mais amplo, que pode representar o efeito de processos de diferenciação mais variados na formação dessas rochas, tais como desgaseificação e imiscibilidade de líquidos, além da cristalização fracionada. Essa interpretação é coerente com a composição isotópica de S da barita, que apresenta amplos intervalos em Catalão I e II, mas restritos e próximos de 0‰ para Salitre e Tapira.

Em todos os complexos nos quais bebedouritos/jacupiranguitos e foscoritos foram analisados, essas rochas exibem valores de $\delta^{34}\text{S}$ sistematicamente mais próximos de 0‰ do que os carbonatitos associados. Nos complexos onde se obteve dados de rochas silicáticas ultramáficas e foscoritos, as primeiras são ainda mais próximas de 0‰ que as últimas. Esses dados sugerem que $\delta^{34}\text{S}$ torna-se progressivamente mais baixo com a evolução do magma. Rochas tardias como carbonatitos e, provavelmente, nelsonitos tendem a ser afetadas por outros processos de diferenciação (imiscibilidade de líquidos e desgaseificação) além da cristalização fracionada, o que pode estar relacionado com os amplos intervalos de valores para $\delta^{34}\text{S}$ observados nessas rochas.

Os sulfetos metassomáticos mostram valores de $\delta^{34}\text{S}$ distintamente negativos como mostrado por Drüppel *et al.* (2006) em fenitos de Swartboisdrif.

Em algumas amostras de carbonatito e nelsonito, observou-se diferenças sistemáticas nas composições isotópicas entre núcleo e borda dos cristais de sulfetos, indicando que não foi alcançado equilíbrio isotópico durante a cristalização. Em todos os casos, os isótopos na borda são mais pesados do que no núcleo correspondente. Muitas dessas amostras têm evidências petrográficas de resfriamento rápido, levando a concluir que tal diferença é causada por desgaseificação de espécies voláteis contendo enxofre, e que o magma evolui de alto conteúdo em ^{32}S para uma composição mais pesada, enriquecida em ^{34}S com a evolução da desgaseificação. A amostra de Tapira mostra

desgaseificação de enxofre em um estágio anterior da evolução do magma se comparada às amostras de Catalão I.

Zheng (1990) fez cálculos baseados em estudos experimentais e mostrou que a destilação *Rayleigh* durante a desgaseificação, tanto de SO₂ como de H₂S pode afetar de maneira importante a composição isotópica do enxofre que restou no magma, dependendo da razão sulfato/sulfeto, que é controlada pela fO₂, da fração que resta de enxofre e da temperatura no momento da desgaseificação. No mesmo estudo, Zheng (1990) demonstrou que em alta fO₂ o δ³⁴S das rochas formadas será desviado para valores mais altos, devido à perda do equilíbrio por desgaseificação, enquanto que em baixa fO₂, o δ³⁴S das rochas cristalizadas é deslocado para valores mais negativos. Além disso, em sistemas carbonatíticos o estado de óxido-redução é altamente dependente da desgaseificação de CO₂ (Gomide *et al.* 2009, Junqueira-Brod *et al.*, em preparação). Portanto, o estado redox de um sistema vai depender de uma complexa interação entre diferentes eventos e condições de desgaseificação, além de cristalização fracionada e possivelmente imiscibilidade de líquidos. Estudos complementares são necessários para uma melhor compreensão desses controles e interações.

Os resultados apresentados neste trabalho, indicam que à medida que a diferenciação progride desde as rochas ultramáficas (jacupiranguito, bebedourito), passando por foscoritos, até nelsonitos e carbonatitos, ocorre consumo preferencial de isótopos mais pesados de enxofre na fase sólida, deixando o magma residual enriquecido em ³²S, o que se traduz em menor valor de δ³⁴S. Por outro lado, as variações observadas do núcleo para a borda dos grãos em sulfetos, em amostras com evidências petrográficas de desgaseificação mostraram que, neste processo, o resíduo evoluiu para maiores valores de δ³⁴S e que, portanto, a desgaseificação de enxofre aconteceu em alta fO₂.

O fracionamento isotópico sulfeto-sulfato permitiu o cálculo de temperaturas de cristalização para carbonatitos de Catalão II (aproximadamente 550°C) e Catalão I (aproximadamente 750°C para um carbonatito pouco evoluído e 475°C para um carbonatito tardio) compatíveis com as temperaturas esperadas para esse tipo de magma.

Os intervalos de composição de isótopos de enxofre nos complexos da PIAP e Jacupiranga são comparáveis aos de carbonatitos de outras províncias e localidades (Mitchell & Krouse 1975; Nikiforov *et al.* 2006; Shin & Lee 2007; Druppel 2006; Farrel *et al.* 2010) e com as variações esperadas para isótopos de enxofre em rochas ígneas (-5‰ a +15‰, Seal *et al.*, 2006), kimberlitos (-13‰ a +5‰, Seal

et al., 2006) e carbonatitos (-13‰ a +2‰, Deines, 1989). Os dados de isótopos de enxofre existentes na literatura, para diversos carbonatitos mundiais de diferentes idades (Paleoproterozoico a Eoceno) indicam uma clara tendência de diminuição do $\delta^{34}\text{S}$ em sulfetos dos carbonatitos mais antigos para os mais jovens, o que pode sugerir uma evolução de longo prazo da composição dos isótopos de enxofre do manto.

REFERÊNCIAS BIBLIOGRÁFICAS

- Almeida, F.F.M. 1983. Relações Tectônicas das rochas alcalinas mesozóicas da região meridional da Plataforma Sul-Americana. Revista Brasileira de Geociências 13, 139-158.
- Almeida, F. F. M., Svisero, D. P. Structural setting and tectonic control of kimberlite and associated rocks of Brazil. 5th Int Kimberlite Conf. Ext. Abstr., p. 3-5, 1991.
- Bailey, D.K. and Hampton, C.M. 1990. Volatiles in alkaline magmatism. Lithos 26, 157-165.
- Barbosa, E.S.R., Brod, J.A., Junqueira-Brod, T.C., Gaspar, J.C., Ribeiro, C.C., Boaventura, G.R., 2004. Petrografia e geoquímica de carbonatitos do Complexo de Salitre, Congresso Brasileiro de Geologia, XLII.
- Barbosa, E.S.R., Junqueira-Brod, T.C., Brod, J.A., Dantas, E.L., 2008. Petrology of bebedourites from the Salitre phoscorite-carbonatite complex, Brazil, 9th International Kimberlite Conference, Frankfurt.
- Barbosa, E.S.R. 2009. Mineralogia e Petrologia do Complexo Carbonatítico-Foscorítico de Salitre, MG. Tese (Doutorado em Geologia) – Universidade de Brasília.
- Barbosa, E.S.R., Brod, J.A., Junqueira-Brod, T.C., Cordeiro, P.F.O., Santos, R.V., Dantas, E.L., 2009. Mineralogia e geoquímica dos foscoritos do Complexo de Salitre, MG, Simpósio de Geologia do Centro-Oeste, XI, Cuiabá, MT.
- Bizzi, L.A., Dewit, M.J., Smith, C.B., McDonald, I., Armstrong, R.A., 1995. Heterogeneous Enriched Mantle Materials and Dupal-Type Magmatism Along the SW Margin of the São-Francisco Craton, Brazil. Journal of Geodynamics, 20(4): 469-491.
- Brod, J.A., 1999. Petrology and geochemistry of the Tapira alkaline complex, Minas Gerais State, Brazil. Ph. D. Thesis, University of Durham, Durham, UK, 486 pp.
- Brod, J. A., Gaspar, J. C., de Araújo, D. P., Gibson, S. A., Thompson, R. N. & Junqueira-Brod, T. C. (2001). Phlogopite and tetra-ferriphlogopite from Brazilian carbonatite complexes: petrogenetic constraints and implications for mineral-chemistry systematics. Journal of Asian Earth Sciences 19, 265-296.
- Brod, J.A., Gibson, S.A., Thompson, R.N., Junqueira-Brod, T.C., Seer, H.J., Moraes, L.C., Boaventura, G.R.. 2000. The kamafugite-carbonatite association in the Alto Paranaíba Igneous Province, southeastern Brazil. Revista Brasileira de Geociências 30 (3), 404-408.

- Brod, A. J., Junqueira-Brod, T. C., Gaspar, J. C., Gibson, S. A., Thompsom, R. N. 2003. Mineral-Chemistry fingerprints of liquid immiscibility and fractionation in the Tapira alkaline-carbonatite complex (Minas Gerais, Brazil). 8th International Kimberlite Conference Long Abstract.
- Brod, J.A., Ribeiro, C.C., Gaspar, J.C., Junqueira-Brod, T.C., Barbosa, E.S.R., Riffel, B.F., Silva, J.F., Chaban, N., Ferrari, A.J.D. 2004. Excursão 1: Geologia e Mineralizações dos Complexos Alcalino-Carbonatíticos da Província Ígnea do Alto Paranaíba. São Paulo: Sociedade Brasileira de Geologia, (Guia de excursão).
- Brod, J. A. ; Barbosa, E.S.R. ; Junqueira-Brod, T. C. ; Gaspar, J.C. ; Diniz-Pinto, H.S. ; Sgarbi, P. B. A. ; Petrinovic, I.A. 2005 . The Late-Cretaceous Goiás Alkaline Province (GAP), Central Brazil. In: Piero Comin-Chiaromonti; Celso de Barros Gomes. (Org.). Mesozoic and Cenozoic alkaline magmatism in the Brazilian Platform. São Paulo: Edusp, p. 261-316.
- Carlson, R.W., Araújo, A.L.N., Junqueira-Brod, T.C., Gaspar, J.C., Brod, J.A., Petrinovic, I.A., Hollanda, M.H.B.M., Pimentel, M.M., Sichel, S.E. 2007. Chemical and Isotopic Relationships between Peridotite Xenoliths and Mafic-Ultrapotassic Rocks from Southern Brazil. Chemical Geology, v. 242, p. 418-437.
- Carvalho, W.T., Bressan, S.R. 1997. Depósitos de Fosfato, Nióbio, Titânio, Terras Raras e Vermiculita de Catalão I - Goiás. In: Schobbenhaus Filho, C., Queiroz, E.T., Coelho, C.E.S. (Eds.), Principais Depósitos Minerais do Brasil. DNPM, Brasília, pp. 69-93.
- Comin-Chiaromonti, P., Gomes, C.B., 1996. Alkaline magmatism in Central-Eastern Paraguay. Relationships with coeval magmatism in Brazil. Edusp/Fapesp, São Paulo, 458 pp.
- Comin-Chiaromonti, P. & Gomes, C. B. (eds). 2005. Mesozoic to Cenozoic Alkaline Magmatism in the Brazilian Platform. 750 pp.
- Coplen, T.B., and Krouse, H.R. 1998. Sulphur isotope data consistency improved: Nature, v. 392, p. 32.
- Cordeiro, P.F.O., Brod, J.A., Dantas, E.L., Barbosa, E.S.R. 2010. Mineral chemistry, isotope geochemistry and petrogenesis of niobium-rich rocks from the Catalão I carbonatite-phoscorite complex, Central Brazil. Lithos 118, 223-237.
- Cordeiro, P.F.O., Brod, J.A., Santos, R.V., Dantas, E.L., Oliveira, C.G., Barbosa, E.S.R. 2011. Stable (C, O) and radiogenic (Sr, Nd) isotopes of carbonates as indicators of magmatic and post-magmatic

- processes of phoscorite-series rocks and carbonatites from Catalão I, central Brazil. Contributions to Mineralogy and Petrology, 161(3): 451-464.
- Craddock, P.R., Rouxel, O.J., Ball, L.A., Bach, W. 2008. Sulfur isotope measurement of sulfate and sulfide by high-resolution MC-ICP-MS. Chemical Geology, v.253, p.102-113.
- Deer, W.A., Howie, R.A., Zussman, J. 1992. An Introduction to the Rock-Forming Minerals. Longman Pub Group.
- Deines, P. 1989. Stable isotope variations in carbonatites. In: Bell K. (ed) Carbonatites: genesis and evolution, Unwin Hyman, p 301-359.
- Ding, T., Valkiers, S., Kipphardt, H., De Bièvre, P., Taylor, P.D.P., Gonfiantini, R., Krouse, R. 2001. Calibrated sulfur isotope abundance ratios of three IAEA sulfur isotope reference materials and V-CDT with reassessment of the atomic weight of sulfur. *Geochimica et Cosmochimica Acta* 65, 2433-2437.
- Downes, H., Balaganskaya, E., Beard, A., Liferovich, R., Demaiffe, D. 2005. Petrogenetic process in the ultramafic, alkaline and carbonatitic magmatism in the Kola Alkaline Province: A review. *Lithos* 85, 48-75.
- Drüppel, K., Wagner, T., Boyce, A. J. 2006. Evolution of Sulfide Mineralization in Ferrocarbonatite, Swartbooisdrif, Northwestern Namibia: Constraints from Mineral Compositions and Sulfur Isotopes. *The Canadian Mineralogist* 44, 877-894.
- Duke, G.I. 2009. Black Hills-Alberta carbonatite-kimberlite linear trend: Slab edge at depth? *Tectonophysics* 454, 185-194.
- Ernesto, M., Marques, L.S., Piccirillo, E.M., Molina, E.C., Ussami, N., Comin-Chiaromonti, P., Bellieni, G. 2002. Paraná Magmatic Province-Tristan da Cunha plume system: fixed versus mobile plume, petrogenetic considerations and alternative heat sources. *Journal of Volcanology and Geothermal Research* 2484, 1-22.
- Ernesto, M. 2005. Paleomagnetism of the post-paleozoic alkaline magmatism in the Brazilian platform: questioning the mantle plume model. In: Comin-Chiaromonti, P. & Gomes, C. B. (eds). Mesozoic to Cenozoic Alkaline Magmatism in the Brazilian Platform. 750 pp.
- Farrel, S., Bell, K., Clark, I. 2010. Sulphur isotopes in carbonatites and associated silicate rocks from the Superior Province, Canada. *Miner. Petrol.* 98, 209-226.

- Gibson, S.A., Thompson, R.N., Dickin, A.P., Leonardos, O.H. 1995a. High-Ti and low-Ti mafic potassic magmas: Key to plume-lithosphere interactions and continental flood-basalt genesis. *Earth Planetary Science Letters* 136, 149-165.
- Gibson, S. A., Thompson, R. N., Leonardos, O. H., Dickin, A. P. & Mitchell, J. G. 1995b. The Late Cretaceous impact of the Trindade mantle plume - evidence from large-volume, mafic, potassic magmatism in SE Brazil. *Journal of Petrology* 36, 189-229.
- Gibson, S.A., Thompson, R.N., Weska, R., Dickin, A.P. and Leonardos, O.H. 1997. Late Cretaceous rift-related upwelling and melting of the Trindade starting mantle plume head beneath western Brazil. *Contributions to Mineralogy and Petrology* 126, 303-314.
- Gomes, C.B., Ruberti, E., Morbidelli, L. 1990. Carbonatite complexes from Brazil: A review. *Journal of South American Earth Sciences* 3, 51-63.
- Gomide, C.S., Brod, J.A., Palmieri, M., Santos, R.V., Junqueira-Brod, T.C., Marchão, M.O., Silva, P.G.N., Braga, L.M.V., Paulino, F., Silveira, D.A. 2008. Estudo preliminar de isótopos estáveis de carbono e oxigênio na associação kamafugito-carbonatito-foscorito da Província Ígnea do Alto Paranaíba. IV Simpósio de Vulcanismo, Foz do Iguaçu-PR.
- Gomide, C.S., Junqueira-Brod, T.C., Brod, J.A., Dardenne, M.A., Palmieri, M., Santos, R.V. Relações entre Geoquímica e processos de desgasificação em carbonatitos do complexo de Catalão I, Goiás. 2009. XI Simpósio de Geologia do Centro-Oeste, Cuiabá, MT, 1 pp.
- Gomide, C.S., Brod, J.A., Buhn, B.M. 2010. Sulfur isotopes from de Catalão I alkaline carbonatite complex, Alto Paranaiba Igneous Province, GO, Brazil. VII South American Symposium on Isotope Geology, Brasilia, Brazil.
- Grasso, C.B., Ribeiro, C.C., Brod, J.A., Gaspar, J.C., 2006. Mapeamento de detalhe (1:2000) das frentes de lavra da mina da Fosfértil Fertilizantes Fosfatados S.A. In: Silva, M.G., Franca-Rocha, W.J.S. (Editors), Congresso Brasileiro de Geologia, XLIII. SBG, Aracaju, pp. 796-801.
- Grasso, C.B., Brod, J.A., 2009. As séries bebedourítica, carbonatítica e foscorítica no complexo de Serra Negra, MG, Simpósio de Geologia do Centro-Oeste, Cuiabá, MT, pp. 1 pp.
- Grasso, C.B., Brod, J.A., Santos, R.V., 2010. Oxygen and carbon isotope study of the Serra Negra Complex, Alto Paranaíba Igneous Province, SE Brazil, South American Symposium on Isotope Geology, VII, Brasília, pp. 273-276.

- Issa Filho, A., Lima, P.R.A.S., Souza, O.M., 1984. Aspectos da geologia do complexo carbonatítico do Barreiro, Araxá, MG, Brasil. In: CBMM (Ed.), Complexos Carbonatíticos do Brasil: Geologia. CBMM, São Paulo, pp. 20-44.
- Jácomo, M.H., Junqueira-Brod, T.C., Pires, A.C.B., Brod, J.A., Palmieri, M., Ferrari, A.J.D., 2010. Associação de magnetometria, gamaespectrometria, geoquímica e petrografia para modelamento tridimensional da mineralização de nióbio do depósito Morro do Padre, Goiás, Brasil, IV Simpósio Brasileiro de Geofísica, Brasília, pp. 4.
- Jones, A. P. & Wyllie, P. J. (1983). Low-temperature glass quenched from a synthetic, rare earth carbonatite: implications for the origin of the Mountain Pass deposit, California. *Economic Geology* 78, 1721-1723.
- Junqueira-Brod, T.C., Gomide C.S., Brod, J.A., Dardenne, M.A., Palmieri, M., Grasso, C., Santos, R.V. Fluidisation processes and breccia formation int the Catalão I and Catalão II Complexes, Alto Paranaíba Igneous Province - APIP, Central Brazil – Evidence for magma fragmentation inside carbonatite magma chambers. In Preparation.
- Kajiwra, Y. and Krouse, H.R. 1971. Sulfur isotope partitioning in metallic sulfide systems. *Canadian Journal of Earth Sciences* 8, 1397-1408.
- Klein, C. 2002. Mineral Science, 405 pp.
- Krafft, M. & Keller, J. (1989). Temperature-Measurements in Carbonatite Lava Lakes and Flows from Oldoinyo-Lengai, Tanzania. *Science* 245, 168-170.
- Leonardos, O. H., Ulbrich, M. N., Gaspar, J. C. 1991. The Mata da Corda volcanic rocks. 5th Int. Kimberlite Conf. Field Guide 65-73.
- Machado Junior D.L. 1992. Geologia do complexo alcalino-carbonatítico de Catalão II (GO). 37 Congresso Brasileiro Geologia (Bol. Res. Exp.). São Paulo, 94-95.
- Mariano A.N., Marchetto M. 1991. Serra Negra and Salitre carbonatite alkaline igneous complex. In O.H. Leonardos, H.O.A. Meyer, J.C. Gaspar (Eds.), 5th Internat. Kimb. Conf. (Field Guide Book). Araxá, CPRM, Sp. Publ. 3/91. 75-79.
- Mitchell, R. H., Krouse, H. R. 1975. Sulphur isotope geochemistry of carbonatites. *Geochimica et Cosmochimica Acta*, 39 (11), 1505-1513.

- Miyoshi, T., Sakai, H., Chiba, H. 1984. Experimental study of sulfur isotope fractionation factors between sulfate and sulfide in high temperature melts. *Geochemical Journal*, 18: 75-84.
- Morbidelli, L., Gomes, C.B., Beccaluva, L., Brotzu, P., Conte, A.M., Ruberti, E., Traversa, G. 1995. Mineralogical, petrological and geochemical aspects of alkaline and alkaline-carbonatite associations from Brazil. *Earth Science Reviews*, v.39. p.135-168.
- Nikiforov, A. V., Bolonim, A. V., Pokrovsky, B. G., Sugorakova, A. M., Chugaev, A. V., Lykhin, D. A. 2006. Isotope Geochemistry (O, C, S, Sr) and Rb-Sr Age of Carbonatites in Central Tuva. *Geology of Ore Deposits* 48 (4), 256–276.
- Oliveira, I.W.B., Sachs, L.L.B., Silva, V.A., Batista, I.H., 2004. In: Schobbenhaus,C., Gonçalves,J.H., Santos, J.O.S., Abram, M.B., Leão Neto, R., Matos, G.M.M., Vidotti, R.M., Ramos, M.A.B., Jesus, J.D.A. de (eds.). *Carta Geológica do Brasil ao Milionésimo: Sistema de Informações Geográficas - SIG e 46 folhas na escala 1 : 1.000.000*. Brasília: CPRM, 2004. 41 CD-ROM's.
- Palmieri, M., Ferrari, A.J.D., Brod, J.A., Barbosa, P.A.R., 2006. Geologia da mina de fosfato da Copebrás no Complexo Foscortítico-Carbonatítico de Catalão I, 43 Congresso Brasileiro de Geologia. Aracajú. Sociedade Brasileira de Geologia, Aracajú, SE, pp. 791-795.
- Palmieri, M., Silva, S.E., Brod, J.A., Ferrari, A.J.D., Barbosa, P.A.R., Jácomo, M.H., Junqueira-Brod, T.C., Cordeiro, P.F.O., 2009. A mineralização de nióbio do Alvo Morro do Padre, Catalão II, GO, Simpósio de Geologia do Centro-Oeste, XI, Cuiabá, MT, pp. 32.
- Palmieri, M., 2011. Modelo Geológico e Avaliação de Recursos Minerais do Depósito de Nióbio Morro do Padre, Complexo alcalino-carbonatítico Catalão II, GO, dissertação de mestrado. Universidade de Brasília, Brasília.
- Qi, H.P., and Coplen, T.B. 2003. Evaluation of the $^{34}\text{S}/^{32}\text{S}$ ratio of Soufre de Lacq elemental sulfur isotopic reference material by continuous flow isotope-ratio mass spectrometry: Chemical Geology 199, 183-187.
- Ribeiro, C.C., Brod, J.A., Junqueira-Brod, T.C., Gaspar, J.C., Petrinovic, I.A., 2005. Mineralogical and field aspects of magma fragmentation deposits in a carbonate-phosphate magma chamber: evidence from the Catalao I complex, Brazil. *Journal of South American Earth Sciences*, 18(3-4): 355-369.

- Ribeiro, C.C. 2008. Geologia, geometalurgia, controles e gênese dos depósitos de fósforo, terras raras e titânio do Complexo Carbonatítico de Catalão I, GO. Tese (Doutorado em Geologia) - Universidade de Brasília.
- Ruberti, E., Gomes, C.B., Comin-Chiaromonti, P. 2005. The alkaline magmatism from the Ponta Grossa Arch. In: Comin-Chiaromonti, P. & Gomes, C. B. (eds). Mesozoic to Cenozoic Alkaline Magmatism in the Brazilian Platform. 750 pp.
- Santos, R. V. & Clayton, R. N. (1995). Variations of oxygen and carbon isotopes in carbonatites: a study of Brazilian alkaline complexes. *Geochimica et Cosmochimica Acta* 59, 1339-1352.
- Seal, R.R. 2006. Sulfur Isotope Geochemistry of Sulfide Minerals. *Reviews in Mineralogy & Geochemistry*, v.61, p.633-677.
- Seer H.J. 1999. Evolução Tectônica dos Grupos Araxá e Ibiá na Sinforma de Araxá-MG. Universidade de Brasília (Tese de Doutorado) 267p.
- Shin, D.B. and Lee, M.J. 2007. Oxygen and sulfur isotope characteristics of Salmagora Complex, Kola Peninsula. Goldschmidt Conference Abstracts A932.
- Sonoki I.K, Garda G.M., 1988. Idades K-Ar de rochas alcalinas do Brasil Meridional e Paraguai Oriental: compilação e adaptação as novas constantes de decaimento. *Boletim IG USP Serie Científica*, v. 19 p. 63-85.
- Thermo Finnigan. 2003. Finnigan Neptune Hardware Manual. Product Marketins Thermo Electron Corporation, Bremen, Germany,
- Thompson, R.N., Gibson, S.A., Mitchell, J.G., Dickin, A.P., Leonardos, O.H., Brod, J.A., Greenwood, J.C. 1998. Migrating Cretaceous-Eocene Magmatism in the Serra do Mar Alkaline Province, SE Brazil: Melts from the Deflected Trindade Mantle Plume? *Journal of Petrology* 39, 1493-1526.
- Thompson, R.N., Smith, P.M., Gibson, S.A., Mattey, D.P., Dickin, A.P. 2002. Ankerite carbonatite from Swartbooisdrif, Namibia: the firt evidence for magmatic ferrocarbonatite. *Contributions to Mineralogy and Petrology* 143, 377-395.
- Traversa, G., Gomes, C.B., Brotzu, P., Buraglini, N., Morbidelli, L., Principato, M.S., Ronca, S., Ruberti, E., 2001. Petrography and mineral chemistry of carbonatites and mica-rich rocks from the Araxá complex (Alto Paranaiba Province, Brazil). *Anais Da Academia Brasileira De Ciencias*, 73(1): 71-98.

- Wyllie, P.J. (1966): Experimental studies of carbonatite problems: the origin and differentiation of carbonatite magmas, in "Carbonatites", O.F. Tuttle and J. Gittins, eds. New York: Wiley, 311-352.
- Woolley, A.R., Kjarsgaard, B.A., 2008. Carbonatite Occurrences of the World: Map and Database, Geological Survey of Canada. 1 CD-ROM + 1 map.
- Zheng, YF. 1990. Sulfur Isotope Fractionation in Magmatic Systems: Models of Rayleigh Distillation and Selective Flux. Chinese Journal of Geochemistry 9 (1).

ANEXOS

Análises de Isótopos de Enxofre

Amostra	$\delta^{34}\text{S}$ ‰ V-CDT	Mineral	Rocha	Complexo
144,05	7.22	Barita	Carbonatito	Catalao II
273600	12.16	Barita	Carbonatito	Catalao II
165911	-5.28	Bornita	Nelsonito	Catalao II
CP1	-6.25	Calcopirita	Carbonatito	Catalao II
165903	-6.10	Calcopirita	Nelsonito	Catalao II
165911	-5.62	Calcopirita	Nelsonito	Catalao II
cp3	-7.08	Calcopirita	Nelsonito	Catalao II
273600	-9.17	Pirita	Carbonatito	Catalao II
15340F	-12.31	Pirita	Carbonatito	Catalao II
272551	-11.73	Pirita	Carbonatito	Catalao II
272843	-8.89	Pirita	Carbonatito	Catalao II
165907a1	-5.09	Pirita	Carbonatito	Catalao II
165903	-4.86	Pirita	Nelsonito	Catalao II
cp2	-5.98	Pirita	Nelsonito	Catalao II
272561	-6.68	Pirrotita	Carbonatito	Catalao II
C1-BAV	3.27	Barita	Carbonatito	Catalao I
C1-DQ	5.70	Barita	Carbonatito	Catalao I
C1-SH1-BH	9.13	Barita	Carbonatito	Catalao I
C1-SH1-BV	12.88	Barita	Carbonatito	Catalao I
AB322,30	-6.66	Pirita	Carbonatito	Catalao I
C1DQ	-7.04	Pirita	Carbonatito	Catalao I
C1PG	-9.50	Pirita	Carbonatito	Catalao I
C1CO3nucleo	-8.05	Pirita	Carbonatito	Catalao I
C1CO3borda	-4.31	Pirita	Carbonatito	Catalao I
C1CO3_nucleo	-9.54	Pirita	Carbonatito	Catalao I
C1CO3_borda	-5.80	Pirita	Carbonatito	Catalao I
C1-SH2	-24.55	Pirita	Carbonatito	Catalao I
C1-SH1nucleo	-17.46	Pirita	Carbonatito	Catalao I
C1-SH1borda	-12.98	Pirita	Carbonatito	Catalao I
C1-SH3nucleo	-23.45	Pirita	Carbonatito	Catalao I
C1-SH3borda	-20.55	Pirita	Carbonatito	Catalao I
CB02	-5.59	Pirita	Carbonatito	Catalao I
CB11	-5.19	Pirita	Carbonatito	Catalao I
CB12	-10.92	Pirita	Carbonatito	Catalao I
J90,50	-3.78	Pirita	Carbonatito	Catalao I
L152,50	-2.20	Pirita	Carbonatito	Catalao I
NRD216	-7.42	Pirita	Carbonatito	Catalao I
CB14nucleo	-6.37	Pirita	Foscorito	Catalao I
CB14borda	-4.56	Pirita	Foscorito	Catalao I

Análises de Isótopos de Enxofre (cont.)

Amostra	$\delta^{34}\text{S}$ ‰ V-CDT	Mineral	Rocha	Complexo
CB16	-17.36	Pirita	Fenito	Catalao I
Mina2	-9.47	Pirita	Magnetitito	Catalao I
NRD-134	-5.20	Pirita	Magnetitito	Catalao I
NRD-304	-7.88	Pirita	Magnetitito	Catalao I
CB04nucleo	-4.48	Pirita	Nelsonito	Catalao I
CB04borda	-2.83	Pirita	Nelsonito	Catalao I
AC328.30Inucleo	-6.41	Pirita	Nelsonito	Catalao I
AC328.30lborda	-3.69	Pirita	Nelsonito	Catalao I
AC328.30Fnucleo	-8.21	Pirita	Nelsonito	Catalao I
AC328.30Fborda	-7.57	Pirita	Nelsonito	Catalao I
NRD164	-8.01	Pirita	Nelsonito	Catalao I
NRD164	-9.60	Pirita	Nelsonito	Catalao I
NRD230	-2.58	Pirita	Nelsonito	Catalao I
NRD256	-7.10	Pirita	Nelsonito	Catalao I
NRD326.1	-6.75	Pirita	Nelsonito	Catalao I
FVL-109c	-2.14	Barita	Carbonatito	Salitre
ASL12B	0.51	Barita	Carbonatito	Salitre
SF101,5	-5.72	Calcopirita	Foscorito	Salitre
SL296A	-4.66	Pirita	Bebedourito	Salitre
SL296A	-5.03	Pirita	Bebedourito	Salitre
ASL19	-7.25	Pirita	Carbonatito	Salitre
F0287	-7.72	Pirita	Carbonatito	Salitre
FVL-109c	-5.70	Pirita	Carbonatito	Salitre
F78,4	-8.77	Pirita	Carbonatito	Salitre
FVL184	-5.65	Pirita	Carbonatito	Salitre
FVL-58	-5.02	Pirita	Carbonatito	Salitre
SF102,4	-5.98	Pirita	Foscorito	Salitre
ASL15	-2.84	Pirrotita	Carbonatito	Salitre
F78,4	-6.81	Pirrotita	Carbonatito	Salitre
FVL93,80	-12.36	Pirrotita	Carbonatito	Salitre
SL10A77	-6.44	Pirrotita	Carbonatito	Salitre
SL360	-6.08	Pirrotita	Carbonatito	Salitre
LG08	-8.13	Calcopirita	Carbonatito	Serra Negra
LG08	-7.61	Pirita	Carbonatito	Serra Negra
LG38	-8.78	Pirita	Carbonatito	Serra Negra
C601	-8.24	Pirrotita	Carbonatito	Serra Negra
AX-AM20C	-4.40	Pirita	Carbonatito	Araxa
AX-C8-15	-9.62	Pirita	Carbonatito	Araxa
B9-CX44	-11.63	Pirita	Carbonatito	Araxa
AXP3A1	-5.12	Pirita	Carbonatito	Araxa
C8-03	-8.64	Pirita	Carbonatito	Araxa

Análises de Isótopos de Enxofre (cont.)

Amostra	$\delta^{34}\text{S} \text{‰ V-CDT}$	Mineral	Rocha	Complexo
C8-2	-11.61	Pirita	Carbonatito	Araxá
C8-3H	-8.91	Pirita	Carbonatito	Araxá
C8-5	-10.74	Pirita	Carbonatito	Araxá
C8-5D	-9.61	Pirita	Carbonatito	Araxá
C8-7G	-10.40	Pirita	Carbonatito	Araxá
C8-9HID	-8.87	Pirita	Carbonatito	Araxá
C8-9MAG	-10.26	Pirita	Carbonatito	Araxá
C9-13	-7.00	Pirita	Carbonatito	Araxá
C8-A3	-7.59	Pirita	Foscorito	Araxá
AX47	-7.93	Pirrotita	Carbonatito	Araxá
Ax57	-9.44	Pirrotita	Carbonatito	Araxá
C8-3E	-11.69	Pirrotita	Carbonatito	Araxá
AT-140	-3.94	Barita	Carbonatito	Tapira
AT135	-1.63	Barita	Carbonatito	Tapira
AT-137	-1.31	Barita	Carbonatito	Tapira
AT-138	16.75	Barita	Carbonatito	Tapira
1E53C	-6.49	Calcopirita	Bebedourito	Tapira
1E53C	-6.31	Pirita	Bebedourito	Tapira
B1-43	-9.55	Pirita	Bebedourito	Tapira
AT01	-2.59	Pirita	Bebedourito	Tapira
AT-103	-13.15	Pirita	Carbonatito	Tapira
AT140	-11.59	Pirita	Carbonatito	Tapira
AT-46	-7.93	Pirita	Carbonatito	Tapira
AT-53	-6.79	Pirita	Carbonatito	Tapira
AT-54	-6.85	Pirita	Carbonatito	Tapira
4-S-22	-7.90	Pirita	Carbonatito	Tapira
FENTAP	-8.61	Pirita	Fenito	Tapira
TP-90-10	-2.19	Pirrotita	Bebedourito	Tapira
AT-128	-4.47	Pirrotita	Carbonatito	Tapira
AT-137	-8.15	Pirrotita	Carbonatito	Tapira
AT-49	-9.01	Pirrotita	Carbonatito	Tapira
TAP-S	-3.95	Pirrotita	Carbonatito	Tapira
JC-05	-1.70	Calcopirita	Bebedourito	Jacupiranga
J-13-B	-0.84	Pirita	Bebedourito	Jacupiranga
80-DIQUE	-6.09	Pirita	Carbonatito	Jacupiranga
C1	-3.15	Pirita	Carbonatito	Jacupiranga
140-N-3B	-5.70	Pirita	Carbonatito	Jacupiranga
C-3-B	-5.56	Pirita	Carbonatito	Jacupiranga
150-5-3E	-4.99	Pirita	Carbonatito	Jacupiranga
C1	-3.34	Pirrotita	Carbonatito	Jacupiranga
150-5-3D	-3.88	Pirrotita	Carbonatito	Jacupiranga

Análises de Isótopos de Enxofre (cont.)

Amostra	$\delta^{34}\text{S}$ ‰ V-CDT	Mineral	Rocha	Complexo
160-5	-4.40	Pirrotita	Carbonatito	Jacupiranga
C4	-3.48	Pirrotita	Carbonatito	Jacupiranga
C5	-5.23	Pirrotita	Carbonatito	Jacupiranga
CL2-50	-4.04	Pirrotita	Carbonatito	Jacupiranga
170-5-2B	-3.96	Pirrotita	Carbonatito	Jacupiranga
C3	-5.37	Pirrotita	Carbonatito	Jacupiranga
CL2-50	-4.04	Pirrotita	Carbonatito	Jacupiranga
JC-01	-3.15	Pirrotita	Carbonatito	Jacupiranga
JC-02	-5.36	Pirrotita	Carbonatito	Jacupiranga

Dados de Química Mineral de Barita

Amostra Rocha	273600 1 carbonatito	273600 2 carbonatito	273600 3 carbonatito	273600 5 carbonatito	273600 6 carbonatito	273600 7 carbonatito	273600 8 carbonatito	14405 2 carbonatito	14405 4 carbonatito	BAV 3 massive Barita	BAV 4 massive Barita	BAV 1 massive Barita
Complexo	Catalão II	Catalão II	Catalão II	Catalão I	Catalão I	Catalão I						
BaO	67.66	67.34	64.99	64.14	66.21	65.01	65.78	67.04	65.17	67.71	66.50	64.48
SO ₃	33.26	32.99	32.77	33.24	33.97	34.19	32.76	34.24	34.29	33.86	33.71	34.19
SeO ₂	0.36	0.00	0.78	0.60	0.00	0.92	0.42	0.00	0.50	0.00	0.00	0.54
MgO	0.00	0.00	0.00	0.01	0.00	0.01	0.00	0.00	0.00	0.00	0.00	0.01
SiO ₂	0.00	0.00	0.00	0.07	0.00	0.00	0.00	0.00	0.00	0.00	0.00	0.00
Al ₂ O ₃	0.06	0.07	0.10	0.11	0.11	0.01	0.13	0.05	0.11	0.07	0.05	0.08
P ₂ O ₅	0.10	0.09	0.13	0.06	0.00	0.12	0.00	0.00	0.07	0.00	0.00	0.00
CaO	0.01	0.01	0.00	0.00	0.02	0.00	0.00	0.04	0.00	0.01	0.02	0.01
Cr ₂ O ₃	0.00	0.00	0.00	0.00	0.00	0.00	0.00	0.00	0.00	0.00	0.00	0.00
FeO	0.02	0.09	0.04	0.00	0.00	0.09	0.00	0.00	0.11	0.04	0.00	0.00
SrO	0.05	0.12	0.35	0.18	0.07	0.00	0.06	0.00	0.00	0.00	0.00	0.01
PbO	0.00	0.00	0.00	0.00	0.00	0.00	0.00	0.00	0.00	0.00	0.00	0.00
MnO	0.00	0.01	0.01	0.06	0.01	0.03	0.01	0.00	0.02	0.02	0.00	0.02
Total	101.52	100.71	99.16	98.46	100.38	100.38	99.16	101.37	100.26	101.71	100.27	99.33
Atomos por fórmula (base de 4 O)												
Ba	1.0381	1.0437	1.0106	0.9932	1.0107	0.9814	1.0284	1.0153	0.9849	1.0309	1.0213	0.9811
Pb	0.0000	0.0000	0.0000	0.0000	0.0000	0.0000	0.0000	0.0000	0.0000	0.0000	0.0000	0.0000
Sr	0.0011	0.0028	0.0080	0.0040	0.0016	0.0000	0.0014	0.0000	0.0000	0.0000	0.0000	0.0001
Ca	0.0003	0.0002	0.0000	0.0000	0.0008	0.0000	0.0000	0.0017	0.0000	0.0002	0.0007	0.0005
Si	0.0000	0.0000	0.0000	0.0028	0.0000	0.0000	0.0000	0.0000	0.0000	0.0000	0.0000	0.0000
Al	0.0030	0.0033	0.0045	0.0051	0.0048	0.0005	0.0059	0.0021	0.0048	0.0034	0.0021	0.0035
P	0.0032	0.0030	0.0045	0.0018	0.0000	0.0038	0.0000	0.0000	0.0022	0.0000	0.0000	0.0000
Cr	0.0000	0.0000	0.0000	0.0000	0.0000	0.0000	0.0000	0.0000	0.0000	0.0000	0.0000	0.0000
Fe	0.0006	0.0029	0.0014	0.0000	0.0000	0.0028	0.0000	0.0000	0.0034	0.0014	0.0000	0.0000
Mg	0.0000	0.0000	0.0000	0.0004	0.0000	0.0008	0.0000	0.0000	0.0000	0.0001	0.0000	0.0003
Mn	0.0000	0.0003	0.0002	0.0019	0.0004	0.0008	0.0003	0.0000	0.0007	0.0008	0.0000	0.0006
S	0.9774	0.9792	0.9761	0.9857	0.9931	0.9885	0.9810	0.9933	0.9925	0.9872	0.9916	0.9965
Se	0.0076	0.0000	0.0167	0.0129	0.0000	0.0192	0.0091	0.0000	0.0105	0.0000	0.0000	0.0114
total	2.03	2.04	2.02	2.01	2.01	2.00	2.03	2.01	2.00	2.02	2.02	1.99

Dados de Química Mineral de Barita (cont.)

Amostra Rocha	BAV 2 massive Barita	DQVM 2 carbonatito	DQVM 3 carbonatito	B1 C1 carbonatito	DQVM 6 carbonatito	DQRS 1 carbonatito	SH1BH 2 carbonatito	SH1BH 3 carbonatito	SH1BH 5 carbonatito	ASL12B 2 carbonatito	ASL12B 4 carbonatito	FVL109 3 carbonatito
Complexo	Catalão I	Catalão I	Catalão I	Catalão I	Catalão I	Catalão I	Catalão I	Catalão I	Catalão I	Salitre	Salitre	Salitre
BaO	65.58	65.77	66.73	66.99	66.72	64.59	66.27	65.54	67.53	64.61	62.25	64.61
SO ₃	34.30	33.90	33.40	33.81	33.93	33.17	33.62	34.08	33.74	34.27	34.34	32.82
SeO ₂	0.00	1.08	0.00	0.30	0.14	0.56	0.00	0.00	0.00	0.00	0.67	0.64
MgO	0.00	0.00	0.00	0.01	0.00	0.00	0.02	0.01	0.03	0.01	0.00	0.01
SiO ₂	0.00	0.00	0.00	0.00	0.00	0.00	0.00	0.00	0.00	0.00	0.00	0.00
Al ₂ O ₃	0.09	0.05	0.01	0.12	0.06	0.08	0.04	0.04	0.13	0.08	0.12	0.06
P ₂ O ₅	0.09	0.09	0.10	0.00	0.00	0.00	0.00	0.00	0.09	0.02	0.01	0.06
CaO	0.06	0.00	0.03	0.00	0.00	0.00	0.00	0.02	0.00	0.00	0.00	0.02
Cr ₂ O ₃	0.00	0.00	0.00	0.00	0.00	0.00	0.00	0.00	0.00	0.00	0.00	0.00
FeO	0.00	0.00	0.00	0.00	0.00	0.04	0.02	0.03	0.00	0.01	0.09	0.00
SrO	0.10	0.00	0.20	0.44	0.56	0.05	0.09	0.06	0.05	1.11	1.45	1.04
PbO	0.00	0.00	0.00	0.00	0.00	0.00	0.00	0.00	0.00	0.00	0.00	0.00
MnO	0.00	0.02	0.01	0.00	0.03	0.00	0.00	0.00	0.01	0.02	0.00	0.05
Total	100.22	100.91	100.49	101.67	101.44	98.50	100.05	99.78	101.57	100.14	98.93	99.31
Atomos por fórmula (base de 4 O)												
Ba	0.9941	0.9955	1.0280	1.0177	1.0140	1.0043	1.0201	1.0014	1.0286	0.9799	0.9419	1.0046
Pb	0.0000	0.0000	0.0000	0.0000	0.0000	0.0000	0.0000	0.0000	0.0000	0.0000	0.0000	0.0000
Sr	0.0023	0.0000	0.0046	0.0099	0.0127	0.0012	0.0019	0.0013	0.0011	0.0250	0.0324	0.0239
Ca	0.0024	0.0000	0.0014	0.0000	0.0000	0.0002	0.0000	0.0010	0.0000	0.0000	0.0000	0.0007
Si	0.0000	0.0000	0.0000	0.0000	0.0000	0.0000	0.0000	0.0000	0.0000	0.0000	0.0001	0.0000
Al	0.0043	0.0022	0.0006	0.0055	0.0027	0.0039	0.0019	0.0017	0.0059	0.0037	0.0055	0.0028
P	0.0030	0.0030	0.0032	0.0000	0.0000	0.0000	0.0000	0.0000	0.0028	0.0008	0.0004	0.0020
Cr	0.0000	0.0000	0.0000	0.0000	0.0000	0.0000	0.0000	0.0000	0.0000	0.0000	0.0000	0.0000
Fe	0.0000	0.0000	0.0000	0.0000	0.0000	0.0014	0.0006	0.0010	0.0000	0.0002	0.0028	0.0000
Mg	0.0002	0.0000	0.0000	0.0003	0.0000	0.0000	0.0013	0.0003	0.0016	0.0005	0.0001	0.0007
Mn	0.0000	0.0007	0.0003	0.0000	0.0009	0.0000	0.0000	0.0000	0.0003	0.0007	0.0000	0.0015
S	0.9957	0.9827	0.9856	0.9837	0.9875	0.9877	0.9910	0.9974	0.9842	0.9954	0.9952	0.9773
Se	0.0000	0.0226	0.0000	0.0063	0.0029	0.0120	0.0000	0.0000	0.0000	0.0000	0.0139	0.0138
total	2.00	2.01	2.02	2.02	2.02	2.01	2.02	2.00	2.02	2.01	1.99	2.03

Dados de Química Mineral de Barita (cont.)

Amostra	FVL109 5	FVL109 7	AT140VM 1	AT140VM 2	AT140VM 7	AT140VM 8	AT137BVM 1	AT137BVM 4	AT132 1
Rocha	carbonatito								
Complexo	Salitre	Salitre	Tapira						
BaO	62.05	61.69	67.34	67.48	65.11	66.23	66.43	66.93	65.58
SO ₃	34.14	34.49	33.98	33.71	33.74	34.46	31.80	33.87	33.53
SeO ₂	0.97	0.24	0.00	0.00	0.34	0.56	0.00	0.20	0.00
MgO	0.00	0.00	0.00	0.00	0.00	0.00	0.00	0.00	0.00
SiO ₂	0.01	0.00	0.00	0.00	0.00	0.00	0.00	0.00	0.09
Al ₂ O ₃	0.06	0.06	0.12	0.11	0.07	0.17	0.12	0.14	0.05
P ₂ O ₅	0.00	0.00	0.05	0.10	0.00	0.02	0.13	0.01	0.00
CaO	0.00	0.00	0.03	0.00	0.00	0.00	0.03	0.00	0.12
Cr ₂ O ₃	0.00	0.00	0.00	0.00	0.00	0.00	0.00	0.00	0.00
FeO	0.14	0.09	0.00	0.00	0.00	0.00	0.07	0.09	0.04
SrO	1.87	1.72	0.00	0.00	0.02	0.06	0.48	0.04	0.12
PbO	0.00	0.00	0.00	0.00	0.00	0.00	0.00	0.00	0.00
MnO	0.00	0.00	0.00	0.00	0.01	0.06	0.00	0.00	0.00
Total	99.24	98.29	101.52	101.40	99.29	101.56	99.05	101.28	99.52
Atomos por fórmula (base de 4 O)									
Ba	0.9391	0.9365	1.0223	1.0295	1.0008	0.9928	1.0573	1.0179	1.0109
Pb	0.0000	0.0000	0.0000	0.0000	0.0000	0.0000	0.0000	0.0000	0.0000
Sr	0.0419	0.0387	0.0000	0.0000	0.0004	0.0013	0.0112	0.0010	0.0027
Ca	0.0000	0.0000	0.0013	0.0000	0.0000	0.0000	0.0012	0.0000	0.0048
Si	0.0004	0.0000	0.0000	0.0000	0.0000	0.0000	0.0000	0.0000	0.0037
Al	0.0028	0.0025	0.0057	0.0049	0.0031	0.0075	0.0056	0.0063	0.0023
P	0.0000	0.0000	0.0016	0.0032	0.0000	0.0006	0.0046	0.0002	0.0000
Cr	0.0000	0.0000	0.0000	0.0000	0.0000	0.0000	0.0000	0.0000	0.0000
Fe	0.0046	0.0030	0.0000	0.0000	0.0000	0.0000	0.0023	0.0028	0.0012
Mg	0.0000	0.0001	0.0000	0.0000	0.0000	0.0000	0.0000	0.0000	0.0000
Mn	0.0000	0.0000	0.0000	0.0000	0.0003	0.0018	0.0000	0.0000	0.0000
S	0.9897	1.0026	0.9880	0.9850	0.9932	0.9894	0.9693	0.9867	0.9899
Se	0.0202	0.0051	0.0000	0.0000	0.0072	0.0116	0.0000	0.0042	0.0000
total	2.00	1.99	2.02	2.02	2.00	2.00	2.05	2.02	2.02

Dados de Química Mineral de Sulfeto

Amostra	272843	272843	272485B	272485B	272485B	272485A	272561	272561	272561	272551PO	272551PO	272551PY	272551PY
mineral	núcleo	borda	núcleo	borda	núcleo	borda	borda	núcleo	borda	núcleo	núcleo	núcleo	borda
Rocha	pirita												
Complexo	Catalão II												
Fe	46.645	46.429	46.747	46.627	47.017	46.852	47.549	46.468	46.488	47.564	46.559	46.65	45.956
Cu	0.005	0.029	0	0.041	0.023	0.003	0.02	0.011	0.003	0.001	0.015	0.012	0.021
Pb	0.286	0.25	0.284	0	0.361	0.337	0.303	0.358	0	0.273	0.336	0	0.315
Co	0.051	0.039	0.057	0.143	0.055	0.044	0.378	0.208	0.298	0.14	0.131	0.02	0.143
Ag	0	0	0.007	0	0.002	0.009	0.042	0	0.002	0	0	0	0
Zn	0.01	0.041	0	0	0.002	0	0	0	0	0	0	0.009	0
Ni	0.011	0	0.019	0	0.016	0	0.009	0	0	0	0	0.006	0
Pt	0	0	0	0	0.002	0.023	0.02	0.009	0	0.003	0.001	0	0.005
Pd	0	0	0	0	0	0	0	0	0	0.006	0.017	0	0.004
S	53.312	53.791	53.732	53.884	53.288	53.469	50.289	53.421	53.555	50.653	52.124	53.456	53.018
As	0	0	0.029	0	0	0	0	0	0.006	0.075	0.006	0.004	0
Se	0.033	0.12	0	0.013	0	0.031	0.031	0.035	0.054	0.046	0	0	0
Total	100.353	100.699	100.875	100.708	100.766	100.768	98.641	100.51	100.406	98.761	99.189	100.157	99.462
proporção atômica para 3 íons													
Fe	1.002	0.992	0.998	0.995	1.007	1.003	1.052	0.997	0.996	1.049	1.015	1.001	0.995
Cu	0.000	0.001	0.000	0.001	0.000	0.000	0.000	0.000	0.000	0.000	0.000	0.000	0.000
Pb	0.002	0.001	0.002	0.000	0.002	0.002	0.002	0.002	0.000	0.002	0.002	0.000	0.002
Co	0.001	0.001	0.001	0.003	0.001	0.001	0.008	0.004	0.006	0.003	0.003	0.000	0.003
Ag	0.000	0.000	0.000	0.000	0.000	0.000	0.000	0.000	0.000	0.000	0.000	0.000	0.000
Zn	0.000	0.001	0.000	0.000	0.000	0.000	0.000	0.000	0.000	0.000	0.000	0.000	0.000
Ni	0.000	0.000	0.000	0.000	0.000	0.000	0.000	0.000	0.000	0.000	0.000	0.000	0.000
Pt	0.000	0.000	0.000	0.000	0.000	0.000	0.000	0.000	0.000	0.000	0.000	0.000	0.000
Pd	0.000	0.000	0.000	0.000	0.000	0.000	0.000	0.000	0.000	0.000	0.000	0.000	0.000
S	1.994	2.002	1.998	2.002	1.989	1.993	1.937	1.996	1.997	1.945	1.979	1.998	2.000
As	0.000	0.000	0.000	0.000	0.000	0.000	0.000	0.000	0.000	0.001	0.000	0.000	0.000
Se	0.001	0.002	0.000	0.000	0.000	0.000	0.000	0.001	0.001	0.001	0.000	0.000	0.000
total	3	3	3	3	3	3	3	3	3	3	3	3	3
Σ cations	1.005	0.996	1.001	0.998	1.011	1.006	1.063	1.003	1.002	1.053	1.020	1.002	1.000
Σ anions	1.995	2.004	1.999	2.002	1.989	1.994	1.937	1.997	1.998	1.947	1.980	1.998	2.000

Dados de Química Mineral de Sulfeto (cont.)

Amostra	272551PY	141484	141484	165907.2	165907.2	165907.1	165907.1	140N3B	140N3B	140N3B	80DIQUE	80DIQUE	80DIQUE
mineral	borda	borda	borda	núcleo	núcleo	borda	núcleo	borda	borda	borda	núcleo	borda	borda
Rocha	pirita												
Complexo	Catalão II												
Fe	46.828	46.603	47.399	46.258	45.766	46.159	45.888	46.651	46.422	46.277	44.786	45.155	45.516
Cu	0	0.055	0.051	0.042	0.019	0.054	0.055	0.009	0.02	0	0.008	0.019	0.028
Pb	0.275	0.275	0.255	0.323	0	0.273	0.286	0.288	0	0.023	0.309	0.297	0.318
Co	0.053	0.082	0.114	0.069	0.299	0.108	0.085	0.056	0.051	0.09	0.232	0.258	0.093
Ag	0	0	0.001	0	0.004	0.018	0	0.002	0	0.002	0	0.001	0.014
Zn	0.017	0	0	0	0.006	0	0	0	0	0.002	0	0	0
Ni	0	0	0.008	0	0	0	0.008	0	0	0	0	0	0
Pt	0.002	0.008	0.001	0	0.006	0	0	0	0.021	0	0	0	0
Pd	0	0	0	0	0	0.003	0.005	0	0	0	0	0	0
S	53.454	53.31	50.996	53.007	52.905	52.548	51.595	53.551	52.261	52.957	52.283	52.968	52.608
As	0	0	0	0	0.01	0.016	0	0.003	0	0.016	0	0	0
Se	0.044	0.027	0.006	0.018	0.009	0	0.004	0.094	0.017	0.002	0.102	0	0
Total	100.673	100.36	98.831	99.717	99.024	99.179	97.926	100.654	98.792	99.369	97.72	98.698	98.577
proporção atômica para 3 íons													
Fe	1.003	1.001	1.042	1.000	0.993	1.004	1.013	0.999	1.013	1.002	0.986	0.983	0.994
Cu	0.000	0.001	0.001	0.001	0.000	0.001	0.001	0.000	0.000	0.000	0.000	0.000	0.001
Pb	0.002	0.002	0.002	0.002	0.000	0.002	0.002	0.002	0.000	0.000	0.002	0.002	0.002
Co	0.001	0.002	0.002	0.001	0.006	0.002	0.002	0.001	0.001	0.002	0.005	0.005	0.002
Ag	0.000	0.000	0.000	0.000	0.000	0.000	0.000	0.000	0.000	0.000	0.000	0.000	0.000
Zn	0.000	0.000	0.000	0.000	0.000	0.000	0.000	0.000	0.000	0.000	0.000	0.000	0.000
Ni	0.000	0.000	0.000	0.000	0.000	0.000	0.000	0.000	0.000	0.000	0.000	0.000	0.000
Pt	0.000	0.000	0.000	0.000	0.000	0.000	0.000	0.000	0.000	0.000	0.000	0.000	0.000
Pd	0.000	0.000	0.000	0.000	0.000	0.000	0.000	0.000	0.000	0.000	0.000	0.000	0.000
S	1.994	1.994	1.953	1.996	2.000	1.991	1.983	1.997	1.985	1.996	2.005	2.009	2.001
As	0.000	0.000	0.000	0.000	0.000	0.000	0.000	0.000	0.000	0.000	0.000	0.000	0.000
Se	0.001	0.000	0.000	0.000	0.000	0.000	0.000	0.001	0.000	0.000	0.002	0.000	0.000
total	3	3	3	3	3	3	3	3	3	3	3	3	3
Σ cations	1.006	1.005	1.047	1.004	1.000	1.009	1.017	1.002	1.014	1.004	0.993	0.991	0.999
Σ anions	1.994	1.995	1.953	1.996	2.000	1.991	1.983	1.998	1.986	1.996	2.007	2.009	2.001

Dados de Química Mineral de Sulfeto (cont.)

Amostra	153_4F núcleo	153_4F borda	153_4F borda	CP3 pirita	CP2 pirita	CP3 núcleo	CP2 pirita	CP2 núcleo	CO3S1 pirita	CO3S1 carbonatito	SH2 pirita	SH2 carbonatito	CO3S2 pirita	
mineral	pirita	pirita	pirita	nelsonito	nelsonito	nelsonito	nelsonito	nelsonito	carbonatito	carbonatito	núcleo	borda	núcleo	
Rocha	carbonatito	carbonatito	carbonatito	Catalão II	Catalão II	Catalão II	Catalão II	Catalão I	Catalão I	Catalão I	borda	pirita	pirita	
Complexo	Catalão II	Catalão II	Catalão II	Catalão II	Catalão II	Catalão II	Catalão II	Catalão I	Catalão I	Catalão I	pirita	carbonatito	carbonatito	
Fe	46.077	44.732	45.246	46.327	46.065	46.409	46.042	46.423	46.57	46.585	46.68	46.83	46.46	
Cu	0.034	0.044	0.022	0.195	0.041	0.335	0.03	0	0.013	0.012	0.008	0	0	
Pb	0.329	0.377	0.332	0.342	0.013	0.342	0	0.295	0.252	0.261	0	0.35	0.332	
Co	0.336	0.433	0.342	0.163	0.052	0.084	0.017	0.096	0.033	0.082	0.063	0.062	0.036	
Ag	0	0	0.017	0.018	0.007	0.003	0.002	0	0	0	0.006	0	0	
Zn	0.016	0.007	0.005	0.01	0	0	0.014	0.006	0	0	0	0.022	0	
Ni	0	0.034	0	0	0	0.018	0.003	0.032	0	0.01	0	0	0.001	
Pt	0	0	0	0.009	0	0.013	0	0.005	0	0	0	0	0.015	
Pd	0.008	0.003	0	0.001	0.001	0	0.005	0	0	0	0	0	0.012	
S	53.226	52.809	52.247	53.347	53.189	53.432	52.894	53.651	53.437	53.41	53.208	53.208	53.442	
As	0.018	0.064	0.099	0	0	0.002	0	0.001	0	0	0	0	0.002	
Se	0	0	0	0.013	0.051	0.086	0	0.048	0.001	0.019	0.044	0.022	0.087	
Total	100.044	98.503	98.31	100.425	99.419	100.724	99.007	100.557	100.306	100.379	100.009	100.494	100.387	
proporção atômica para 3 íons														
Fe	0.993	0.977	0.993	0.995	0.995	0.994	0.999	0.994	1.000	1.000	1.004	1.006	0.997	
Cu	0.001	0.001	0.000	0.004	0.001	0.006	0.001	0.000	0.000	0.000	0.000	0.000	0.000	
Pb	0.002	0.002	0.002	0.002	0.000	0.002	0.000	0.002	0.001	0.002	0.000	0.002	0.002	
Co	0.007	0.009	0.007	0.003	0.001	0.002	0.000	0.002	0.001	0.002	0.001	0.001	0.001	
Ag	0.000	0.000	0.000	0.000	0.000	0.000	0.000	0.000	0.000	0.000	0.000	0.000	0.000	
Zn	0.000	0.000	0.000	0.000	0.000	0.000	0.000	0.000	0.000	0.000	0.000	0.000	0.000	
Ni	0.000	0.001	0.000	0.000	0.000	0.000	0.000	0.001	0.000	0.000	0.000	0.000	0.000	
Pt	0.000	0.000	0.000	0.000	0.000	0.000	0.000	0.000	0.000	0.000	0.000	0.000	0.000	
Pd	0.000	0.000	0.000	0.000	0.000	0.000	0.000	0.000	0.000	0.000	0.000	0.000	0.000	
S	1.997	2.009	1.996	1.995	2.002	1.994	1.999	2.001	1.998	1.996	1.994	1.990	1.998	
As	0.000	0.001	0.002	0.000	0.000	0.000	0.000	0.000	0.000	0.000	0.000	0.000	0.000	
Se	0.000	0.000	0.000	0.000	0.001	0.001	0.000	0.001	0.000	0.000	0.001	0.000	0.001	
total	3	3	3	3	3	3	3	3	3	3	3	3	3	
Σ cations	1.003	0.990	1.002	1.004	0.997	1.005	1.001	0.998	1.002	1.003	1.006	1.009	1.000	
Σ anions	1.997	2.010	1.998	1.996	2.003	1.995	1.999	2.002	1.998	1.997	1.994	1.991	2.000	

Dados de Química Mineral de Sulfeto (cont.)

Amostra	CO3S2	S24170B	S24170B	SH1	SH1	C1DQ	C1DQ	C1DQ	C1DQ	SH	SH	AO418_70	AO418_70
mineral	borda pirita	núcleo pirita	borda pirita										
Rocha	carbonatito	carbonatito	carb/nelsonito										
Complexo	Catalão I	Catalão I	Catalão I										
Fe	46.774	46.049	46.747	46.905	46.84	46.5	46.907	46.736	46.011	46.348	46.672	46.227	46.108
Cu	0.012	0.006	0	0.017	0.002	0	0.008	0	0	0	0.001	0.007	0.013
Pb	0.323	0.308	0.342	0.202	0.35	0.292	0.192	0.395	0.247	0.34	0.296	0.296	0
Co	0.046	0.58	0.051	0.101	0.073	0.06	0.07	0.051	0.069	0.059	0.073	0.083	0.085
Ag	0	0.026	0	0.017	0.016	0	0	0.007	0.001	0	0	0	0.004
Zn	0	0	0.001	0	0	0.002	0	0.01	0	0	0	0	0
Ni	0.007	0	0	0.012	0	0	0	0	0.005	0.009	0.018	0.037	0
Pt	0.037	0	0.009	0	0.007	0.011	0	0.027	0.017	0.008	0	0	0.01
Pd	0.004	0.003	0.01	0.006	0.009	0	0	0	0	0	0	0.002	0
S	53.545	52.923	53.576	53.308	53.382	53.724	53.95	53.952	53.622	53.519	53.565	52.773	53.238
As	0	0.001	0	0	0	0	0	0	0	0.006	0	0.006	0
Se	0	0	0.027	0.04	0.012	0	0	0.002	0.097	0.102	0.027	0	0
Total	100.748	99.896	100.763	100.608	100.691	100.589	101.127	101.18	100.069	100.391	100.652	99.431	99.458
proporção atômica para 3 íons													
Fe	1.001	0.995	1.000	1.005	1.004	0.995	0.998	0.995	0.989	0.995	0.999	1.002	0.996
Cu	0.000	0.000	0.000	0.000	0.000	0.000	0.000	0.000	0.000	0.000	0.000	0.000	0.000
Pb	0.002	0.002	0.002	0.001	0.002	0.002	0.001	0.002	0.001	0.002	0.002	0.002	0.000
Co	0.001	0.012	0.001	0.002	0.001	0.001	0.001	0.001	0.001	0.001	0.001	0.002	0.002
Ag	0.000	0.000	0.000	0.000	0.000	0.000	0.000	0.000	0.000	0.000	0.000	0.000	0.000
Zn	0.000	0.000	0.000	0.000	0.000	0.000	0.000	0.000	0.000	0.000	0.000	0.000	0.000
Ni	0.000	0.000	0.000	0.000	0.000	0.000	0.000	0.000	0.000	0.000	0.000	0.001	0.000
Pt	0.000	0.000	0.000	0.000	0.000	0.000	0.000	0.000	0.000	0.000	0.000	0.000	0.000
Pd	0.000	0.000	0.000	0.000	0.000	0.000	0.000	0.000	0.000	0.000	0.000	0.000	0.000
S	1.996	1.991	1.996	1.990	1.992	2.002	1.999	2.001	2.007	2.000	1.997	1.993	2.002
As	0.000	0.000	0.000	0.000	0.000	0.000	0.000	0.000	0.000	0.000	0.000	0.000	0.000
Se	0.000	0.000	0.000	0.001	0.000	0.000	0.000	0.000	0.001	0.002	0.000	0.000	0.000
total	3	3	3	3	3	3	3	3	3	3	3	3	3
Σ cations	1.004	1.009	1.003	1.009	1.008	0.998	1.001	0.999	0.992	0.998	1.003	1.007	0.998
Σ anions	1.996	1.991	1.997	1.991	1.992	2.002	1.999	2.001	2.008	2.002	1.997	1.993	2.002

Dados de Química Mineral de Sulfeto (cont.)

Amostra	AO418_70	J9050	J9050	J9050	AM3780	AC3283F	AC3283F	AC3283F	AB3223	AB3223	AB3223	L15250	L15250
mineral	borda pirita	núcleo pirita	borda pirita	borda pirita	núcleo pirita	borda pirita	núcleo pirita	borda pirita	núcleo pirita	borda pirita	borda pirita	núcleo pirita	borda pirita
Rocha	carb/nelsonito	carbonatito	carbonatito	carbonatito	carbonatito	nelsonito	nelsonito	nelsonito	ap carbonat	ap carbonat	ap carbonat	carbonatito	carbonatito
Complexo	Catalão I	Catalão I	Catalão I	Catalão I	Catalão I	Catalão I	Catalão I	Catalão I	Catalão I	Catalão I	Catalão I	Catalão I	Catalão I
Fe	46.43	45.323	45.123	45.183	45.624	45.756	45.663	45.603	46.514	46.381	46.409	46.199	45.983
Cu	0.011	0	0.029	0.014	0	0.012	0	0.003	0	0	0.046	0.025	0.059
Pb	0	0.312	0.34	0.328	0.333	0.392	0	0.17	0	0.278	0.237	0.296	0
Co	0.088	0.043	0.073	0.06	0.063	0.139	0.067	0.072	0.078	0.072	0.038	0.057	0.21
Ag	0.025	0	0.022	0	0	0.001	0	0.014	0	0.009	0.01	0.004	0.004
Zn	0	0	0	0	0	0	0.004	0	0	0	0.016	0	0
Ni	0.013	0.003	0	0.019	0.003	0	0	0	0	0	0.013	0	0
Pt	0	0	0	0	0.008	0	0.024	0.011	0.015	0.006	0	0	0
Pd	0	0.006	0.006	0	0	0	0	0.001	0.007	0.01	0	0	0.001
S	53.217	52.697	52.888	52.636	53.119	52.4	53.037	53.048	53.461	53.466	53.517	53.156	53.178
As	0	0.005	0	0.013	0.002	0	0.003	0	0	0.008	0.001	0	0
Se	0	0.045	0.011	0.073	0.005	0.063	0.037	0	0.08	0	0.059	0	0.113
Total	99.784	98.434	98.492	98.326	99.157	98.763	98.835	98.922	100.155	100.23	100.346	99.737	99.548
proporção atômica para 3 íons													
Fe	1.000	0.991	0.985	0.989	0.990	1.000	0.992	0.991	0.998	0.996	0.996	0.998	0.993
Cu	0.000	0.000	0.001	0.000	0.000	0.000	0.000	0.000	0.000	0.000	0.001	0.000	0.001
Pb	0.000	0.002	0.002	0.002	0.002	0.002	0.000	0.001	0.000	0.002	0.001	0.002	0.000
Co	0.002	0.001	0.002	0.001	0.001	0.003	0.001	0.001	0.002	0.001	0.001	0.001	0.004
Ag	0.000	0.000	0.000	0.000	0.000	0.000	0.000	0.000	0.000	0.000	0.000	0.000	0.000
Zn	0.000	0.000	0.000	0.000	0.000	0.000	0.000	0.000	0.000	0.000	0.000	0.000	0.000
Ni	0.000	0.000	0.000	0.000	0.000	0.000	0.000	0.000	0.000	0.000	0.000	0.000	0.000
Pt	0.000	0.000	0.000	0.000	0.000	0.000	0.000	0.000	0.000	0.000	0.000	0.000	0.000
Pd	0.000	0.000	0.000	0.000	0.000	0.000	0.000	0.000	0.000	0.000	0.000	0.000	0.000
S	1.997	2.006	2.011	2.006	2.007	1.994	2.006	2.007	1.999	2.000	2.000	1.999	2.000
As	0.000	0.000	0.000	0.000	0.000	0.000	0.000	0.000	0.000	0.000	0.000	0.000	0.000
Se	0.000	0.001	0.000	0.001	0.000	0.001	0.001	0.000	0.001	0.000	0.001	0.000	0.002
total	3	3	3	3	3	3	3	3	3	3	3	3	3
Σ cations	1.003	0.993	0.989	0.993	0.993	1.005	0.993	0.993	1.000	1.000	0.999	1.001	0.998
Σ anions	1.997	2.007	2.011	2.007	2.007	1.995	2.007	2.007	2.007	2.000	2.001	1.999	2.002

Dados de Química Mineral de Sulfeto (cont.)

Amostra	L15250 borda pirita carbonatito Catalão I	L15250 borda pirita carbonatito Catalão I	CB15H núcleo pirita carbonatito Catalão I	CB15H borda pirita carbonatito Catalão I	CB15M núcleo pirita carbonatito Catalão I	CB15M borda pirita carbonatito Catalão I	CB15M borda pirita carbonatito Catalão I	NRD326 núcleo pirita nelsonito Catalão I	NRD326 borda pirita nelsonito Catalão I	NRD326 borda pirita nelsonito Catalão I	NRD304 núcleo pirita nelsonito Catalão I	NRD304 borda pirita nelsonito Catalão I	
mineral													
Rocha													
Complexo													
Fe	46.694	46.317	46.142	46.537	46.336	46.866	46.032	46.604	45.577	45.566	46.217	46.872	46.658
Cu	0.019	0.001	0.058	0.05	0.022	0.021	0.031	0.004	0.01	0.048	0.035	0.05	0.036
Pb	0.336	0.358	0.388	0.301	0.29	0.308	0.365	0.265	0.239	0.339	0.25	0.284	0.322
Co	0.363	0.095	0.06	0.068	0.052	0.077	0.047	0.031	0.057	0.03	0.029	0.041	0.052
Ag	0	0	0	0.031	0	0	0	0	0.004	0	0.004	0.007	0
Zn	0.007	0.003	0.015	0	0	0	0	0.004	0	0.005	0	0.016	0
Ni	0.018	0.011	0	0.014	0	0	0	0	0	0	0.005	0	0
Pt	0	0	0	0.005	0.013	0	0	0	0	0.023	0	0.008	0
Pd	0	0	0.017	0.003	0	0.005	0	0	0	0	0.001	0	0
S	52.417	53.291	53.288	53.156	53.095	53.197	53.223	53.383	53.062	52.839	53.28	54.091	53.946
As	0	0	0	0	0	0.008	0	0	0	0	0	0	0.004
Se	0	0	0.002	0	0	0.054	0	0.014	0.001	0.137	0	0.018	0.101
Total	99.854	100.076	99.97	100.165	99.808	100.536	99.698	100.305	98.95	98.987	99.821	101.387	101.119
proporção atômica para 3 íons													
Fe	1.012	0.997	0.995	1.002	1.000	1.006	0.994	1.001	0.990	0.992	0.996	0.995	0.994
Cu	0.000	0.000	0.001	0.001	0.000	0.000	0.001	0.000	0.000	0.001	0.001	0.001	0.001
Pb	0.002	0.002	0.002	0.002	0.002	0.002	0.002	0.002	0.001	0.002	0.001	0.002	0.002
Co	0.007	0.002	0.001	0.001	0.001	0.002	0.001	0.001	0.001	0.001	0.001	0.001	0.001
Ag	0.000	0.000	0.000	0.000	0.000	0.000	0.000	0.000	0.000	0.000	0.000	0.000	0.000
Zn	0.000	0.000	0.000	0.000	0.000	0.000	0.000	0.000	0.000	0.000	0.000	0.000	0.000
Ni	0.000	0.000	0.000	0.000	0.000	0.000	0.000	0.000	0.000	0.000	0.000	0.000	0.000
Pt	0.000	0.000	0.000	0.000	0.000	0.000	0.000	0.000	0.000	0.000	0.000	0.000	0.000
Pd	0.000	0.000	0.000	0.000	0.000	0.000	0.000	0.000	0.000	0.000	0.000	0.000	0.000
S	1.978	1.998	2.000	1.993	1.996	1.989	2.002	1.997	2.007	2.003	2.001	2.001	2.001
As	0.000	0.000	0.000	0.000	0.000	0.000	0.000	0.000	0.000	0.000	0.000	0.000	0.000
Se	0.000	0.000	0.000	0.000	0.000	0.001	0.000	0.000	0.000	0.002	0.000	0.000	0.002
total	3	3	3	3	3	3	3	3	3	3	3	3	3
Σ cations	1.022	1.002	1.000	1.007	1.004	1.010	0.998	1.003	0.993	0.995	0.999	0.999	0.997
Σ anions	1.978	1.998	2.000	1.993	1.996	1.990	2.002	1.997	2.007	2.005	2.001	2.001	2.003

Dados de Química Mineral de Sulfeto (cont.)

Amostra	NRD304 borda pirita nelsonito Catalão I	NRD304 núcleo pirita nelsonito Catalão I	NRD304 núcleo pirita nelsonito Catalão I	NRD256 núcleo pirita nelsonito Catalão I	NRD256 borda pirita nelsonito Catalão I	NRD256 borda pirita nelsonito Catalão I	NRD256 núcleo pirita nelson/carb Catalão I	NRD230 borda pirita nelson/carb Catalão I	NRD230 borda pirita nelson/carb Catalão I	NRD218 núcleo pirita carbonatito Catalão I	NRD218 borda pirita carbonatito Catalão I	NRD218 borda pirita carbonatito Catalão I	
mineral													
Rocha													
Complexo													
Fe	46.516	46.849	46.622	47.002	46.618	46.5	46.936	46.562	46.24	46.789	46.273	46.291	46.365
Cu	0.033	0.004	0.017	0.023	0.029	0	0.03	0.028	0.029	0.043	0.032	0.01	0.025
Pb	0.258	0.306	0.234	0.306	0.245	0.345	0.416	0.342	0.356	0.294	0.258	0.233	0.276
Co	0.071	0.081	0.072	0.069	0.052	0.078	0.056	0.079	0.099	0.077	0.047	0.058	0.049
Ag	0	0	0	0	0	0	0	0	0.007	0	0	0.006	0
Zn	0	0	0	0.005	0.026	0	0	0	0.004	0	0.003	0	0.014
Ni	0	0.018	0	0	0.009	0	0.001	0.006	0	0	0	0	0.011
Pt	0.014	0	0.018	0	0	0	0	0.031	0.029	0	0	0	0
Pd	0	0	0	0.001	0	0	0	0.003	0.008	0.005	0.016	0	0
S	53.864	53.743	53.919	53.607	53.461	53.784	53.604	53.478	53.458	53.852	53.099	53.721	53.929
As	0	0	0.002	0	0.001	0.002	0	0	0	0	0	0	0.009
Se	0.067	0.083	0.035	0.072	0.019	0	0.056	0.027	0.008	0.043	0.093	0.079	0
Total	100.823	101.084	100.919	101.085	100.46	100.709	101.099	100.522	100.235	101.135	99.81	100.414	100.678
proporção atômica para 3 íons													
Fe	0.993	0.999	0.994	1.003	1.000	0.994	1.002	0.998	0.994	0.997	0.999	0.992	0.990
Cu	0.001	0.000	0.000	0.000	0.001	0.000	0.001	0.001	0.001	0.001	0.001	0.000	0.000
Pb	0.001	0.002	0.001	0.002	0.001	0.002	0.002	0.002	0.002	0.002	0.002	0.001	0.002
Co	0.001	0.002	0.001	0.001	0.001	0.002	0.001	0.002	0.002	0.002	0.001	0.001	0.001
Ag	0.000	0.000	0.000	0.000	0.000	0.000	0.000	0.000	0.000	0.000	0.000	0.000	0.000
Zn	0.000	0.000	0.000	0.000	0.000	0.000	0.000	0.000	0.000	0.000	0.000	0.000	0.000
Ni	0.000	0.000	0.000	0.000	0.000	0.000	0.000	0.000	0.000	0.000	0.000	0.000	0.000
Pt	0.000	0.000	0.000	0.000	0.000	0.000	0.000	0.000	0.000	0.000	0.000	0.000	0.000
Pd	0.000	0.000	0.000	0.000	0.000	0.000	0.000	0.000	0.000	0.000	0.000	0.000	0.000
S	2.002	1.996	2.002	1.992	1.996	2.002	1.993	1.997	2.001	1.998	1.996	2.004	2.006
As	0.000	0.000	0.000	0.000	0.000	0.000	0.000	0.000	0.000	0.000	0.000	0.000	0.000
Se	0.001	0.001	0.001	0.001	0.000	0.000	0.001	0.000	0.000	0.001	0.001	0.001	0.000
total	3	3	3	3	3	3	3	3	3	3	3	3	3
Σ cations	0.997	1.003	0.997	1.007	1.003	0.998	1.006	1.003	0.999	1.001	1.002	0.995	0.994
Σ anions	2.003	1.997	2.003	1.993	1.997	2.002	1.994	1.997	2.001	1.999	1.998	2.005	2.006

Dados de Química Mineral de Sulfeto (cont.)

Amostra	NRD218 núcleo	NRD218 borda	NRD218 borda	NRD326.2 núcleo	NRD326.2 borda	NRD326.2 núcleo	C1PG borda	C1PG pirita	C1PG carbonatito	C1PG carbonatito	C1PG borda	C1PG pirita	C1PG carbonatito	C1PG borda	núcleo
mineral	pirita	pirita	pirita	pirita	pirita	pirita	pirita	pirita	carbonatito	carbonatito	pirita	pirita	carbonatito	pirita	núcleo
Rocha	carbonatito	carbonatito	carbonatito	carbonatito	nelsonito	nelsonito	carbonatito	carbonatito	carbonatito	carbonatito	carbonatito	carbonatito	carbonatito	carbonatito	núcleo
Complexo	Catalão I	Catalão I	Catalão I	Catalão I	Catalão I	Catalão I	Catalão I	Catalão I	Catalão I	Catalão I	Catalão I	Catalão I	Catalão I	Catalão I	Catalão I
Fe	46.362	45.954	46.345	43.1	46.845	45.559	46.484	46.552	46.547	46.643	46.515	46.691	46.595		
Cu	0.039	0.029	0.035	0.024	0.009	0.032	0	0.012	0.024	0.036	0.025	0	0		
Pb	0.304	0.349	0.302	0.386	0.339	0.338	0.328	0.289	0.345	0.34	0.332	0.314	0.384		
Co	0.057	0.052	0.067	2.517	0.065	0.48	0.098	0.095	0.053	0.077	0.058	0.062	0.123		
Ag	0.006	0	0	0.008	0.02	0	0.004	0	0	0.001	0	0	0.006		
Zn	0	0	0	0	0	0.004	0	0	0	0.005	0.004	0	0		
Ni	0	0.014	0.006	0.039	0	0	0.021	0.013	0	0.019	0.015	0	0		
Pt	0	0	0	0.025	0	0	0	0.011	0	0	0	0.002	0		
Pd	0	0.006	0	0	0	0.005	0.011	0.005	0	0	0	0	0		
S	53.509	53.243	53.467	51.754	53.423	52.762	53.7	53.346	53.302	53.899	54.11	53.59	53.611		
As	0	0	0	0	0	0	0.004	0	0	0	0	0.006	0.112		
Se	0	0.031	0.025	0	0.052	0	0	0.112	0	0	0.132	0	0		
Total	100.277	99.678	100.247	97.853	100.753	99.18	100.65	100.435	100.271	101.02	101.191	100.665	100.831		
proporção atômica para 3 íons															
Fe	0.995	0.993	0.996	0.952	1.003	0.990	0.995	0.999	1.001	0.994	0.989	0.999	0.997		
Cu	0.001	0.001	0.001	0.000	0.000	0.001	0.000	0.000	0.000	0.001	0.000	0.000	0.000		
Pb	0.002	0.002	0.002	0.002	0.002	0.002	0.002	0.002	0.002	0.002	0.002	0.002	0.002		
Co	0.001	0.001	0.001	0.053	0.001	0.010	0.002	0.002	0.001	0.002	0.001	0.001	0.002		
Ag	0.000	0.000	0.000	0.000	0.000	0.000	0.000	0.000	0.000	0.000	0.000	0.000	0.000		
Zn	0.000	0.000	0.000	0.000	0.000	0.000	0.000	0.000	0.000	0.000	0.000	0.000	0.000		
Ni	0.000	0.000	0.000	0.001	0.000	0.000	0.000	0.000	0.000	0.000	0.000	0.000	0.000		
Pt	0.000	0.000	0.000	0.000	0.000	0.000	0.000	0.000	0.000	0.000	0.000	0.000	0.000		
Pd	0.000	0.000	0.000	0.000	0.000	0.000	0.000	0.000	0.000	0.000	0.000	0.000	0.000		
S	2.001	2.003	2.000	1.991	1.992	1.997	2.001	1.995	1.996	2.001	2.005	1.998	1.997		
As	0.000	0.000	0.000	0.000	0.000	0.000	0.000	0.000	0.000	0.000	0.000	0.000	0.002		
Se	0.000	0.000	0.000	0.000	0.001	0.000	0.000	0.002	0.000	0.000	0.002	0.000	0.000		
total	3	3	3	3	3	3	3	3	3	3	3	3	3		
Σ cations	0.999	0.997	0.999	1.009	1.007	1.003	0.999	1.004	1.004	0.999	0.993	1.002	1.001		
Σ anions	2.001	2.003	2.001	1.991	1.993	1.997	2.001	1.996	1.996	2.001	2.007	1.998	1.999		

Dados de Química Mineral de Sulfeto (cont.)

Amostra	CB12 borda	CB12 pirita	CB11 carbonatito	CB11 núcleo	CB11 pirita	CB07 carbonatito	CB07 borda	CB07 pirita	CB07 foscorito	CB07 borda	CB07 pirita	CB04 borda	CB04 pirita	CB04 carbonatito
mineral														
Rocha	Catalão I	Catalão I	Catalão I	Catalão I	Catalão I	Foscorito	Catalão I	Catalão I	Catalão I	Catalão I	Catalão I	Catalão I	Catalão I	Catalão I
Complexo						Catalão I								
Fe	46.645	46.546	46.624	46.439	46.631	47.073	46.772	46.742	47.08	47.061	46.908	46.65	46.633	
Cu	0.001	0.015	0	0	0.037	0.011	0	0.021	0.019	0.023	0.008	0.009	0	
Pb	0.351	0.336	0.355	0.264	0.324	0.332	0.325	0.329	0.294	0.358	0.311	0.305	0.283	
Co	0.082	0.158	0.056	0.198	0.172	0.024	0.056	0.046	0.029	0.083	0.067	0.036	0.045	
Ag	0	0.017	0.038	0.003	0.008	0	0	0	0.027	0	0.004	0	0.004	
Zn	0.018	0	0	0	0	0	0.008	0	0.004	0.001	0	0	0	
Ni	0	0	0	0	0	0	0	0	0	0	0	0	0.005	
Pt	0.009	0	0	0	0	0	0	0	0.002	0	0.019	0	0	
Pd	0.01	0	0	0	0	0	0.003	0	0	0	0.004	0	0.008	
S	53.874	53.428	53.63	53.33	53.18	53.792	53.71	53.947	53.676	54.362	53.826	53.492	53.921	
As	0.015	0.069	0.003	0.001	0	0	0	0	0	0	0	0	0	
Se	0	0.035	0.068	0.069	0	0	0.026	0.051	0.029	0.031	0.011	0	0.062	
Total	101.005	100.604	100.774	100.304	100.352	101.232	100.9	101.136	101.16	101.919	101.158	100.492	100.961	
proporção atômica para 3 íons														
Fe	0.995	0.998	0.997	0.998	1.003	1.002	0.999	0.995	1.004	0.995	0.999	1.000	0.994	
Cu	0.000	0.000	0.000	0.000	0.001	0.000	0.000	0.000	0.000	0.000	0.000	0.000	0.000	
Pb	0.002	0.002	0.002	0.002	0.002	0.002	0.002	0.002	0.002	0.002	0.002	0.002	0.002	
Co	0.002	0.003	0.001	0.004	0.004	0.000	0.001	0.001	0.001	0.002	0.001	0.001	0.001	
Ag	0.000	0.000	0.000	0.000	0.000	0.000	0.000	0.000	0.000	0.000	0.000	0.000	0.000	
Zn	0.000	0.000	0.000	0.000	0.000	0.000	0.000	0.000	0.000	0.000	0.000	0.000	0.000	
Ni	0.000	0.000	0.000	0.000	0.000	0.000	0.000	0.000	0.000	0.000	0.000	0.000	0.000	
Pt	0.000	0.000	0.000	0.000	0.000	0.000	0.000	0.000	0.000	0.000	0.000	0.000	0.000	
Pd	0.000	0.000	0.000	0.000	0.000	0.000	0.000	0.000	0.000	0.000	0.000	0.000	0.000	
S	2.001	1.995	1.998	1.996	1.991	1.995	1.998	2.001	1.993	2.001	1.997	1.997	2.002	
As	0.000	0.001	0.000	0.000	0.000	0.000	0.000	0.000	0.000	0.000	0.000	0.000	0.000	
Se	0.000	0.001	0.001	0.001	0.000	0.000	0.000	0.001	0.000	0.000	0.000	0.000	0.001	
total	3	3	3	3	3	3	3	3	3	3	3	3	3	
Σ cations	0.999	1.004	1.001	1.003	1.009	1.005	1.002	0.999	1.007	0.999	1.003	1.003	0.997	
Σ anions	2.001	1.996	1.999	1.997	1.991	1.995	1.998	2.001	1.993	2.001	1.997	1.997	2.003	

Dados de Química Mineral de Sulfeto (cont.)

Amostra	CB02 núcleo	CB02 borda	CB02 borda	CB14 núcleo	CB14 borda	CB16 núcleo	CB16 pirita	NRD204 núcleo	NRD204 borda	NRD204 pirita	NRD178 núcleo	NRD178 borda	NRD178 pirita	NRD178 borda
mineral	pirita	pirita	pirita	pirita	pirita	pirita	nelsonito	nelsonito	nelsonito	nelsonito	Catalão I	Catalão I	Catalão I	Catalão I
Rocha	carbonatito	carbonatito	carbonatito	foscorito	foscorito	fenite	Catalão I	Catalão I	Catalão I	Catalão I	Catalão I	Catalão I	Catalão I	Catalão I
Complexo	Catalão I	Catalão I	Catalão I	Catalão I	Catalão I	Catalão I	Catalão I	Catalão I	Catalão I	Catalão I	Catalão I	Catalão I	Catalão I	Catalão I
Fe	46.812	46.544	46.829	47.077	46.748	46.046	45.855	46.952	46.769	46.8	46.565	46.69	46.678	
Cu	0.01	0.009	0.004	0	0.016	0.006	0.015	0.004	0	0.017	0.029	0	0.026	
Pb	0.306	0.364	0.31	0.294	0.346	0.173	0.208	0.267	0.193	0.181	0.289	0.31	0.319	
Co	0.081	0.074	0.077	0.061	0.062	0.047	0.03	0.061	0.028	0.054	0.083	0.083	0.048	
Ag	0	0	0	0	0	0.006	0.001	0	0	0.022	0.013	0	0	
Zn	0	0	0.005	0	0	0	0.005	0	0.007	0.002	0	0.008	0	
Ni	0	0	0	0.002	0	0	0.014	0	0.022	0	0	0	0	
Pt	0	0.004	0	0.01	0	0	0	0	0	0	0.033	0.015	0	
Pd	0	0	0	0	0	0	0	0	0	0.006	0.002	0.002	0.009	
S	53.506	53.528	53.902	53.808	53.629	53.278	53.285	53.707	53.522	53.654	54.145	53.946	53.355	
As	0.01	0.001	0.002	0	0	0.002	0	0	0	0	0	0.003	0	
Se	0.067	0.005	0.01	0.052	0.046	0.006	0.029	0.048	0.018	0	0.1	0	0.015	
Total	100.792	100.529	101.139	101.304	100.847	99.564	99.442	101.039	100.559	100.736	101.259	101.057	100.45	
proporção atômica para 3 íons														
Fe	1.002	0.998	0.997	1.002	0.999	0.994	0.991	1.001	1.001	1.000	0.990	0.995	1.002	
Cu	0.000	0.000	0.000	0.000	0.000	0.000	0.000	0.000	0.000	0.000	0.001	0.000	0.000	
Pb	0.002	0.002	0.002	0.002	0.002	0.001	0.001	0.002	0.001	0.001	0.002	0.002	0.002	
Co	0.002	0.002	0.002	0.001	0.001	0.001	0.001	0.001	0.001	0.001	0.002	0.002	0.001	
Ag	0.000	0.000	0.000	0.000	0.000	0.000	0.000	0.000	0.000	0.000	0.000	0.000	0.000	
Zn	0.000	0.000	0.000	0.000	0.000	0.000	0.000	0.000	0.000	0.000	0.000	0.000	0.000	
Ni	0.000	0.000	0.000	0.000	0.000	0.000	0.000	0.000	0.000	0.000	0.000	0.000	0.000	
Pt	0.000	0.000	0.000	0.000	0.000	0.000	0.000	0.000	0.000	0.000	0.000	0.000	0.000	
Pd	0.000	0.000	0.000	0.000	0.000	0.000	0.000	0.000	0.000	0.000	0.000	0.000	0.000	
S	1.994	1.998	1.999	1.994	1.996	2.003	2.006	1.995	1.996	1.997	2.004	2.002	1.994	
As	0.000	0.000	0.000	0.000	0.000	0.000	0.000	0.000	0.000	0.000	0.000	0.000	0.000	
Se	0.001	0.000	0.000	0.001	0.001	0.000	0.000	0.001	0.000	0.000	0.002	0.000	0.000	
total	3	3	3	3	3	3	3	3	3	3	3	3	3	
Σ cations	1.005	1.002	1.001	1.005	1.003	0.996	0.994	1.004	1.004	1.003	0.994	0.998	1.005	
Σ anions	1.995	1.998	1.999	1.995	1.997	2.004	2.006	1.996	1.996	1.997	2.006	2.002	1.995	

Dados de Química Mineral de Sulfeto (cont.)

Amostra	NRD164 núcleo	NRD164 borda	NRD164 núcleo	NRD134 núcleo	NRD134 borda	NRD134 pirita	NRD134 magnetitite	NRD134 borda	MINA2 borda	MINA2 pirita	NRD216B núcleo	NRD216B pirita	241_70A C1 núcleo	241_70A C1 borda	
mineral	pirita	pirita	pirita	pirita	pirita	pirita	magnetitite	pirita	pirita	magnetitite	carbonatito	carbonatito	pirita	pirita	
Rocha	nelsonito	nelsonito	nelsonito	Catalão I	Catalão I	Catalão I	Catalão I	Catalão I	Catalão I	Catalão I	Catalão I	Catalão I	carbonatito	carbonatito	
Complexo	Catalão I	Catalão I	Catalão I	Catalão I	Catalão I	Catalão I	Catalão I	Catalão I	Catalão I	Catalão I	Catalão I	Catalão I	Catalão I	Catalão I	
Fe	45.902	45.719	46.291	46.67	46.729	44.952	46.534	46.21	44.697	46.351	46.686	46.736	46.675		
Cu	0.034	0	0.02	0.014	0	0	0.025	0.005	0.007	0.046	0.011	0.003	0.009		
Pb	0.297	0.256	0.3	0.274	0.344	0.289	0.329	0.355	0.288	0.322	0.267	0.036	0		
Co	0.063	0.057	0.069	0.239	0.319	2.135	0.272	0.056	0.761	0.037	0.056	0.08	0.031		
Ag	0.026	0	0	0.001	0	0.017	0	0	0.011	0.003	0	0	0.018		
Zn	0	0.005	0	0	0	0.003	0.003	0	0	0.01	0	0.001	0		
Ni	0	0	0.005	0.001	0.001	0	0	0	0	0.004	0	0	0		
Pt	0	0	0.032	0	0	0	0.002	0	0	0.018	0	0	0.003		
Pd	0.005	0.009	0	0	0	0	0	0	0	0.001	0	0	0		
S	52.082	51.862	52.589	53.215	53.066	52.399	52.893	53.072	51.575	52.788	53.761	52.37	52.578		
As	0.006	0	0.004	0	0	0.007	0	0.005	0	0.005	0	0	0		
Se	0.075	0.015	0.014	0.097	0.041	0.134	0.03	0	0.019	0.131	0.016	0.02	0		
Total	98.49	97.923	99.324	100.511	100.5	99.936	100.088	99.703	97.358	99.715	100.798	99.246	99.314		
proporção atômica para 3 íons															
Fe	1.006	1.007	1.006	1.002	1.004	0.974	1.004	0.999	0.991	1.004	0.997	1.016	1.013		
Cu	0.001	0.000	0.000	0.000	0.000	0.000	0.000	0.000	0.000	0.001	0.000	0.000	0.000		
Pb	0.002	0.002	0.002	0.002	0.002	0.002	0.002	0.002	0.002	0.002	0.002	0.000	0.000		
Co	0.001	0.001	0.001	0.005	0.006	0.044	0.006	0.001	0.016	0.001	0.001	0.002	0.001		
Ag	0.000	0.000	0.000	0.000	0.000	0.000	0.000	0.000	0.000	0.000	0.000	0.000	0.000		
Zn	0.000	0.000	0.000	0.000	0.000	0.000	0.000	0.000	0.000	0.000	0.000	0.000	0.000		
Ni	0.000	0.000	0.000	0.000	0.000	0.000	0.000	0.000	0.000	0.000	0.000	0.000	0.000		
Pt	0.000	0.000	0.000	0.000	0.000	0.000	0.000	0.000	0.000	0.000	0.000	0.000	0.000		
Pd	0.000	0.000	0.000	0.000	0.000	0.000	0.000	0.000	0.000	0.000	0.000	0.000	0.000		
S	1.988	1.990	1.990	1.990	1.986	1.978	1.988	1.998	1.991	1.990	2.000	1.982	1.986		
As	0.000	0.000	0.000	0.000	0.000	0.000	0.000	0.000	0.000	0.000	0.000	0.000	0.000		
Se	0.001	0.000	0.000	0.001	0.001	0.002	0.000	0.000	0.000	0.002	0.000	0.000	0.000		
total	3	3	3	3	3	3	3	3	3	3	3	3	3	3	
Σ cations	1.010	1.010	1.010	1.009	1.013	1.020	1.012	1.002	1.009	1.007	1.000	1.018	1.014		
Σ anions	1.990	1.990	1.990	1.991	1.987	1.980	1.988	1.998	1.991	1.993	2.000	1.982	1.986		

Dados de Química Mineral de Sulfeto (cont.)

Amostra	241_70A C1 borda pirita carbonatito Catalão I	241_70A C1 borda pirita carbonatito Catalão I	241_70A C2 núcleo pirita carbonatito Catalão I	241_70A C2 borda pirita carbonatito Catalão I	241_70A C2 núcleo pirita carbonatito Catalão I	241_70A C2 borda pirita carbonatito Catalão I	241_70A C2 borda pirita carbonatito Catalão I	AE460 C1 núcleo pirita nels (dyke) Catalão I	AE460 C1 borda pirita nels (dyke) Catalão I	AE460 C1 borda pirita nels (dyke) Catalão I	AE460 C2 núcleo pirita nels (dyke) Catalão I	AE460 C2 borda pirita nels (dyke) Catalão I	
mineral													
Rocha													
Complexo													
Fe	46.47	46.844	46.745	46.978	46.972	46.802	46.53	46.736	46.956	46.756	46.835	46.926	46.657
Cu	0.025	0	0	0	0	0.01	0	0.003	0	0	0	0.023	0
Pb	0	0	0	0	0	0	0	0	0.01	0	0	0	0
Co	0.07	0.067	0.07	0.022	0.039	0.075	0.039	0.056	0.09	0.069	0.072	0.057	0.089
Ag	0	0	0.006	0	0.008	0	0	0	0	0	0.008	0	0.002
Zn	0.005	0	0	0	0.013	0	0.01	0	0	0	0	0	0
Ni	0.004	0.008	0.001	0	0	0	0	0.005	0	0.002	0	0.008	0
Pt	0	0	0	0	0	0	0	0	0.001	0	0	0	0
Pd	0	0.003	0	0	0.014	0	0	0.003	0	0	0	0	0
S	52.169	52.547	52.159	52.316	52.015	51.773	51.007	51.506	50.826	50.363	50.636	50.404	50.379
As	0	0.001	0	0	0	0	0	0	0	0	0	0.002	0
Se	0.006	0.016	0	0.004	0.134	0.04	0	0	0.015	0.022	0.019	0.157	0.029
Total	98.749	99.486	98.981	99.32	99.195	98.69	97.596	98.306	97.89	97.223	97.57	97.577	97.156
proporção atômica para 3 íons													
Fe	1.014	1.015	1.019	1.020	1.023	1.024	1.031	1.027	1.039	1.042	1.040	1.044	1.041
Cu	0.000	0.000	0.000	0.000	0.000	0.000	0.000	0.000	0.000	0.000	0.000	0.000	0.000
Pb	0.000	0.000	0.000	0.000	0.000	0.000	0.000	0.000	0.000	0.000	0.000	0.000	0.000
Co	0.001	0.001	0.001	0.000	0.001	0.002	0.001	0.001	0.002	0.001	0.002	0.001	0.002
Ag	0.000	0.000	0.000	0.000	0.000	0.000	0.000	0.000	0.000	0.000	0.000	0.000	0.000
Zn	0.000	0.000	0.000	0.000	0.000	0.000	0.000	0.000	0.000	0.000	0.000	0.000	0.000
Ni	0.000	0.000	0.000	0.000	0.000	0.000	0.000	0.000	0.000	0.000	0.000	0.000	0.000
Pt	0.000	0.000	0.000	0.000	0.000	0.000	0.000	0.000	0.000	0.000	0.000	0.000	0.000
Pd	0.000	0.000	0.000	0.000	0.000	0.000	0.000	0.000	0.000	0.000	0.000	0.000	0.000
S	1.983	1.983	1.980	1.979	1.973	1.973	1.968	1.972	1.959	1.956	1.958	1.952	1.957
As	0.000	0.000	0.000	0.000	0.000	0.000	0.000	0.000	0.000	0.000	0.000	0.000	0.000
Se	0.000	0.000	0.000	0.000	0.002	0.001	0.000	0.000	0.000	0.000	0.000	0.002	0.000
total	3	3	3	3	3	3	3	3	3	3	3	3	3
Σ cations	1.017	1.017	1.020	1.021	1.025	1.026	1.032	1.028	1.041	1.044	1.042	1.045	1.043
Σ anions	1.983	1.983	1.980	1.979	1.975	1.974	1.968	1.972	1.959	1.956	1.958	1.955	1.957

Dados de Química Mineral de Sulfeto (cont.)

Amostra	AE460 C3 borda	AE460 C3 pirita	SF1024 núcleo	SF1024 pirita	SF1024 phl. fosc	SF1024 Salitre	SF1024 Salitre	C60_1 pirita	F109CP carbonatito	F109CP Salitre	F109CP Salitre	SL296A pirita	FF413 bebedourito	FF413 Salitre
mineral														
Rocha	nels (dyke)	nels (dyke)	pirita	pirita	phl. fosc	phl. fosc	phl. fosc	carbonatito	carbonatito	carbonatito	carbonatito	bebedourito	pirita	pirita
Complexo	Catalão I	Catalão I	borda	borda	borda	borda	borda	borda	borda	borda	borda	Salitre	Salitre	Salitre
Fe	47.022	46.617	46.854	48.01	46.454	46.742	46.68	46.545	46.783	46.565	46.248	45.471	45.712	
Cu	0.023	0.012	0.039	0.026	0.036	0.027	0.047	0.045	0.028	0.075	0.016	0.038	0.018	
Pb	0	0	0.347	0.238	0.407	0.21	0.376	0	0.376	0.247	0.013	0.294	0.315	
Co	0.052	0.045	0.104	0.039	0.074	0.086	0.149	0.061	0.151	0.049	0.553	0.156	0.082	
Ag	0	0	0	0	0.026	0.002	0	0	0.009	0	0	0.001	0	
Zn	0	0	0	0.003	0	0.01	0	0.006	0.002	0	0	0.001	0.004	
Ni	0.005	0.023	0.001	0	0	0	0	0	0.017	0	0.169	0.704	0.154	
Pt	0	0	0.019	0	0	0.018	0.002	0.012	0.01	0	0	0	0	
Pd	0	0.001	0	0	0	0	0	0	0	0.001	0	0	0	
S	50.679	50.633	53.417	50.765	53.622	53.653	54.121	53.658	53.574	53.582	53.307	52.345	52.712	
As	0.007	0	0.003	0.016	0.001	0.002	0	0	0	0.004	0.012	0	0.001	
Se	0.013	0.041	0.047	0	0	0.029	0.043	0.022	0	0	0.051	0	0.064	
Total	97.801	97.372	100.831	99.097	100.62	100.779	101.418	100.349	100.95	100.523	100.369	99.01	99.062	
proporção atômica para 3 íons														
Fe	1.042	1.037	1.003	1.055	0.995	0.999	0.991	0.997	1.000	0.997	0.992	0.992	0.995	
Cu	0.000	0.000	0.001	0.001	0.001	0.001	0.001	0.001	0.001	0.001	0.000	0.001	0.000	
Pb	0.000	0.000	0.002	0.001	0.002	0.001	0.002	0.000	0.002	0.001	0.000	0.002	0.002	
Co	0.001	0.001	0.002	0.001	0.002	0.002	0.003	0.001	0.003	0.001	0.011	0.003	0.002	
Ag	0.000	0.000	0.000	0.000	0.000	0.000	0.000	0.000	0.000	0.000	0.000	0.000	0.000	
Zn	0.000	0.000	0.000	0.000	0.000	0.000	0.000	0.000	0.000	0.000	0.000	0.000	0.000	
Ni	0.000	0.000	0.000	0.000	0.000	0.000	0.000	0.000	0.000	0.000	0.003	0.015	0.003	
Pt	0.000	0.000	0.000	0.000	0.000	0.000	0.000	0.000	0.000	0.000	0.000	0.000	0.000	
Pd	0.000	0.000	0.000	0.000	0.000	0.000	0.000	0.000	0.000	0.000	0.000	0.000	0.000	
S	1.956	1.961	1.991	1.942	2.000	1.997	2.002	2.001	1.994	1.999	1.992	1.988	1.997	
As	0.000	0.000	0.000	0.000	0.000	0.000	0.000	0.000	0.000	0.000	0.000	0.000	0.000	
Se	0.000	0.001	0.001	0.000	0.000	0.000	0.001	0.000	0.000	0.000	0.001	0.000	0.001	
total	3	3	3	3	3	3	3	3	3	3	3	3	3	
Σ cations	1.044	1.038	1.008	1.057	1.000	1.003	0.997	0.999	1.006	1.001	1.007	1.012	1.002	
Σ anions	1.956	1.962	1.992	1.943	2.000	1.997	2.003	2.001	1.994	1.999	1.993	1.988	1.998	

Dados de Química Mineral de Sulfeto (cont.)

Amostra	F784 borda pirita carbonatito Complexo Fe	F784 núcleo pirita carbonatito Salitre	SLE277A1 borda pirita carbonatito Salitre	SLE277A1 núcleo pirita carbonatito Salitre	FVL184 borda pirita carbonatito Salitre	C8-9HID núcleo pirita carbonatito Araxá	C8-9HID borda pirita carbonatito Araxá	C8-5D núcleo pirita carbonatito Araxá	C8-5D borda pirita carbonatito Araxá	C8-2 núcleo pirita carbonatito Araxá	C8-2 borda pirita carbonatito Araxá	C8-2 núcleo pirita carbonatito Araxá	C8-2 núcleo pirita carbonatito Araxá	
mineral														
Rocha														
Complexo														
Fe	46.28	47.086	46.233	46.849	47.083	46.326	46.502	45.992	46.385	46.728	46.836	46.738	46.776	
Cu	0	0	0.031	0	0.011	0.01	0.031	0.013	0.009	0.002	0	0	0.013	
Pb	0.305	0.368	0.371	0.398	0	0	0	0.062	0	0	0	0	0	
Co	0.178	0.123	0.172	0.191	0.09	0.05	0.163	0.074	0.151	0.035	0.059	0.043	0.045	
Ag	0	0	0.01	0	0	0	0	0.004	0	0	0	0.007	0.004	
Zn	0	0	0.002	0.012	0	0	0	0	0	0	0	0	0.021	
Ni	0.032	0.031	0.009	0.009	0.013	0.114	0.037	0.015	0.022	0.003	0	0.043	0	
Pt	0	0.014	0	0	0	0	0	0.007	0	0	0	0	0	
Pd	0.011	0	0	0	0	0.005	0	0	0.002	0.007	0	0	0.006	
S	52.406	53.616	53.258	52.824	53.163	53.445	53.591	51.678	52.841	53.788	52.986	53.559	53.671	
As	0	0	0	0	0.003	0	0.056	1.343	0.431	0.011	0.497	0.009	0	
Se	0.053	0	0	0.05	0.015	0.049	0	0	0	0.039	0	0.051	0.131	
Total	99.265	101.238	100.086	100.333	100.378	99.999	100.38	99.188	99.841	100.613	100.378	100.45	100.667	
proporção atômica para 3 íons														
Fe	1.007	1.004	0.996	1.010	1.010	0.996	0.996	1.006	1.002	0.998	1.007	1.001	0.999	
Cu	0.000	0.000	0.001	0.000	0.000	0.000	0.001	0.000	0.000	0.000	0.000	0.000	0.000	
Pb	0.002	0.002	0.002	0.002	0.000	0.000	0.000	0.000	0.000	0.000	0.000	0.000	0.000	
Co	0.004	0.002	0.004	0.004	0.002	0.001	0.003	0.002	0.003	0.001	0.001	0.001	0.001	
Ag	0.000	0.000	0.000	0.000	0.000	0.000	0.000	0.000	0.000	0.000	0.000	0.000	0.000	
Zn	0.000	0.000	0.000	0.000	0.000	0.000	0.000	0.000	0.000	0.000	0.000	0.000	0.000	
Ni	0.001	0.001	0.000	0.000	0.000	0.002	0.001	0.000	0.000	0.000	0.000	0.001	0.000	
Pt	0.000	0.000	0.000	0.000	0.000	0.000	0.000	0.000	0.000	0.000	0.000	0.000	0.000	
Pd	0.000	0.000	0.000	0.000	0.000	0.000	0.000	0.000	0.000	0.000	0.000	0.000	0.000	
S	1.986	1.991	1.998	1.983	1.987	2.000	1.999	1.969	1.988	2.000	1.984	1.997	1.997	
As	0.000	0.000	0.000	0.000	0.000	0.000	0.001	0.022	0.007	0.000	0.008	0.000	0.000	
Se	0.001	0.000	0.000	0.001	0.000	0.001	0.000	0.000	0.000	0.001	0.000	0.001	0.002	
total	3	3	3	3	3	3	3	3	3	3	3	3	3	
Σ cations	1.013	1.009	1.002	1.016	1.013	0.999	1.000	1.009	1.006	0.999	1.008	1.002	1.001	
Σ anions	1.987	1.991	1.998	1.984	1.987	2.001	2.000	1.991	1.994	2.001	1.992	1.998	1.999	

Dados de Química Mineral de Sulfeto (cont.)

Amostra	C9-13	C9-13	C8-A3	C8-A3	C8-7G	C8-7G	C8-9MAG	C8-9MAG	C815	C815	C815	B944	B944	
mineral	borda	núcleo	núcleo	borda	núcleo	borda	núcleo	borda	borda	núcleo	borda	núcleo	borda	
Rocha	pirita	pirita	pirita	pirita	pirita	pirita	pirita	pirita	pirita	pirita	pirita	pirita	pirita	
Complexo	carbonatito	carbonatito	foscorito	foscorito	carbonatito									
Amostra	Araxá	Araxá	Araxá	Araxá	Araxá	Araxá	Araxá	Araxá	Araxá	Araxá	Araxá	Araxá	Araxá	
Fe	46.53	46.851	46.132	46.743	46.27	45.991	46.704	46.578	46.455	46.609	46.104	45.824	45.824	
Cu	0.04	0	0.056	0.007	0.018	0.024	0.01	0	0.017	0.037	0.006	0.001	0.02	
Pb	0	0.002	0	0	0.075	0.028	0	0	0.374	0.234	0.38	0.295	0.333	
Co	0.244	0.072	0.346	0.079	0.185	0.406	0.05	0.065	0.031	0.05	0.15	0.088	0.102	
Ag	0.021	0	0	0	0.021	0	0	0	0.001	0.024	0	0	0	
Zn	0.003	0	0	0	0.005	0	0.011	0	0.014	0	0.009	0.014	0	
Ni	0.063	0	0.097	0	0	0.032	0.053	0.084	0.002	0	0.129	0	0	
Pt	0.008	0	0.023	0	0.01	0	0.008	0	0	0.017	0	0	0.002	
Pd	0	0.003	0	0	0	0.002	0.003	0	0	0	0	0	0	
S	53.389	53.236	52.507	53.227	53.368	53.028	53.083	52.693	52.955	53.222	52.74	52.652	52.56	
As	0.039	0.026	0.017	0.016	0.074	0.409	0	0.001	0.003	0.013	0	0.004	0	
Se	0	0.022	0	0.006	0	0	0	0.059	0	0.039	0.022	0.046	0	
Total	100.337	100.212	99.178	100.078	100.026	99.92	99.922	99.48	99.852	100.245	99.54	98.924	98.841	
proporção atômica para 3 íons														
Fe	0.998	1.006	1.002	1.005	0.995	0.992	1.006	1.009	1.004	1.002	1.000	0.998	0.999	
Cu	0.001	0.000	0.001	0.000	0.000	0.000	0.000	0.000	0.000	0.001	0.000	0.000	0.000	
Pb	0.000	0.000	0.000	0.000	0.000	0.000	0.000	0.000	0.002	0.001	0.002	0.002	0.002	
Co	0.005	0.001	0.007	0.002	0.004	0.008	0.001	0.001	0.001	0.001	0.003	0.002	0.002	
Ag	0.000	0.000	0.000	0.000	0.000	0.000	0.000	0.000	0.000	0.000	0.000	0.000	0.000	
Zn	0.000	0.000	0.000	0.000	0.000	0.000	0.000	0.000	0.000	0.000	0.000	0.000	0.000	
Ni	0.001	0.000	0.002	0.000	0.000	0.001	0.001	0.002	0.000	0.000	0.003	0.000	0.000	
Pt	0.000	0.000	0.000	0.000	0.000	0.000	0.000	0.000	0.000	0.000	0.000	0.000	0.000	
Pd	0.000	0.000	0.000	0.000	0.000	0.000	0.000	0.000	0.000	0.000	0.000	0.000	0.000	
S	1.994	1.991	1.987	1.993	1.999	1.992	1.991	1.987	1.993	1.993	1.992	1.997	1.996	
As	0.001	0.000	0.000	0.000	0.001	0.007	0.000	0.000	0.000	0.000	0.000	0.000	0.000	
Se	0.000	0.000	0.000	0.000	0.000	0.000	0.000	0.001	0.000	0.001	0.000	0.001	0.000	
total	3	3	3	3	3	3	3	3	3	3	3	3	3	
Σ cations	1.005	1.008	1.013	1.007	1.000	1.002	1.009	1.012	1.007	1.006	1.008	1.002	1.004	
Σ anions	1.995	1.992	1.987	1.993	2.000	1.998	1.991	1.988	1.993	1.994	1.992	1.998	1.996	

Dados de Química Mineral de Sulfeto (cont.)

Amostra	B944	BC3H	BC3H	BC3H	AM20C C1	AM20C C1	AM20C C1	AM20C C1	AM20C C2	AM20C C2	AT103	AT103	AT103	
mineral	borda	núcleo	borda	borda	núcleo	borda	núcleo	borda	núcleo	núcleo	borda	borda	borda	
Rocha	pirita													
Complexo	carbonatito													
Araxá	Araxá	Araxá	Araxá	Araxá	Araxá	Araxá	Araxá	Araxá	Araxá	Araxá	Tapira	Tapira	Tapira	
Fe	46.03	46.377	46.287	46.099	46.506	46.913	46.692	46.519	46.149	46.083	46.465	45.942	45.381	
Cu	0.017	0.008	0	0.005	0.003	0.002	0	0.001	0	0	0	0.027	0	
Pb	0.288	0.349	0.297	0.014	0.123	0	0	0.067	0	0	0.336	0.301	0.337	
Co	0.078	0.134	0.234	0.163	0.201	0.164	0.11	0.148	0.413	0.609	0.127	0.181	0.217	
Ag	0	0	0	0	0.001	0	0.006	0.006	0.022	0.001	0	0	0	
Zn	0	0	0	0.01	0	0	0.023	0.176	0.192	0.274	0	0	0.009	
Ni	0.001	0	0	0	0	0.007	0.003	0.012	0	0	0.022	0	0.034	
Pt	0	0	0	0.009	0	0	0	0	0	0	0.045	0	0	
Pd	0.002	0	0	0	0	0	0.007	0.011	0	0	0	0.004	0	
S	52.783	53.189	53.479	53.118	51.44	51.858	51.225	51.646	50.597	51.737	52.833	52.359	51.425	
As	0	0	0.142	0	0	0.007	0	0	0.098	0	0	0.001	0.007	
Se	0.026	0	0	0.04	0	0	0.072	0	0	0	0.102	0.106	0.026	
Total	99.225	100.057	100.439	99.458	98.274	98.951	98.138	98.586	97.471	98.704	99.93	98.921	97.436	
proporção atômica para 3 íons														
Fe	1.000	0.999	0.993	0.996	1.023	1.024	1.029	1.020	1.026	1.009	1.004	1.002	1.006	
Cu	0.000	0.000	0.000	0.000	0.000	0.000	0.000	0.000	0.000	0.000	0.000	0.001	0.000	
Pb	0.002	0.002	0.002	0.000	0.001	0.000	0.000	0.000	0.000	0.000	0.002	0.002	0.002	
Co	0.002	0.003	0.005	0.003	0.004	0.003	0.002	0.003	0.009	0.013	0.003	0.004	0.005	
Ag	0.000	0.000	0.000	0.000	0.000	0.000	0.000	0.000	0.000	0.000	0.000	0.000	0.000	
Zn	0.000	0.000	0.000	0.000	0.000	0.000	0.000	0.003	0.004	0.005	0.000	0.000	0.000	
Ni	0.000	0.000	0.000	0.000	0.000	0.000	0.000	0.000	0.000	0.000	0.000	0.000	0.001	
Pt	0.000	0.000	0.000	0.000	0.000	0.000	0.000	0.000	0.000	0.000	0.000	0.000	0.000	
Pd	0.000	0.000	0.000	0.000	0.000	0.000	0.000	0.000	0.000	0.000	0.000	0.000	0.000	
S	1.996	1.996	1.998	1.999	1.972	1.972	1.967	1.973	1.960	1.973	1.989	1.990	1.986	
As	0.000	0.000	0.002	0.000	0.000	0.000	0.000	0.000	0.002	0.000	0.000	0.000	0.000	
Se	0.000	0.000	0.000	0.001	0.000	0.000	0.001	0.000	0.000	0.000	0.002	0.002	0.000	
total	3	3	3	3	3	3	3	3	3	3	3	3	3	
Σ cations	1.003	1.004	1.000	1.000	1.028	1.028	1.032	1.027	1.039	1.027	1.010	1.009	1.014	
Σ anions	1.997	1.996	2.000	2.000	1.972	1.972	1.968	1.973	1.961	1.973	1.990	1.991	1.986	

Dados de Química Mineral de Sulfeto (cont.)

Amostra	AT139S núcleo	AT139S borda	AT139S núcleo	AT135S borda	AT135S pirita	AT135S carbonatito	AT135S borda	AT140S núcleo	AT46 borda	AT46 pirita	B143 núcleo	B143 pirita	B143 borda	AT54 núcleo
mineral	pirita	pirita	pirita	pirita	pirita	carbonatito	pirita	pirita	carbonatito	carbonatito	bebedourito	pirita	pirita	pirita
Rocha	carbonatito	carbonatito	carbonatito	carbonatito	carbonatito		carbonatito	carbonatito	Tapira	Tapira	Tapira	Tapira	Tapira	carbonatito
Complexo	Tapira	Tapira	Tapira	Tapira	Tapira		Tapira	Tapira	Tapira	Tapira	Tapira	Tapira	Tapira	Tapira
Fe	46.524	45.944	45.455	46.145	46.71	46.619	45.737	44.027	43.489	46.132	46.407	46.402	46.487	
Cu	0.031	0.046	0.073	0.034	0.018	0.038	0.079	0.006	0	0.028	0	0.039	0	
Pb	0.384	0.315	0.801	0	0.354	0.012	0.294	0	0	0.342	0.287	0.37	0.297	
Co	0.087	0.064	0.074	0.325	0.059	0.15	0.174	1.864	2.703	0.06	0.071	0.042	0.084	
Ag	0.001	0	0	0.004	0.005	0	0.002	0	0.008	0	0	0.001	0	
Zn	0	0	0	0	0.007	0.006	0.008	0	0	0	0	0.01	0	
Ni	0	0	0	0.089	0	0.006	0.01	0.438	0	0.015	0.001	0	0	
Pt	0	0	0	0	0	0.013	0.011	0	0	0	0.016	0	0.004	
Pd	0	0	0	0	0	0	0	0	0	0.009	0.007	0	0	
S	53.907	53.163	52.469	52.396	53.528	52.812	51.819	53.045	52.848	52.752	53.33	53.662	53.718	
As	0.214	0.234	0.429	0	0.003	0	0	0.058	0.03	0.879	0.001	0.419	0	
Se	0	0	0	0.004	0.026	0.035	0	0	0.084	0	0.039	0.042	0	
Total	101.148	99.766	99.301	98.997	100.71	99.691	98.134	99.438	99.162	100.217	100.159	100.987	100.59	
proporção atômica para 3 íons														
Fe	0.991	0.992	0.992	1.004	1.000	1.008	1.007	0.953	0.944	0.997	0.998	0.992	0.995	
Cu	0.001	0.001	0.001	0.001	0.000	0.001	0.002	0.000	0.000	0.001	0.000	0.001	0.000	
Pb	0.002	0.002	0.005	0.000	0.002	0.000	0.002	0.000	0.000	0.002	0.002	0.002	0.002	
Co	0.002	0.001	0.002	0.007	0.001	0.003	0.004	0.038	0.056	0.001	0.001	0.001	0.002	
Ag	0.000	0.000	0.000	0.000	0.000	0.000	0.000	0.000	0.000	0.000	0.000	0.000	0.000	
Zn	0.000	0.000	0.000	0.000	0.000	0.000	0.000	0.000	0.000	0.000	0.000	0.000	0.000	
Ni	0.000	0.000	0.000	0.002	0.000	0.000	0.000	0.009	0.000	0.000	0.000	0.000	0.000	
Pt	0.000	0.000	0.000	0.000	0.000	0.000	0.000	0.000	0.000	0.000	0.000	0.000	0.000	
Pd	0.000	0.000	0.000	0.000	0.000	0.000	0.000	0.000	0.000	0.000	0.000	0.000	0.000	
S	2.001	2.000	1.994	1.986	1.996	1.988	1.986	1.999	1.998	1.985	1.998	1.997	2.002	
As	0.003	0.004	0.007	0.000	0.000	0.000	0.000	0.001	0.000	0.014	0.000	0.007	0.000	
Se	0.000	0.000	0.000	0.000	0.000	0.001	0.000	0.000	0.001	0.000	0.001	0.001	0.000	
total	3	3	3	3	3	3	3	3	3	3	3	3	3	
Σ cations	0.996	0.996	0.999	1.014	1.004	1.012	1.014	1.000	1.000	1.001	1.002	0.996	0.998	
Σ anions	2.004	2.004	2.001	1.986	1.996	1.988	1.986	2.000	2.000	1.999	1.998	2.004	2.002	

Dados de Química Mineral de Sulfeto (cont.)

Amostra	AT54 borda	AT54 pirita	AT53 borda	AT53 pirita	FENTAP núcleo	FENTAP pirita	FENTAP fenite	LG08 borda	LG08 pirita	LG08 carbonatito	4S22 borda	4S22 pirita	4S22 carbonatito
mineral	borda	pirita	borda	pirita	borda	pirita	borda	núcleo	pirita	carbonatito	borda	pirita	carbonatito
Rocha	carbonatito	carbonatito	carbonatito	carbonatito	carbonatito	carbonatito	carbonatito	carbonatito	carbonatito	carbonatito	carbonatito	carbonatito	carbonatito
Complexo	Tapira	Tapira	Tapira	Tapira	Tapira	Tapira	Tapira	Tapira	Tapira	Tapira	Tapira	Tapira	Tapira
Fe	46.576	46.871	46.146	46.462	46.242	45.639	45.458	46.225	46.441	46.649	46.684	46.65	46.796
Cu	0.026	0.024	0.008	0.02	0.005	0.021	0	0.002	0.004	0.024	0.029	0.006	0.003
Pb	0.349	0.333	0.34	0.312	0.293	0.316	0.315	0.258	0.316	0.333	0.306	0.281	0.347
Co	0.116	0.083	0.079	0.077	0.121	0.217	0.203	0.356	0.36	0.432	0.294	0.401	0.299
Ag	0.025	0	0.02	0	0	0.015	0.002	0.001	0	0	0.01	0	0
Zn	0.019	0	0	0.006	0.002	0	0	0	0.003	0	0	0	0.013
Ni	0.014	0	0.03	0	0.27	0.532	0.576	0	0.006	0	0	0.001	0.006
Pt	0.026	0	0	0.001	0.005	0	0	0.022	0	0	0	0	0.006
Pd	0	0.012	0	0	0	0	0	0.009	0	0	0.002	0	0.002
S	53.677	53.828	50.901	52.708	53.074	52.71	53.041	52.414	53.342	52.79	53.371	53.015	52.93
As	0	0	0.009	0	0	0	0	0.003	0.007	0	0.003	0	0
Se	0.002	0	0.061	0	0.025	0.055	0	0.027	0.088	0.011	0.068	0	0.077
Total	100.83	101.151	97.594	99.586	100.037	99.505	99.595	99.317	100.567	100.239	100.767	100.354	100.479
proporção atômica para 3 íons													
Fe	0.996	0.999	1.025	1.007	0.997	0.990	0.984	1.005	0.996	1.006	1.000	1.004	1.007
Cu	0.000	0.000	0.000	0.000	0.000	0.000	0.000	0.000	0.000	0.000	0.001	0.000	0.000
Pb	0.002	0.002	0.002	0.002	0.002	0.002	0.002	0.002	0.002	0.002	0.002	0.002	0.002
Co	0.002	0.002	0.002	0.002	0.002	0.004	0.004	0.007	0.007	0.009	0.006	0.008	0.006
Ag	0.000	0.000	0.000	0.000	0.000	0.000	0.000	0.000	0.000	0.000	0.000	0.000	0.000
Zn	0.000	0.000	0.000	0.000	0.000	0.000	0.000	0.000	0.000	0.000	0.000	0.000	0.000
Ni	0.000	0.000	0.001	0.000	0.006	0.011	0.012	0.000	0.000	0.000	0.000	0.000	0.000
Pt	0.000	0.000	0.000	0.000	0.000	0.000	0.000	0.000	0.000	0.000	0.000	0.000	0.000
Pd	0.000	0.000	0.000	0.000	0.000	0.000	0.000	0.000	0.000	0.000	0.000	0.000	0.000
S	1.998	1.997	1.969	1.989	1.993	1.991	1.999	1.985	1.993	1.983	1.991	1.986	1.983
As	0.000	0.000	0.000	0.000	0.000	0.000	0.000	0.000	0.000	0.000	0.000	0.000	0.000
Se	0.000	0.000	0.001	0.000	0.000	0.001	0.000	0.000	0.001	0.000	0.001	0.000	0.001
total	3	3	3	3	3	3	3	3	3	3	3	3	3
Σ cations	1.002	1.003	1.030	1.011	1.007	1.008	1.001	1.014	1.006	1.017	1.008	1.014	1.015
Σ anions	1.998	1.997	1.970	1.989	1.993	1.992	1.999	1.986	1.994	1.983	1.992	1.986	1.985

Dados de Química Mineral de Sulfeto (cont.)

Amostra	1E53C	CB07	CB07	CB07	LG38	LG38	LG38	LG38	LG38	LG38	AT01	AT01	LG08
mineral	núcleo	núcleo	borda	borda	núcleo	borda	núcleo	borda	núcleo	borda	vein	vein	núcleo
Rocha	pirita	pirita	pirita	pirita	pirita	pirita	pirita	pirita	pirita	pirita	pirita	pirita	pirita
Complexo	foscorito	foscorito	foscorito	foscorito	carbonatito	carbonatito	carbonatito	carbonatito	carbonatito	carbonatito	bebedourito	bebedourito	carbonatito
Fe	46.474	46.805	46.215	46.733	47.193	46.642	46.789	46.749	46.944	46.2	46.74	46.897	46.791
Cu	0.202	0	0.018	0	0	0	0	0.008	0.023	0	0.01	0.02	0
Pb	0.426	0.358	0.33	0.351	0.311	0	0	0.005	0.009	0	0.279	0.38	0.336
Co	0.117	0.059	0.051	0.069	0.071	0.073	0.116	0.074	0.073	0.414	0.181	0.114	0.168
Ag	0.004	0	0	0	0	0.003	0	0	0	0.015	0	0	0.029
Zn	0.013	0.014	0.003	0	0.006	0	0	0.007	0.011	0	0	0	0.008
Ni	0.169	0	0	0	0	0	0.001	0.001	0.004	0.009	0.026	0.018	0.004
Pt	0	0.029	0	0	0	0	0	0.007	0.01	0	0.003	0.005	0.008
Pd	0	0.001	0	0	0	0	0	0	0	0.003	0	0	0.002
S	53.496	53.615	53.111	53.44	53.168	52.928	53.059	53.269	53.382	53.344	52.689	53.533	53.036
As	0	0	0	0	0.007	0.023	0.015	0	0.099	0.052	0	0	0
Se	0	0.023	0.015	0.102	0	0	0.047	0	0	0.035	0.02	0.053	0.076
Total	100.901	100.904	99.743	100.695	100.756	99.669	100.027	100.12	100.555	100.072	99.948	101.02	100.458
proporção atômica para 3 íons													
Fe	0.994	1.000	0.998	1.001	1.012	1.007	1.007	1.005	1.005	0.993	1.010	1.002	1.006
Cu	0.004	0.000	0.000	0.000	0.000	0.000	0.000	0.000	0.000	0.000	0.000	0.000	0.000
Pb	0.002	0.002	0.002	0.002	0.002	0.000	0.000	0.000	0.000	0.000	0.002	0.002	0.002
Co	0.002	0.001	0.001	0.001	0.001	0.001	0.002	0.002	0.001	0.008	0.004	0.002	0.003
Ag	0.000	0.000	0.000	0.000	0.000	0.000	0.000	0.000	0.000	0.000	0.000	0.000	0.000
Zn	0.000	0.000	0.000	0.000	0.000	0.000	0.000	0.000	0.000	0.000	0.000	0.000	0.000
Ni	0.003	0.000	0.000	0.000	0.000	0.000	0.000	0.000	0.000	0.000	0.001	0.000	0.000
Pt	0.000	0.000	0.000	0.000	0.000	0.000	0.000	0.000	0.000	0.000	0.000	0.000	0.000
Pd	0.000	0.000	0.000	0.000	0.000	0.000	0.000	0.000	0.000	0.000	0.000	0.000	0.000
S	1.993	1.996	1.998	1.994	1.985	1.991	1.989	1.994	1.991	1.997	1.983	1.992	1.987
As	0.000	0.000	0.000	0.000	0.000	0.000	0.000	0.000	0.002	0.001	0.000	0.000	0.000
Se	0.000	0.000	0.000	0.002	0.000	0.000	0.001	0.000	0.000	0.001	0.000	0.001	0.001
total	3	3	3	3	3	3	3	3	3	3	3	3	3
Σ cations	1.007	1.004	1.002	1.005	1.015	1.009	1.010	1.006	1.008	1.002	1.016	1.007	1.012
Σ anions	1.993	1.996	1.998	1.995	1.985	1.991	1.990	1.994	1.992	1.998	1.984	1.993	1.988

Dados de Química Mineral de Sulfeto (cont.)

Amostra	LG08	J13B	J13B	J13B	C1	272561	141484	10A77	10A77	10A77	C60_1	C60_1	93_8	
mineral	núcleo	núcleo	borda	borda	borda	núcleo	núcleo	núcleo	borda	borda	núcleo	borda	núcleo	
Rocha	pirita	pirita	pirita	pirita	pirita	pirrotita	pirrotita	pirrotita	pirrotita	pirrotita	pirrotita	pirrotita	pirrotita	
Complexo	carbonatito	jacupiranguito	jacupiranguito	jacupiranguito	carbonatito	carbonatito	brecha	apatitite	apatitite	apatitite	carbonatito	carbonatito	carbonatito	
Tapira		Jacupiranga	Jacupiranga	Jacupiranga	Jacupiranga	Catalão II	Catalão II	Salitre	Salitre	Salitre	Salitre	Salitre	Salitre	
Fe	46.63	46.146	46.215	46.19	45.325	59.347	59.275	60.994	60.652	60.341	59.476	59.876	60.062	
Cu	0.029	0.054	0.017	0.013	0.032	0.018	0.022	0.042	0.037	0.034	0	0.031	0.035	
Pb	0.334	0.037	0	0	0.239	0.219	0.222	0.254	0.038	0.301	0.242	0.229	0	
Co	0.316	0.228	0.064	0.16	0.315	0.378	0.113	0.191	0.189	0.245	0.133	0.094	0.163	
Ag	0	0	0.001	0	0	0.004	0	0	0.01	0	0	0	0	
Zn	0	0	0.01	0	0	0	0.002	0.012	0.001	0	0.005	0	0	
Ni	0	0.027	0	0.095	0.025	0	0.003	0	0	0	0	0	0	
Pt	0.018	0.016	0.001	0.021	0.005	0	0	0	0.012	0.034	0.002	0	0.002	
Pd	0	0	0	0.002	0.003	0	0	0	0	0	0	0	0.003	
S	53.304	53.373	53.304	53.349	52.025	39.314	39.386	38.863	38.853	38.831	39.631	39.877	38.929	
As	0	0	0	0	0.007	0.009	0	0	0.008	0	0.003	0.004	0	
Se	0.05	0	0	0	0.022	0	0.034	0.07	0.069	0	0	0.019	0.061	
Total	100.681	99.881	99.612	99.83	97.998	99.289	99.057	100.426	99.869	99.786	99.492	100.13	99.255	
proporção atômica para 3 íons														
Fe	1.000	0.993	0.996	0.994	0.997	0.867	0.864	0.901	0.896	0.892	0.862	0.862	0.885	
Cu	0.001	0.001	0.000	0.000	0.001	0.000	0.000	0.001	0.000	0.000	0.000	0.000	0.000	
Pb	0.002	0.000	0.000	0.000	0.001	0.001	0.001	0.001	0.000	0.001	0.001	0.001	0.000	
Co	0.006	0.005	0.001	0.003	0.007	0.005	0.002	0.003	0.003	0.003	0.002	0.001	0.002	
Ag	0.000	0.000	0.000	0.000	0.000	0.000	0.000	0.000	0.000	0.000	0.000	0.000	0.000	
Zn	0.000	0.000	0.000	0.000	0.000	0.000	0.000	0.000	0.000	0.000	0.000	0.000	0.000	
Ni	0.000	0.001	0.000	0.002	0.001	0.000	0.000	0.000	0.000	0.000	0.000	0.000	0.000	
Pt	0.000	0.000	0.000	0.000	0.000	0.000	0.000	0.000	0.000	0.000	0.000	0.000	0.000	
Pd	0.000	0.000	0.000	0.000	0.000	0.000	0.000	0.000	0.000	0.000	0.000	0.000	0.000	
S	1.990	2.000	2.002	2.000	1.993	1.000	1.000	0.999	0.999	1.000	1.000	1.000	0.999	
As	0.000	0.000	0.000	0.000	0.000	0.000	0.000	0.000	0.000	0.000	0.000	0.000	0.000	
Se	0.001	0.000	0.000	0.000	0.000	0.000	0.000	0.001	0.001	0.000	0.000	0.000	0.001	
total	3	3	3	3	3	1.873	1.867	1.905	1.899	1.897	1.865	1.865	1.888	
Σ cations	1.009	1.000	0.998	1.000	1.006	0.873	0.867	0.905	0.899	0.897	0.865	0.865	0.888	
Σ anions	1.991	2.000	2.002	2.000	1.994	1	1	1	1	1	1	1	1	

Dados de Química Mineral de Sulfeto (cont.)

Amostra	93_8 borda pirrotita carbonatito Rocha Complexo	93_8 borda pirrotita carbonatito Salitre	C60_2 núcleo pirrotita carbonatito Salitre	C60_2 borda pirrotita carbonatito Salitre	C60_2 borda pirrotita carbonatito Salitre	ASL15 núcleo pirrotita carbonatito Salitre	F784 núcleo pirrotita carbonatito Salitre	F784 borda pirrotita carbonatito Salitre	F784 borda pirrotita carbonatito Salitre	SLE277A1 núcleo pirrotita carbonatito Salitre	SLE277A1 borda pirrotita carbonatito Salitre	SLE277A1 borda pirrotita carbonatito Salitre	FVL184 borda pirrotita carbonatito Salitre
Fe	60.393	60.691	59.624	59.689	59.245	59.777	60.083	60.118	59.858	59.961	59.847	59.723	60.107
Cu	0.035	0.031	0.049	0.052	0.016	0.017	0	0.007	0	0	0	0	0.041
Pb	0.22	0.26	0.045	0.269	0.144	0.192	0.217	0.246	0.251	0.213	0.216	0.227	0.237
Co	0.183	0.162	0.142	0.164	0.138	0.367	0.117	0.103	0.094	0.179	0.201	0.219	0.083
Ag	0.004	0	0	0	0.004	0	0	0	0.004	0	0.001	0	0.011
Zn	0	0	0.001	0	0	0.005	0	0	0	0	0	0	0
Ni	0.006	0.019	0	0	0.011	0	0	0	0	0.036	0.006	0.037	0.001
Pt	0	0.007	0	0	0	0	0	0.048	0	0.012	0	0	0
Pd	0	0	0	0.005	0	0.001	0	0.002	0	0	0	0	0.012
S	38.84	38.856	39.776	39.807	39.992	38.847	39.493	39.704	39.521	39.494	39.551	39.571	39.328
As	0	0	0	0.004	0	0	0	0	0	0	0	0	0
Se	0	0.03	0.019	0.093	0.05	0	0.019	0	0.071	0.06	0.083	0.084	0
Total	99.681	100.056	99.656	100.083	99.6	99.206	99.929	100.228	99.799	99.955	99.905	99.861	99.82
Proporção atômica para 1 S													
Fe	0.893	0.897	0.861	0.860	0.850	0.884	0.873	0.869	0.869	0.871	0.868	0.866	0.878
Cu	0.000	0.000	0.001	0.001	0.000	0.000	0.000	0.000	0.000	0.000	0.000	0.000	0.001
Pb	0.001	0.001	0.000	0.001	0.001	0.001	0.001	0.001	0.001	0.001	0.001	0.001	0.001
Co	0.003	0.002	0.002	0.002	0.002	0.005	0.002	0.001	0.001	0.002	0.003	0.003	0.001
Ag	0.000	0.000	0.000	0.000	0.000	0.000	0.000	0.000	0.000	0.000	0.000	0.000	0.000
Zn	0.000	0.000	0.000	0.000	0.000	0.000	0.000	0.000	0.000	0.000	0.000	0.000	0.000
Ni	0.000	0.000	0.000	0.000	0.000	0.000	0.000	0.000	0.000	0.000	0.000	0.001	0.000
Pt	0.000	0.000	0.000	0.000	0.000	0.000	0.000	0.000	0.000	0.000	0.000	0.000	0.000
Pd	0.000	0.000	0.000	0.000	0.000	0.000	0.000	0.000	0.000	0.000	0.000	0.000	0.000
S	1.000	1.000	1.000	0.999	0.999	1.000	1.000	1.000	0.999	0.999	0.999	0.999	1.000
As	0.000	0.000	0.000	0.000	0.000	0.000	0.000	0.000	0.000	0.000	0.000	0.000	0.000
Se	0.000	0.000	0.000	0.001	0.001	0.000	0.000	0.000	0.001	0.001	0.001	0.001	0.000
total	1.897	1.901	1.863	1.864	1.853	1.890	1.876	1.872	1.871	1.875	1.872	1.870	1.880
Σ cations	0.897	0.901	0.863	0.864	0.853	0.890	0.876	0.872	0.871	0.875	0.872	0.870	0.880
Σ anions	1	1	1	1	1	1	1	1	1	1	1	1	1

Dados de Química Mineral de Sulfeto (cont.)

Amostra	FVL184	SLE360	SLE360	SLE360	BC3E	BC3E	BC3E	AT138	AT138	AT138	AT138	AT138	AT138	
mineral	borda pirrotita	núcleo pirrotita	núcleo pirrotita	borda pirrotita	borda pirrotita	borda pirrotita	borda pirrotita	núcleo pirrotita	borda pirrotita	núcleo pirrotita	borda pirrotita	núcleo pirrotita	borda pirrotita	
Rocha	carbonatito	carbonatito	carbonatito	carbonatito	carbonatito	carbonatito	carbonatito	carbonatito	carbonatito	carbonatito	carbonatito	carbonatito	carbonatito	
Complexo	Salitre	Salitre	Salitre	Salitre	Araxá	Araxá	Araxá	Tapira	Tapira	Tapira	Tapira	Tapira	Tapira	
Fe	59.986	60.164	60.028	60.321	59.353	59.505	59.391	59.729	59.339	59.401	58.919	59.297	59.546	
Cu	0	0	0.006	0.011	0	0.032	0.012	0.027	0.012	0.024	0.043	0.033	0.012	
Pb	0	0.028	0.013	0	0.211	0	0.185	0.261	0.222	0.235	0.285	0.014	0.044	
Co	0.083	0.112	0.106	0.134	0.166	0.172	0.155	0.156	0.126	0.196	0.175	0.173	0.221	
Ag	0	0	0.013	0.011	0	0	0	0	0	0	0	0	0	
Zn	0.017	0	0	0	0	0	0	0	0	0	0	0	0	
Ni	0	0.014	0.019	0.027	0	0	0.012	0.008	0.049	0.021	0.042	0	0.098	
Pt	0	0	0	0.012	0.003	0	0	0	0	0	0	0	0.005	
Pd	0.005	0	0	0	0.005	0.004	0	0	0.003	0	0	0.009	0	
S	38.943	40.319	40.246	39.874	39.037	39.488	39.307	39.735	39.373	39.481	39.254	39.239	39.497	
As	0	0	0	0	0	0.003	0	0	0	0	0	0	0	
Se	0	0.015	0	0.005	0	0.058	0.06	0	0	0.064	0	0.048	0.006	
Total	99.034	100.652	100.431	100.395	98.775	99.262	99.122	99.916	99.124	99.422	98.718	98.813	99.429	
Proporção atômica para 1 S														
Fe	0.884	0.857	0.856	0.869	0.873	0.865	0.867	0.863	0.865	0.863	0.862	0.867	0.866	
Cu	0.000	0.000	0.000	0.000	0.000	0.000	0.000	0.000	0.000	0.000	0.001	0.000	0.000	
Pb	0.000	0.000	0.000	0.000	0.001	0.000	0.001	0.001	0.001	0.001	0.001	0.000	0.000	
Co	0.001	0.002	0.001	0.002	0.002	0.002	0.002	0.002	0.002	0.003	0.002	0.002	0.003	
Ag	0.000	0.000	0.000	0.000	0.000	0.000	0.000	0.000	0.000	0.000	0.000	0.000	0.000	
Zn	0.000	0.000	0.000	0.000	0.000	0.000	0.000	0.000	0.000	0.000	0.000	0.000	0.000	
Ni	0.000	0.000	0.000	0.000	0.000	0.000	0.000	0.000	0.001	0.000	0.001	0.000	0.001	
Pt	0.000	0.000	0.000	0.000	0.000	0.000	0.000	0.000	0.000	0.000	0.000	0.000	0.000	
Pd	0.000	0.000	0.000	0.000	0.000	0.000	0.000	0.000	0.000	0.000	0.000	0.000	0.000	
S	1.000	1.000	1.000	1.000	1.000	0.999	0.999	1.000	1.000	0.999	1.000	1.000	1.000	
As	0.000	0.000	0.000	0.000	0.000	0.000	0.000	0.000	0.000	0.000	0.000	0.000	0.000	
Se	0.000	0.000	0.000	0.000	0.000	0.001	0.001	0.000	0.000	0.001	0.000	0.000	0.000	
total	1.886	1.858	1.858	1.871	1.876	1.868	1.870	1.867	1.869	1.868	1.867	1.870	1.870	
Σ cations	0.886	0.858	0.858	0.871	0.876	0.868	0.870	0.867	0.869	0.868	0.867	0.870	0.870	
Σ anions	1	1	1	1	1	1	1	1	1	1	1	1	1	

Dados de Química Mineral de Sulfeto (cont.)

Amostra	AT137S borda pirrotita carbonatito Rocha Complexo	AT137S borda pirrotita carbonatito Tapira	AT128 borda pirrotita carbonatito Tapira	AT46 núcleo pirrotita carbonatito Tapira	TP9010 núcleo pirrotita bebedourito Tapira	TP9010 núcleo pirrotita bebedourito Tapira	TP9010 borda pirrotita bebedourito Tapira	TP9010 borda pirrotita bebedourito Tapira	AT49 núcleo pirrotita carbonatito Tapira	AT49 borda pirrotita carbonatito Tapira	AT49 borda pirrotita carbonatito Tapira	TAPS núcleo pirrotita carbonatito Tapira	TAPS borda pirrotita carbonatito Tapira	
Fe	59.332	59.405	60.536	59.451	59.69	59.49	59.453	59.664	60.145	59.789	59.974	61.188	60.73	
Cu	0.016	0.032	0	0.005	0	0	0.026	0.023	0	0	0.038	0	0	
Pb	0.206	0.033	0.153	0	0.006	0.019	0.235	0.246	0.27	0.246	0.283	0.267	0.261	
Co	0.217	0.217	0.247	0.103	0.225	0.23	0.295	0.273	0.079	0.109	0.087	0.11	0.09	
Ag	0	0	0.004	0	0	0	0.034	0	0	0.005	0.023	0	0.009	
Zn	0.001	0	0.01	0	0	0.015	0.008	0	0.024	0	0.005	0.005	0.001	
Ni	0.124	0.15	0	0.038	0.013	0.074	0.061	0.065	0	0.018	0.003	0	0.015	
Pt	0	0	0.015	0.023	0	0	0.032	0	0	0.007	0.047	0.024	0	
Pd	0	0.011	0	0	0	0	0.005	0.002	0.001	0.013	0	0	0.008	
S	39.589	39.588	38.149	38.186	39.388	39.355	39.457	39.019	39.414	39.892	39.848	38.23	38.154	
As	0.006	0.007	0	0.012	0	0	0	0	0.004	0	0.009	0.004	0.005	
Se	0.083	0.04	0	0.021	0.044	0.012	0.075	0.051	0.087	0.01	0	0.052	0	
Total	99.574	99.483	99.114	97.839	99.366	99.195	99.681	99.343	100.024	100.089	100.317	99.88	99.273	
Proporção atômica para 1 S														
Fe	0.860	0.861	0.911	0.894	0.870	0.868	0.865	0.878	0.875	0.861	0.864	0.918	0.914	
Cu	0.000	0.000	0.000	0.000	0.000	0.000	0.000	0.000	0.000	0.000	0.000	0.000	0.000	
Pb	0.001	0.000	0.001	0.000	0.000	0.000	0.001	0.001	0.001	0.001	0.001	0.001	0.001	
Co	0.003	0.003	0.004	0.001	0.003	0.003	0.004	0.004	0.001	0.001	0.001	0.002	0.001	
Ag	0.000	0.000	0.000	0.000	0.000	0.000	0.000	0.000	0.000	0.000	0.000	0.000	0.000	
Zn	0.000	0.000	0.000	0.000	0.000	0.000	0.000	0.000	0.000	0.000	0.000	0.000	0.000	
Ni	0.002	0.002	0.000	0.001	0.000	0.001	0.001	0.001	0.000	0.000	0.000	0.000	0.000	
Pt	0.000	0.000	0.000	0.000	0.000	0.000	0.000	0.000	0.000	0.000	0.000	0.000	0.000	
Pd	0.000	0.000	0.000	0.000	0.000	0.000	0.000	0.000	0.000	0.000	0.000	0.000	0.000	
S	0.999	1.000	1.000	1.000	1.000	1.000	0.999	0.999	0.999	1.000	1.000	0.999	1.000	
As	0.000	0.000	0.000	0.000	0.000	0.000	0.000	0.000	0.000	0.000	0.000	0.000	0.000	
Se	0.001	0.000	0.000	0.000	0.000	0.000	0.001	0.001	0.001	0.000	0.000	0.001	0.000	
total	1.865	1.867	1.916	1.896	1.873	1.872	1.871	1.884	1.878	1.863	1.867	1.921	1.917	
Σ cations	0.865	0.867	0.916	0.896	0.873	0.872	0.871	0.884	0.878	0.863	0.867	0.921	0.917	
Σ anions	1	1	1	1	1	1	1	1	1	1	1	1	1	

Dados de Química Mineral de Sulfeto (cont.)

Amostra	TAPS	AT01	AT01	AT01	CL2-50	CL2-50	JC02	JC02	JC02	170 52B	170 52B	170 52B	150 53D	
mineral	borda pirrotita	núcleo pirrotita	borda pirrotita	borda pirrotita	borda pirrotita	borda carbonatito	núcleo pirrotita	borda carbonatito	borda carbonatito	núcleo pirrotita	borda pirrotita	borda carbonatito	núcleo pirrotita	
Rocha	carbonatito	bebedourito	bebedourito	bebedourito	Jacupiranga	Jacupiranga	Jacupiranga	Jacupiranga	Jacupiranga	Jacupiranga	Jacupiranga	Jacupiranga	carbonatito	
Complexo	Tapira	Tapira	Tapira	Tapira	Jacupiranga	Jacupiranga	Jacupiranga	Jacupiranga	Jacupiranga	Jacupiranga	Jacupiranga	Jacupiranga	Jacupiranga	
Fe	60.503	60.179	59.603	59.662	59.762	59.475	59.221	60.184	59.674	60.119	60.081	60.103	60.449	
Cu	0	0.002	0.02	0.001	0.011	0.048	0.042	0.025	0.024	0.027	0.057	0	0.061	
Pb	0.208	0.233	0.251	0.104	0.147	0	0.266	0.071	0.264	0.07	0.187	0.267	0.251	
Co	0.102	0.18	0.154	0.157	0.303	0.366	0.304	0.309	0.189	0.344	0.359	0.306	0.247	
Ag	0	0	0	0.018	0	0.003	0	0	0.029	0.027	0	0	0	
Zn	0.006	0	0	0	0	0	0	0	0	0	0.005	0.005	0.007	
Ni	0	0	0	0.002	0	0	0.04	0.022	0.042	0.01	0.006	0.02	0	
Pt	0.015	0.01	0	0.004	0	0.023	0.004	0	0	0	0.016	0.021	0	
Pd	0.012	0.017	0	0	0.004	0	0.005	0	0	0	0	0	0.001	
S	38.304	39.438	39.756	39.541	38.656	38.248	38.708	38.577	38.63	38.31	38.511	38.443	37.455	
As	0.009	0.007	0.007	0	0	0.014	0.01	0	0	0.007	0	0	0	
Se	0.029	0.048	0.043	0.08	0.016	0.061	0.1	0.049	0.002	0.061	0	0.05	0.009	
Total	99.188	100.114	99.834	99.569	98.899	98.238	98.7	99.237	98.854	98.975	99.222	99.215	98.48	
Proporção atômica para 1 S														
Fe	0.907	0.876	0.860	0.866	0.888	0.892	0.877	0.895	0.887	0.900	0.896	0.897	0.927	
Cu	0.000	0.000	0.000	0.000	0.000	0.001	0.001	0.000	0.000	0.000	0.001	0.000	0.001	
Pb	0.001	0.001	0.001	0.000	0.001	0.000	0.001	0.000	0.001	0.000	0.001	0.001	0.001	
Co	0.001	0.002	0.002	0.002	0.004	0.005	0.004	0.004	0.003	0.005	0.005	0.004	0.004	
Ag	0.000	0.000	0.000	0.000	0.000	0.000	0.000	0.000	0.000	0.000	0.000	0.000	0.000	
Zn	0.000	0.000	0.000	0.000	0.000	0.000	0.000	0.000	0.000	0.000	0.000	0.000	0.000	
Ni	0.000	0.000	0.000	0.000	0.000	0.000	0.001	0.000	0.001	0.000	0.000	0.000	0.000	
Pt	0.000	0.000	0.000	0.000	0.000	0.000	0.000	0.000	0.000	0.000	0.000	0.000	0.000	
Pd	0.000	0.000	0.000	0.000	0.000	0.000	0.000	0.000	0.000	0.000	0.000	0.000	0.000	
S	1.000	0.999	0.999	0.999	1.000	0.999	0.999	0.999	1.000	0.999	1.000	0.999	1.000	
As	0.000	0.000	0.000	0.000	0.000	0.000	0.000	0.000	0.000	0.000	0.000	0.000	0.000	
Se	0.000	0.000	0.000	0.001	0.000	0.001	0.001	0.001	0.000	0.001	0.000	0.001	0.000	
total	1.909	1.879	1.864	1.868	1.893	1.898	1.884	1.901	1.892	1.906	1.903	1.903	1.932	
Σ cations	0.909	0.879	0.864	0.868	0.893	0.898	0.884	0.901	0.892	0.906	0.903	0.903	0.932	
Σ anions	1	1	1	1	1	1	1	1	1	1	1	1	1	

Dados de Química Mineral de Sulfeto (cont.)

Amostra	150 53D	150 53D	C5	C5	C3B	C3B	C3B	C3	C3	C3	160-5	160-5	160-5
mineral	borda	borda	núcleo	borda	núcleo	borda	núcleo	borda	borda	borda	núcleo	borda	borda
Rocha	pirrotita												
Complexo	Jacupiranga												
Fe	60.994	60.636	60.159	60.077	59.515	59.428	58.935	58.79	58.804	59.008	59.838	60.497	60.603
Cu	0.037	0.032	0.032	0.035	0.031	0	0.047	0	0.04	0.015	0.022	0.035	0
Pb	0.231	0.215	0.312	0.22	0.157	0.147	0.199	0.211	0.165	0.137	0.166	0	0.026
Co	0.179	0.188	0.212	0.232	0.306	0.274	0.229	0.197	0.239	0.18	0.321	0.293	0.333
Ag	0	0.008	0	0	0	0	0	0	0	0	0	0	0
Zn	0.002	0	0.007	0	0	0	0.007	0	0.005	0	0	0.006	0
Ni	0	0	0.038	0.044	0.322	0.282	0.095	0.049	0.061	0.063	0	0.007	0.012
Pt	0.021	0.006	0	0.007	0	0	0.001	0.007	0	0.014	0	0	0
Pd	0	0.007	0.011	0	0.002	0.003	0.014	0	0	0	0	0	0
S	37.709	37.968	39.25	39.037	38.622	38.949	40.118	38.711	38.855	38.559	38.821	38.614	38.744
As	0	0	0.011	0	0.014	0	0.003	0	0	0	0.003	0	0
Se	0.006	0	0	0.122	0.032	0.05	0.017	0	0.11	0.075	0.021	0.111	0
Total	99.179	99.06	100.032	99.774	99.001	99.133	99.665	97.965	98.279	98.051	99.192	99.563	99.718
Proporção atômica para 1 S													
Fe	0.929	0.917	0.880	0.883	0.884	0.876	0.843	0.872	0.868	0.878	0.885	0.899	0.898
Cu	0.000	0.000	0.000	0.000	0.000	0.000	0.001	0.000	0.001	0.000	0.000	0.000	0.000
Pb	0.001	0.001	0.001	0.001	0.001	0.001	0.001	0.001	0.001	0.001	0.001	0.000	0.000
Co	0.003	0.003	0.003	0.003	0.004	0.004	0.003	0.003	0.003	0.003	0.004	0.004	0.005
Ag	0.000	0.000	0.000	0.000	0.000	0.000	0.000	0.000	0.000	0.000	0.000	0.000	0.000
Zn	0.000	0.000	0.000	0.000	0.000	0.000	0.000	0.000	0.000	0.000	0.000	0.000	0.000
Ni	0.000	0.000	0.001	0.001	0.005	0.004	0.001	0.001	0.001	0.001	0.000	0.000	0.000
Pt	0.000	0.000	0.000	0.000	0.000	0.000	0.000	0.000	0.000	0.000	0.000	0.000	0.000
Pd	0.000	0.000	0.000	0.000	0.000	0.000	0.000	0.000	0.000	0.000	0.000	0.000	0.000
S	1.000	1.000	1.000	0.999	1.000	0.999	1.000	1.000	0.999	0.999	1.000	0.999	1.000
As	0.000	0.000	0.000	0.000	0.000	0.000	0.000	0.000	0.000	0.000	0.000	0.000	0.000
Se	0.000	0.000	0.000	0.001	0.000	0.001	0.000	0.000	0.001	0.001	0.000	0.001	0.000
total	1.933	1.921	1.885	1.888	1.894	1.884	1.849	1.876	1.873	1.882	1.890	1.903	1.903
Σ cations	0.933	0.921	0.885	0.888	0.894	0.884	0.849	0.876	0.873	0.882	0.890	0.903	0.903
Σ anions	1	1	1	1	1	1	1	1	1	1	1	1	1

Dados de Química Mineral de Sulfeto (cont.)

Amostra	JC01 núcleo pirrotita carbonatito Rocha Complexo	JC01 borda pirrotita carbonatito Jacupiranga	JC01 borda pirrotita carbonatito Jacupiranga	272843 núcleo calcopirita carbonatito Catalão II	272843 borda calcopirita carbonatito Catalão II	272485B1 núcleo calcopirita carbonatito Catalão II	165911C borda calcopirita nelsonito Catalão II							
Fe	60.537	59.818	59.586	30.574	30.138	30.213	30.673	30.14	30.288	30.236	30.513	29.953	30.229	
Cu	0.014	0.011	0.007	33.379	33.205	33.45	33.897	33.486	33.683	33.293	33.548	33.617	33.682	
Pb	0	0	0.016	0.265	0.095	0.277	0.211	0.207	0	0.172	0.267	0.182	0	
Co	0.149	0.111	0.141	0.005	0.07	0.066	0.036	0.05	0.036	0.037	0.03	0.029	0.025	
Ag	0	0.005	0	0.063	0	0.009	0.018	0	0.002	0	0.003	0.029	0	
Zn	0	0.004	0	0.048	0.02	0.017	0.016	0	0	0.008	0.003	0.031	0.013	
Ni	0.027	0.027	0.021	0.006	0	0	0.009	0	0.011	0	0	0.002	0	
Pt	0.001	0	0.018	0	0	0	0	0.008	0	0	0.003	0	0	
Pd	0	0.008	0	0.006	0	0.003	0	0	0.01	0	0.011	0	0	
S	39.203	38.977	38.676	35.304	34.681	34.662	34.833	35.029	34.976	34.782	34.41	34.98	34.804	
As	0.002	0	0	0	0	0	0	0	0.013	0	0.001	0	0	
Se	0.043	0.025	0.058	0.14	0.062	0.002	0.06	0.056	0.033	0	0.071	0	0.032	
Total	99.976	98.986	98.523	99.79	98.271	98.699	99.753	98.976	99.052	98.528	98.86	98.823	98.785	
Proporção atômica para 1 S				Proporção atômica para 4 íons										
Fe	0.886	0.881	0.884	1.005	1.006	1.006	1.012	0.999	1.002	1.007	1.016	0.994	1.003	
Cu	0.000	0.000	0.000	0.965	0.974	0.979	0.982	0.975	0.979	0.974	0.982	0.980	0.983	
Pb	0.000	0.000	0.000	0.002	0.001	0.002	0.002	0.002	0.000	0.002	0.002	0.002	0.000	
Co	0.002	0.002	0.002	0.000	0.002	0.002	0.001	0.002	0.001	0.001	0.001	0.001	0.001	
Ag	0.000	0.000	0.000	0.001	0.000	0.000	0.000	0.000	0.000	0.000	0.000	0.000	0.000	
Zn	0.000	0.000	0.000	0.001	0.001	0.000	0.000	0.000	0.000	0.000	0.000	0.001	0.000	
Ni	0.000	0.000	0.000	0.000	0.000	0.000	0.000	0.000	0.000	0.000	0.000	0.000	0.000	
Pt	0.000	0.000	0.000	0.000	0.000	0.000	0.000	0.000	0.000	0.000	0.000	0.000	0.000	
Pd	0.000	0.000	0.000	0.000	0.000	0.000	0.000	0.000	0.000	0.000	0.000	0.000	0.000	
S	1.000	1.000	0.999	2.022	2.015	2.010	2.001	2.021	2.016	2.017	1.996	2.022	2.012	
As	0.000	0.000	0.000	0.000	0.000	0.000	0.000	0.000	0.000	0.000	0.000	0.000	0.000	
Se	0.000	0.000	0.001	0.003	0.001	0.000	0.001	0.001	0.001	0.000	0.002	0.000	0.001	
total	1.889	1.883	1.887	4	4	4	4	4	4	4	4	4	4	
Σ cations	0.889	0.883	0.887	1.975	1.983	1.990	1.998	1.977	1.983	1.983	2.002	1.978	1.987	
Σ anions	1	1	1	2.025	2.017	2.010	2.002	2.023	2.017	2.017	1.998	2.022	2.013	

Dados de Química Mineral de Sulfeto (cont.)

Amostra	CP1 núcleo calcopirita	CP1 borda calcopirita	CP1 borda calcopirita	CP3 núcleo calcopirita	CP3 borda calcopirita	CP3 borda calcopirita	165911C1 núcleo calcopirita	165911C1 borda calcopirita	165911C1 núcleo calcopirita	165911C1 borda calcopirita	165911C1 borda calcopirita	JC05 núcleo calcopirita
mineral												
Rocha	carbonatito	carbonatito	carbonatito	nelsonito	nelsonito	nelsonito	nelsonito	nelsonito	nelsonito	nelsonito	nelsonito	jacupiranguito
Complexo	Catalão II	Catalão II	Catalão II	Catalão II	Catalão II	Catalão II	Catalão II	Catalão II	Catalão II	Catalão II	Catalão II	Jacupiranga
Fe	30.167	30.569	30.629	30.552	30.47	30.423	30.343	30.248	30.27	30.431	30.422	30.192
Cu	33.324	33.896	33.641	33.489	33.739	34.108	34.29	34.316	34.067	34.165	33.916	33.625
Pb	0.175	0.264	0	0.275	0.202	0.163	0	0	0	0.013	0.01	0.15
Co	0.018	0.036	0.045	0.035	0.079	0.039	0.049	0	0.024	0.037	0.017	0.041
Ag	0.051	0	0.014	0.069	0	0.02	0.045	0.054	0.025	0.063	0.045	0.039
Zn	0.05	0.03	0.022	0.025	0.151	0.036	0	0	0	0	0	0.029
Ni	0	0	0	0	0	0	0.019	0.053	0.013	0.018	0.003	0
Pt	0.003	0	0	0.013	0	0	0	0	0.009	0	0.002	0.023
Pd	0	0	0	0	0.002	0	0.005	0	0	0.001	0.001	0
S	34.286	35.003	35.068	34.752	34.928	35.278	33.759	33.638	33.6	33.644	33.638	34.857
As	0.009	0	0	0	0	0	0	0.003	0.002	0	0	0
Se	0	0.054	0	0	0.046	0.018	0.092	0.038	0	0	0.06	0
Total	98.083	99.852	99.419	99.21	99.617	100.085	98.602	98.35	98.01	98.372	98.114	98.956
Proporção atômica para 4 íons												
Fe	1.011	1.007	1.010	1.013	1.005	0.998	1.016	1.016	1.019	1.022	1.023	1.002
Cu	0.982	0.981	0.975	0.976	0.978	0.983	1.009	1.013	1.008	1.008	1.003	0.980
Pb	0.002	0.002	0.000	0.002	0.002	0.001	0.000	0.000	0.000	0.000	0.000	0.001
Co	0.001	0.001	0.001	0.001	0.002	0.001	0.002	0.000	0.001	0.001	0.001	0.001
Ag	0.001	0.000	0.000	0.001	0.000	0.000	0.001	0.001	0.000	0.001	0.001	0.001
Zn	0.001	0.001	0.001	0.001	0.004	0.001	0.000	0.000	0.000	0.000	0.000	0.001
Ni	0.000	0.000	0.000	0.000	0.000	0.000	0.001	0.002	0.000	0.001	0.000	0.000
Pt	0.000	0.000	0.000	0.000	0.000	0.000	0.000	0.000	0.000	0.000	0.000	0.000
Pd	0.000	0.000	0.000	0.000	0.000	0.000	0.000	0.000	0.000	0.000	0.000	0.000
S	2.002	2.007	2.013	2.006	2.007	2.015	1.969	1.968	1.971	1.967	1.971	2.014
As	0.000	0.000	0.000	0.000	0.000	0.000	0.000	0.000	0.000	0.000	0.000	0.000
Se	0.000	0.001	0.000	0.000	0.001	0.000	0.002	0.001	0.000	0.000	0.001	0.000
total	4	4	4	4	4	4	4	4	4	4	4	4
Σ cations	1.998	1.992	1.987	1.994	1.992	1.985	2.029	2.031	2.029	2.033	2.028	1.986
Σ anions	2.002	2.008	2.013	2.006	2.008	2.015	1.971	1.969	1.971	1.967	1.972	2.014

Dados de Química Mineral de Sulfeto (cont.)

Amostra	JC05 borda calcopirita Rocha Complexo	JC05 borda calcopirita jacupiranguito Jacupiranga	PAL borda calcopirita carbonatito Phalaborwa	PAL núcleo calcopirita carbonatito Phalaborwa	PAL borda calcopirita carbonatito Phalaborwa	165911C1 núcleo bornite nelsonito Catalão II	165911C1 borda bornite nelsonito Catalão II
Fe	30.073	30.176	30.225	30.377	30.494	11.28	11.383
Cu	32.715	33.328	33.62	33.456	33.424	62.129	61.736
Pb	0.202	0.107	0.182	0.174	0.197	0	0
Co	0.04	0.039	0.039	0.003	0.02	0.036	0.008
Ag	0	0.036	0.002	0	0.015	0.237	0.281
Zn	0.029	0.02	0.021	0	0	0	0
Ni	0	0	0.083	0.008	0	0.015	0.063
Pt	0	0	0.011	0	0	0	0
Pd	0	0	0	0	0	0	0.008
S	34.395	35	34.551	34.385	34.665	25.526	25.293
As	0	0	0.009	0	0	0.009	0
Se	0	0.055	0.077	0.043	0	0.03	0.095
Total	97.454	98.761	98.82	98.446	98.815	99.262	98.867
Proporção atômica para 4 íons						atomic proportions for 10 ions	
Fe	1.012	1.001	1.006	1.015	1.014	1.021	1.035
Cu	0.968	0.972	0.983	0.982	0.977	4.940	4.934
Pb	0.002	0.001	0.002	0.002	0.002	0.000	0.000
Co	0.001	0.001	0.001	0.000	0.001	0.003	0.001
Ag	0.000	0.001	0.000	0.000	0.000	0.011	0.013
Zn	0.001	0.001	0.001	0.000	0.000	0.000	0.000
Ni	0.000	0.000	0.003	0.000	0.000	0.001	0.005
Pt	0.000	0.000	0.000	0.000	0.000	0.000	0.000
Pd	0.000	0.000	0.000	0.000	0.000	0.000	0.000
S	2.016	2.022	2.003	2.000	2.007	4.022	4.006
As	0.000	0.000	0.000	0.000	0.000	0.001	0.000
Se	0.000	0.001	0.002	0.001	0.000	0.002	0.006
total	4	4	4	4	4	10	10
Σ cations	1.984	1.976	1.995	1.999	1.993	5.976	5.988
Σ anions	2.016	2.024	2.005	2.001	2.007	4.024	4.012